Aerosol Particle Formation from Photochemical Oxidation of Sulfur Dioxide Vaper(Dissertation_全文)

AUTHOR(S):

Kasahara, Mikio

AEROSOL PARTICLE FORMATION FROM PHOTOCHEMICAL OXIDATION OF SULFUR DIOXIDE VAPOR

FEBRUARY 1975

MIKIO KASAHARA

AEROSOL PARTICLE FORMATION

FROM

PHOTOCHEMICAL OXIDATION OF SULFUR DIOXIDE VAPOR

FEBRUARY 1975

MIKIO KASAHARA

INSTITUTE OF ATOMIC ENERGY

KYOTO UNIVERSITY

PREFACE

Sulfur dioxide is one of the most injurious air pollutants. It is oxidized photochemically by absorbing solar radiation in the atmosphere to form finally sulfuric acid aerosols. Sulfuric acid aerosols have more severe physiological effect on humans than sulfur dioxide, and contribute to material damage, reduction of visibility and so on. Consequently, it is urgently required to make clear the formation mechanism of sulfuric acid aerosols from sulfur dioxide vapor in the atmosphere.

In this study, the formation and evolution mechanism of aerosol particles from photochemical oxidation of sulfur dioxide and properties of formed aerosols are examined experimentally under various environmental conditions in the most simple system of sulfur dioxide - pure air mixture using an artificial light, and also are investigated theoretically.

Further, a role of ultraviolet radiation in the photochemical reaction of air pollutants, in which ultraviolet radiation should be the most fundamental and important factor, is studied to discuss the differences between reaction in the atmosphere and that in the laboratory.

LIST OF PUBLICATIONS ON THIS STUDY

1. Kasahara, M. and Takahashi, K. (1971) : Aerosol formation from photochemical oxidation of sulfur dioxide, Kogai to Taisaku (J. Environ. Poll. Contr.), Vol.7, pp.997-1001 & pp.1151-1160. *review in Japanese* ..... Chapter 2

2. Kasahara, M. and Takahashi, K. (1973) : Ultraviolet irradiation on photochemical reaction of air pollutants, Taikiosenkenkyu (J. Japan Soc. Air Poll.), Vol.8, pp.645-653. *in Japanese* ..... Chapter 3

3. Kasahara, M. and Takahashi, K. (1974) : Numerical calculation of aerosol particle concentration passing through diffusion tube, Techn. Rept. Inst. Atomic Energy, Kyoto Univ., No.165. ..... Chapter 5

4. Takahashi, K., Kasahara, M. and Itoh, M. (1975) : A kinetic model of sulfuric acid aerosol formation from photochemical oxidation of sulfur dioxide vapor, J. Aerosol Sci., Vol.6, in printing. ..... Chapter 6

5. Kasahara, M. and Takahashi, K. (1975) : Experimental studies on aerosol particle formation from photochemical oxidation of sulfur dioxide, Atmos. Environ., in printing. .... Chapter 4 & 5

TABLE OF CONTENTS

page

Preface i
List of Publications on This Study ii
Table of Contents iii
List of Figures vii
List of Tables x

1. Introduction 1
  1.1 General 1
  1.2 Scope of This Study 2
    1.2.1 Object of the Study 2
    1.2.2 Outline of the Study 4
References 6

2. Review of Previous Work 7
  2.1 Sulfur Dioxide in the Atmosphere 7
  2.2 Ultraviolet Irradiation on Photochemical Reaction . . 8
  2.3 Photochemical Oxidation of Sulfur Dioxide in Air . . . 9
    2.3.1 Mechanism of Reactions 9
    2.3.2 Photochemical Reaction of Sulfur Dioxide 10
  2.4 Photochemical Reaction in the System of Sulfur Dioxide and Other Substances 15
    2.4.1 Mechanism of Reactions 15
    2.4.2 Photochemical Reaction in Homogeneous Mixtures . 15
    2.4.3 Photochemical Reaction in Heterogeneous Mixtures . 19
    2.4.4 Reactions of Sulfur Dioxide in Ambient Air . . . 21
  2.5 Aerosol Formation from Photochemical Reaction of SO_2 . 23

2.6 Properties of Particles Formed by Photochemical Reaction 26
2.6.1 Identification of Photochemical Aerosol Particles 28
2.6.2 Physical Properties of Photochemical Aerosol Particles 29
2.7 Theoretical Studies on Aerosol Formation 32
2.7.1 Homogeneous Nucleation 33
2.7.2 Nucleation in Binary Homogeneous System 34
References 37

3. Ultraviolet and Photochemical Reaction of Air Pollutants . 48
3.1 Introduction 48
3.2 Solar Irradiance in the Lower Atmosphere 49
3.2.1 Absorption and Scattering of Solar Radiation in Atmosphere 49
3.2.2 Direct and Scattered Intensity 51
3.2.3 Numerical Calculation and Results 52
3.3 Measurement of Ultraviolet Intensity in Solar Radiation 56
3.3.1 Measurement of Ultraviolet Intensity 56
3.3.2 Analyses of Measured Values 58
3.3.3 Results 58
3.4 Absorption of Radiation in Photochemical Reaction . . 60
3.4.1 Photochemical Reaction in Polluted Air 60
3.4.2 Absorption of Light Energy 61
3.4.3 Specific Absorption Rate Constant by Sulfur Dioxide 64
3.5 Results and Discussion 66
List of Symbols in Chapter 3 69
References 71

4. Aerosol Formation by Photochemical Oxidation of Sulfur Dioxide 74
4.1 Introduction 74
4.2 Experimental Equipment and Procedure 76
4.2.1 Photochemical Reaction Chamber and Related Facilities 76
4.2.2 Measurement Instrument 81
4.2.3 Experimental Procedure 83
4.3 Results and Discussion 85
4.3.1 Variation with Irradiation Time 85
4.3.2 Effects of Environmental Conditions in the Early Stage of Reaction 93
List of Symbols in Chapter 4 100
References 101

5. Physical and Chemical Properties of Photochemical Aerosols from Sulfur Dioxide 103
5.1 Introduction 103
5.2 Theory and Numerical Calculation on Diffusion Tube Method 104
5.2.1 General 104
5.2.2 Theory and Numerical Calculation 105
5.2.3 Determination of Particle Size Distribution . . . 107
5.3 Experimental Equipment and Procedure 109
5.4 Results and Discussion 111
5.4.1 Physical Properties of Aerosols 111
5.4.2 Chemical Properties of Aerosols 120
5.4.3 Photochemical Oxidation Rate of Sulfur Dioxide . 122
List of Symbols in Chapter 5 126
References 127

6. Kinetic Model of Aerosol Formation from Photochemical Oxidation of Sulfur Dioxide 130
6.1 Introduction 130
6.2 Nucleation of Sulfuric Acid Embryos 131
6.3 Kinetic Model of Aerosol Formation and Growth 133
6.4 Computational Method 138
6.5 Results and Discussion 142
6.5.1 Variation of Various Factors with Time 142
6.5.2 Maximum Number Concentration of Vapor Molecule and Particle 144
6.5.3 Maximum Number Formation Rate 147
6.5.4 Particle Radius and Volumetric Formation Rate . . 148
6.5.5 Particulate Fraction of Sulfuric Acid 149
6.5.6 Effect of Particles from Foreign Source 149
6.5.7 Comparison of Theoretical Calculation with Experimental Results 152
List of Symbols in Chapter 6 156
References 158

7. Conclusions and Recommendations 160

Acknowledgments 163

Appendices
Appendix 1 Effect of Impurities in Sample Gas on Experimental Studies A-1
Appendix 2 On the Accuracy of the CNC A-3
Appendix 3 Programme of Kinetic Model of Sulfuric Acid Formation from Photochemical Oxidation of Sulfur Dioxide A-5
Appendix 4 Aerosol Particle Concentration Passing Through Diffusion Tube A-7
Appendix 5 Examples of Original Data in the Experimental Studies A-8

LIST OF FIGURES

Figure		page
3-1	Solar zenith angle z in Kyoto, and relation between z and air mass m	50
3-2	Total, direct and scattering radiation spectra in the lower atmosphere	54
3-3	Total, direct and scattering ultraviolet radiation in the lower atmosphere	55
3-4	Response curve of UV meter	56
3-5	Measured direction	57
3-6	Spacial distribution of scattering u.v. radiation	57
3-7	Theoretical and measured direct u.v. intensity at the earth's surface	59
3-8	Theoretical and measured scattered u.v. intensity at the earth's surface	59
3-9	Spectral absorption of solar radiation by SO_2 for various values of z	65
3-10	Absorption of solar radiation by SO_2	65
3-11	Spectral transmittance of various thicknesses of acrylite and of saran	68
4-1	Schematic flow diagram of the experimental system	77
4-2	Calibration of some hydrocarbons by gas chromatograph	78
4-3	Energy spectrum of blacklight	80
4-4	Variation of particle number concentration with extended time from onset of irradiation	86
4-5	Average value and standard deviation of particle number concentrations obtained in four separate measurements for Run NT(1,60,1)	86

4-6 Effects of the flow condition and the corrected curve for NT(1,60,1) 87
4-7 Variation of the particle number concentration with irradiation time for various SO_2 concentrations 88
4-8 Variation of the particle number concentration with irradiation time for various relative humidities 89
4-9 Effects of SO_2 concentration, relative humidity and relative u.v. intensity on the maximum number concentration 91
4-10 Effects of SO_2 concentration, relative humidity and relative u.v. intensity on irradiation time when particle number concentration reaches maximum 91
4-11 Variation of the particle number concentration with irradiation time for various relative u.v. light intensities 92
4-12 Variation of the particle number concentration with irradiation time in the early stage of reaction 93
4-13 Effects of SO_2 concentration and relative humidity on the maximum number formation rate 94
4-14 Relation between the maximum number formation rate and the maximum particle number concentration . 97
4-15 Relation between the maximum number formation rate and irradiation times when the particle number concentration reaches maximum and when detectable particles are first formed 98

5-1 N/N_o and M/M_o as a function of X/Q 108
5-2 An example of particle size determination 109

5-3 Variation of particle radius of aerosols with irradiation time under various environmental conditions 112
5-4 Variation of particle number concentration of aerosols with irradiation time for various environmental conditions 112
5-5 Variation of volume concentration with irradiation time under various environmental conditions 114
5-6 Variation of surface area concentration with irradiation time under various environmental conditions 114
5-7 Variation of particle number concentration, volume concentration and surface area concentration with irradiation time for Run rT(1,60) 114
5-8 Effect of sulfur dioxide concentration on particle radius at various relative humidities . . . 117
5-9 Effect of relative humidity on particle radius at various sulfur dioxide concentration . . . 117
5-10 Effect of sulfur dioxide concentration and relative humidity on volume concentration 118
5-11 Effect of sulfur dioxide concentration and relative humidity on surface area concentration . . 118

6-1 Nucleation rate of sulfuric acid embryo at 25°C . . 132
6-2 Properties of critical embryo of sulfuric acid . . 134
6-3 Equilibrium water vapor pressure of particle containing sulfuric acid at 25°C 137
6-4 Flow chart for numerical computation of kinetic model 139
6-5 Schema of computation by Improved Cauchy - Polygon method 140

6-6 Time change of some characteristic values in aerosol formation at 50% r.h. and $S = 10^6 cm^{-3} sec^{-1}$. 142
6-7 Time change of number concentration of sulfuric acid vapor molecule 143
6-8 Time change of particle number concentration 143
6-9 Maximum number concentration of vapor molecule and time to reach the maximum concentration 144
6-10 Maximum particle number concentration and time to reach the maximum concentration 144
6-11 Maximum number concentration of vapor molecule and particle, and time to reach the maximum concentration 146
6-12 Maximum number formation rate for various relative humidities 147
6-13 Growth of averaged particle size 148
6-14 Volumetric formation rate of particle 148
6-15 Particulate fraction of sulfuric acid 149
6-16 Effect of foreign particles on change of various factors with time 150
6-17 Effect of foreign particles on particle number concentration change with time 151

LIST OF TABLES

Table page

2-1 Summary of photochemical oxidation of SO_2 14
2-2 Summary of photochemical reaction in homogeneous mixtures, I 18

2-3 Summary of photochemical reaction in homogeneous mixture, II 20
2-4 Summary of photochemical reaction in heterogeneous mixture 22
2-5 Summary of photochemical oxidation in atmosphere . . 24
2-6 Summary of physical properties of photochemical particles 27
2-7 Summary of identification of photochemical particles 30

3-1 Spectral absorption coefficient of SO_2 65
3-2 k_a by SO_2 in lower atmosphere at N 35° 66

4-1 Effective light intensity in reaction chamber . . . 81
4-2 Ranges of environmental factors used in this study . 84
4-3 Properties in formation and evolution processes of sulfuric acid mist under various environmental conditions 95
4-4 Maximum number formation rate as a function of product, $s \times I_r$ 96

5-1 Ranges of environmental factors used in this study . 110
5-2 Volumetric formation rate for Run r_T 115
5-3 Sulfuric acid concentration of a particle 121
5-4 Photochemical oxidation rate for Run $r_T(1,60)$ . . . 123
5-5 Photochemical oxidation rates for Run r_T in % hr^{-1} . 123

6-1 Values of physical and chemical properties of H_2SO_4 and H_2O vapor, at 20°C and 1 atm 136
6-2 Initial properties of newly formed particles applied in this study 141

6-3 Effect of foreign particle on volume concentration and surface area concentration 153
6-4 Experimental results of photochemical oxidation rate and some other factors, and comparison with theoretical values 154

Chapter 1

1. INTRODUCTION

1.1 General

Sulfur dioxide, SO_2, is one of the most common and primary air pollutants existing in the atmosphere as well as carbon monoxide, hydrocarbons, nitrogen oxides, and aerosol particles. It is among the most injurious air pollutants because of its toxicity and pervasiveness, and its concentration is often used as an index which indicates the level of air pollution. Sulfur dioxide absorbs near-ultraviolet radiation and molecules are electrically excited. Some of these excited molecules react chemically to become sulfur trioxide which combines with water in the atmosphere to form sulfuric acid mist. Sulfur dioxide and sulfuric acid mist contribute the effect on humans, animals and plants, materials damage and reduction of visibility as was seen in the serious pollution incident in London in 1952.

Because of the more severe physiological effect of sulfuric acid on humans than that of sulfur dioxide [1] and because of the singularity of sulfuric acid mist as aerosol particles, such as reduction of visibility and multiplicative increase of harmfulness by gas-particle mixture, it is of special interest to elucidate the reaction mechanism and reaction singularities of sulfur dioxide to sulfuric acid aerosols, and to investigate the physical and chemical properties of aerosol particles formed.

Generally, following the order of the steps in the over-all photochemical process, the information required for understanding of photochemical reactions which occur in polluted air may be listed under four general headings : (1) Radiation, (2) Absorption, (3) Primary process, and (4) Secondary reactions [2].

Almost all of the previous experimental studies on photochemical reaction of sulfur dioxide belong to the fourth step, i.e. Secondary reactions. It is, however, difficult to interpret or to compare mutually the results obtained in those studies because of the differences in the experimental conditions, such as chemical compounds, degree of humidity, temperature and intensity of solar radiation in the atmosphere, or such as reactants, its concentrations, type of irradiation sources and type of reaction chamber in the laboratory experiment. And in fact, adequate understanding of photochemical reaction of sulfur dioxide is lacking as shown in the results of photochemical reaction rate, and in the results for the effect of water vapor on photochemical reaction and aerosol formation.

1.2 Scope of This Study

1.2.1 Object of the Study

It is thought to be impossible to disregard sulfuric acid aerosol formation from sulfur dioxide in the atmosphere as is judged in the episode of sulfuric acid rain in summer of last year in Japan. Since sulfuric acid aerosols have severe effects upon human and life-environment and moreover sufficient understanding for aerosol formation of sulfuric acid from sulfur dioxide in the atmosphere is lacking as discribed before, it is urgently required to elucidate the aerosol formation mechanism and its singularities and to make clear the effect of environmental conditions on formation and evolution processes of sulfuric acid aerosols.

The most important formation process of sulfuric acid aerosol in the atmosphere is thought to be photochemical reaction. Accordingly, in this study, ultraviolet radiation is taken up as driving force of reaction of sulfur dioxide to sulfuric acid

aerosols.

In the properties of aerosol particles, the most fundamental and important factors are particle size distribution and concentration of particles. Because they are most effective factors for chemical, physical and physiological phenomena, such as aerosol formation mechanism, reduction of visibility and the toxicity of aerosol contaminants. Therefore, it is very important to determine the formation rate of aerosol particles, to trace formation and growth process of particles with time, and to elucidate the physical and chemical properties of aerosol particles under various environmental conditions.

As the first step to make clear the formation and growth mechanism of sulfuric acid aerosol in the atmosphere, the following subjects are examined experimentally in the most simple system of sulfur dioxide in pure air using an artificial light and are investigated theoretically.

Subject 1 : Formation and evolution mechanism, and its singularity of sulfuric acid aerosols from photochemical reaction of sulfur dioxide,

Subject 2 : Effect of environmental factors on aerosol formation,

Subject 3 : Physical and chemical properties of formed aerosols.

However, since the photochemical reaction of air pollutants is generally occured in the atmosphere by receiving the solar radiation, it is desirable to investigate the photochemical reaction for natural sunlight in the atmosphere. But such a investigation has many difficulties because the environmental conditions, such as chemical compounds, degree of humidity, temperature and intensity of sunlight change momentarily. In this experimental study as well as many other investigations, smog chamber tests are performed using an artificial light. The experimental result obtained

by smog chamber test is finally required to be converted into the case of reaction under the natural sunlight in the atmosphere. Otherwise, at least, the effective intensity of the artificial light for substances in question should be estimated and compared with that of the natural sunlight. For this purpose, the following subject is studied in advance of the aerosol formation study.

Subject 4 : A role of the ultraviolet irradiation in the photochemical reaction of air pollutants.

1.2.2 Outline of the Study

This study consists of two main parts, namely the first step, Radiation, and the fourth step, Secondary process, in the basic steps of the photochemical reaction study described before. The former is the study on Subject 4, and the latter is both experimental and theoretical studies on Subject 1 to 3.

In Chapter 2, the literatures on photochemical reaction and photochemical aerosol formation of sulfur dioxide, including on radiation, are reviewed.

Theoretical calculation and measurements for Subject 4 are made in Chapter 3. To obtain the basic data for the role of ultraviolet intensity in photochemical reaction of air pollutants, ultraviolet intensity at the earth's surface is calculated and measured, and specific absorption rate of solar radiation by sulfur dioxide is also calculated for various environmental conditions. Besides, an equation is proposed for estimating the specific absorption rate of artificial radiation by some air pollutants.

Subjects 1 and 2 are studied experimentally in Chapter 4. The particle number concentration change with time is examined in a systematical way under various environmental conditions, such as sulfur dioxide concentration, relative humidity and ultraviolet light intensity, and the effects of environmental factors on

formation and evolution processes of aerosol particle are investigated. From the detailed measurements of particle number concentration change in the early stage of reaction, the maximum number formation rates of aerosol particles are determined under various environmental conditions.

The study on Subject 3, examination of physical and chemical properties of formed aerosols, is performed in Chapter 5. That is, the particle size distribution of aerosols is measured systematically under various environmental conditions, and the determination of sulfuric acid concentration of particle is attempted. Besides, the volumetric formation rate is calculated, and photochemical reaction rate from sulfur dioxide to aerosol particle is determined. The basic technique used here is diffusion tube method.

Theoretical approach is also an important and effective way to make clear the mechanism of aerosol formation from photochemical oxidation of sulfur dioxide. In Chapter 6, to make clear Subject 1, 2 and 3 theoretically, the nucleation rate for a system of water and sulfuric acid vapor is calculated, and a kinetic model of the photochemical aerosol formation processes from sulfur dioxide in air is proposed.

References

[1] Gartrell, F. E., Thomas, F. W. and Carpenter, S. B. (1963) : Atmospheric oxidation of SO_2 in coal-burning power plant plumes, Amer. Ind. Hyg. Assoc. J., Vol.24, pp.113-120.

[2] Leighton, P. A. (1961) : Photochemistry of air pollution, Academic Press, New York.

Chapter 2

2. Review of Previous Work

In this chapter, the general characteristics of sulfur dioxide in the atmosphere are summarized at first, and subsequently the literatures on photochemical reaction and photochemical aerosol formation of sulfur dioxide are reviewed. The topics covered here are classified into the following six categories; 1) ultraviolet irradiation on photochemical reaction, 2) photochemical reaction of sulfur dioxide in air, 3) photochemical reaction in the system of sulfur dioxide and other substances, 4) aerosol formation from photochemical reaction of sulfur dioxide, 5) properties of aerosol particles formed by photochemical reaction of sulfur dioxide, and 6) theoretical calculations of aerosol formation from sulfur dioxide vapor.

There are several reviews on the photochemistry of air pollutants [1-5]. The popular text of Leighton [6] is an comprehensive review on photochemistry. Altshuller and Bufalini [7,8] reviewed the photochemical aspects of air pollution including the topics of sulfur dioxide photolysis and aerosol. Wagman [9] reviewed the atmospheric aerosol researches and suggested that size analyses of sulfuric acid droplet in atmosphere would be of universal interest. Urone and Schoroeder [10] and Buffalini [11] reviewed the literatures on the reactions of sulfur dioxide in polluted atmosphere and indicated the questions remained unanswered. Kasahara and Takahashi [12] reviewed the literatures on aerosol formation from photochemical oxidation of sulfur dioxide.

2.1 Sulfur Dioxide in the Atmosphere [13,14]

Sulfur dioxide is one of the most common of gaseous contaminants found in the ambient atmosphere. Sulfur dioxide is invisible, nonflammable and acidic gas. It is oxidized to sulfur trioxide in

the atmosphere. Sulfur trioxide is highly hygroscopic gas, which combines with water in the atmosphere to form sulfuric acid mist, or with other materials in the atmosphere to form sulfate compounds. The chief sources of sulfur dioxide are the combustion of fuels, the refining of petroleum, the smelting operations and the manufacture of sulfuric acid [13]. The volcanic gases also may be an important natural source of sulfur dioxide [15]. On atmospheric sulfur dioxide concentration in urban areas, a large number of data have been reported and analyzed [16-20]. Rohrman and Ludwig [21] have reviewed the sources of sulfur dioxide in the atmosphere.

Sulfur dioxide and sulfuric acid aerosols may contribute the effects on humans with damage ranging from eye irritation to death, on animals and plants, materials damage, buildings corrosion, and reduction of visibility as shown in the serious pollution incident in London in 1952. Gartrell et al. [22] suggested that elucidation of the rates of conversion of sulfur dioxide to the acid form is of special important in appraising potential health effects because of the more severe physiological effect of sulfuric acid on humans.

2.2 Ultraviolet Irradiation on Photochemical Reaction

Only a few studies has been performed on the roles of ultraviolet (u.v.) irradiation on photochemical reaction of air pollutants. It is pointed out by Leighton [6] that the examination of intensity and spectral distribution of solar radiation is the most fundamental and important in the photochemistry of air pollutants. Leighton calculated the spectral intensity of solar radiation in the lower atmosphere and the absorption rate of solar radiation by various kinds of air pollutants. Kasahara et al. [23] calculated the specific absorption rate of solar radiation by sulfur dioxide under various environmental conditions, and also proposed the equation to estimate the absorption rate of artificial radiation in

the popular system used in the experimental studies of photochemical reaction.

On the other hand, a lot of measurements of u.v. intensity of solar radiation in the lower atmosphere has been performed [24,25]. However, almost all of them are measurements of total u.v. intensity and measured value of the spectral u.v. intensity is only a few [26,27]. Volz [28] measured the solar radiation and the spectral skylight (skylight scattering function) in maritime aerosols and continental dust. Kasahara et al. [23] also showed the directional distribution of the scattered u.v. intensity of solar radiation. Chisaka et al. [29] measured the u.v. energy distribution in smog chamber and estimated the relative u.v. intensity of artificial radiation in smog chamber to solar radiation in atmosphere.

Some investigations relative to the influence of environmental factors, such as the amounts of particulate matter and water vapor, on the solar radiation have been reported. Shettle and Weinman [30] calculated the solar irradiance passing through vertically inhomogeneous turbid atmospheres. Shettle [31], Unsworth et al. [32] and Kubo [33] examined the effect of smog composition on the transfer of solar radiation. And Twomey [34] examined the effect of cloud drops on the absorption of solar radiation by atmospheric dust.

2.3 Photochemical Oxidation of Sulfur Dioxide in Air

2.3.1 Mechanism of Reactions

Sulfur dioxide, SO_2, absorbs solar radiation whose wavelength is between 2900 and 4000 Å, with the maximum absorption probably occuring between 2900 and 3000 Å, and molecules are excited electronically. That is, the initial step is $SO_2 + h\nu \longrightarrow SO_2^*$ when light is absorbed by SO_2. According to Johnston and Dev Jain [35],

in about 99% of the cases SO_2 absorbes near-ultraviolet radiation to form the excited singlet electronic state.

Some of these excited SO_2 molecules may be deactivated by collision with other molecules. Remains of the excited molecules react chemically in order to form sulfur trioxide, SO_3. (In the absence of oxygen, sulfur and SO_3 are formed [36,37].) A number of studies on the mechanisms of primary photochemical processes [38] and/or of quenching reaction [39,40] of the first excited singlet and triplet state of SO_2 have been performed, and the rate constant [39,41-46] and the quantum yield [47] of these reactions were estimated. Although estimations of quantum yield of SO_2 to SO_3 were also made [48-50], quantitative knowledge of these oxidation processes are still unsatisfactory.

By irradiation of SO_2 in the atmosphere where the oxygen concentration is high in comparison with SO_2, O_3 and SO_3, the following reactions are likely to occur [37,51];

$$SO_2 + h\nu \longrightarrow SO_2^* \qquad (2.1)$$

$$SO_2^* + O_2 \longrightarrow SO_4 \qquad (2.2)$$

$$SO_4 + O_2 \longrightarrow SO_3 + O_3 \qquad (2.3)$$

$$SO_3 + H_2O \longrightarrow H_2SO_4 \ . \qquad (2.4)$$

Later, Blacet [52] supplemented Reaction (2.3) by the following reaction;

$$SO_4 + SO_2 \longrightarrow 2\ SO_3 \ . \qquad (2.5)$$

Another possible over-all reaction is

$$SO_2 + O_3 + h\nu \longrightarrow SO_3 + O_2 \ . \qquad (2.6)$$

Reaction (2.6), however, is negligible in the atmosphere [37].

Recently Vohra et al. [53] proposed a following mechanism of conversion of SO_2 to sulfuric acid aerosols; The singlet excited state of molecular oxygen can oxidize SO_2 molecule by the reaction

$$SO_2 + O_2^* \longrightarrow SO_4 \quad , \tag{2.7}$$

and SO_4 reacts with water as follows;

$$SO_4 + H_2O \longrightarrow HSO_4 + OH \tag{2.8}$$

HSO_4 can further react with water forming H_2SO_4.

A large number of studies on the photochemical reaction rate of SO_2 to SO_3 or to sulfuric acid aerosols has been made, and it was found that the formation rate of SO_3 or sulfuric acid aerosols was first order with respect to SO_2 [36,51]. Then the over-all reaction of SO_2 to SO_3 is presented by

$$-\frac{d(SO_2)}{dt} = \frac{d(SO_3)}{dt} = k\ (SO_2)$$

$$= \Phi\ k_a\ (SO_2) \tag{2.9}$$

where, k = observed reaction rate constant relative to SO_2 concentration,

k_a = specific absorption rate constant, and

Φ = over-all quantum yield.

The values of k for the photochemical reaction of SO_2 have been determined under various conditions as mentioned later.

2.3.2 Photochemical Reaction of Sulfur Dioxide

A large number of investigations have been performed to explain the mechanism of photochemical reaction of SO_2 and to obtain the reaction rate with artificial light or natural sunlight.

Hall [36] found that the formation rate of SO_3 is directly proportional to the SO_2 concentration and is roughly independent of the oxygen concentration, and derived the rate law expressed by Eq.(2.9). He also obtained the first-order rate constant, k, being 5×10^{-4} hr^{-1} (8×10^{-6} min^{-1}) for natural daytime sunlight.

Gerhard and Johnstone [51] also found that the photochemical oxidation of sulfur dioxide is first order with respect to the sulfur dioxide concentration. The oxidation rate is unaffected by the humidity in the range from 30 to 90% r.h., by the presence or absence of salt nuclei or by the concentration of NO_2 in the range studied. The reaction rate for an artificial sunlight and natural sunlight is in the order of 0.68% hr^{-1} (10^{-4} min^{-1}) and 0.1% hr^{-1} (2×10^{-5} min^{-1}), respectively.

Renzetti and Doyle [54] estimated the specific absorption rate, k_a, of sulfur dioxide for a mercury arc radiation used in the experiment to be 0.013 min^{-1}. The average rate of photochemical reaction of sulfur dioxide is 0.0045 min^{-1}. These data give the quantum yield for sulfur dioxide to be 0.3. If the same quantum yield of 0.3 is assumed for natural sunlight, the photochemical reaction rate is 0.04 min^{-1} in the lower atmosphere.

Urone et al. [55] obtained the value in the order of 0.1% hr^{-1} (1.7×10^{-5} min^{-1}) for k of SO_2 in clean air in the presence of water vapor up to 100% r.h. A photon flux of irradiation source used is 5.39×10^{15} photons/sec/cm^2, about seven times the intensity of noonday sunlight.

According to Wilson and Levy [56], the reaction rate of sulfur dioxide in pure air is strongly dependent on water vapor concentration, as well as the result obtained by Shirai et al. [57].

Katz and Gale [58] verified that the photochemical reaction of dilute sulfur dioxide in air follows the first order reversible mechanism that approaches equilibrium at about 50% conversion of

sulfur dioxide to sulfur trioxide or to sulfuric acid. They also found that the conversion rate increases from about $4.7 \times 10^{-5} min^{-1}$ in dry air to about 1.7×10^{-4} min^{-1} in moist air at 50% r.h., and that it increases significantly with the increasing light intensity and with the presence of NO_2.

Cox and Penkett [59] investigated the photochemical reaction of SO_2 at low concentrations in air using natural sunlight. The determination of reaction rate from the aerosol measurement gives up to 0.65% hr^{-1} (1.1×10^{-4} min^{-1}), and values at least as high as this may be expected in the atmosphere. These values are considerably higher than the widely accepted value of 0.1% hr^{-1} (1.7×10^{-5} min^{-1}). It is suggested that participation in the photochemical reaction of trace impurities in the ambient air may contribute to such a high value.

Matteson [60] investigated corona discharge oxidation of sulfur dioxide instead of photochemical oxidation. Residence times, humidity, and oxygen and sulfur dioxide concentrations were varied to study the kinetics of the conversion of sulfur dioxide to acid mist. They reported that the reaction was zeroth order with respect to sulfur dioxide in the range tested.

The rate constant of photochemical reaction of sulfur dioxide in air was estimated by a number of other investigators. In Table 2-1, the results of studies on photochemical oxidation of sulfur dioxide in the presence of oxygen, or in clean air are summarized. The reaction rates of sulfur dioxide obtained by these investigators differ by several order of magnitude. However, since the experimental conditions, such as reactants, reactant concentration, kind of irradiation sources, type of reaction chambers, and relative humidity used by each investigator differ, it is difficult to interpret or to compare with these values.

Table 2-1. Summary of photochemical oxidation of SO_2

Workers	Ref.	Reaction rate (min^{-1})	Experimental condition				Remarks
			r.h.	irradiation	reac. cham.	SO_2 conc.	
Hall	36	8×10^{-6}	0	natural sunlight	quartz tube	SO_2=56 - 230 mmHg	initial conc. of O_2 =5 - 20 mmHg
Gerhard, Johnstone	51	10^{-4} 1.7×10^{-5}	32 - 91	GE sunlamp Type RS 275 natural sunlight	lucite cell	SO_2=5 - 30 ppm in air	reaction rate was unaffected by r.h., visibility not significant
Renzetti, Doyle	54	4.5×10^{-3}	50	GE H400 - H1 medium press. mercury arc lamp	pyrex flask	SO_2=0.2 - 0.6 ppm	k_a=0.013 min^{-1} by sulfur dioxide
Shirai, et al.	57	3.4×10^{-3} at low r.h. - 1.1×10^{-1} at high r.h.	0.007 - 70.7 mg / l (water in air)	low press. mercury lamp		SO_2=50 - 550 ppm	reaction rate increase remarkably with increasing water vapor in air
Urone, et al.	55	10^{-4}	50	intermediate press. u.v. lamp	borosilicate glass	SO_2=8 - 25 ppm	reaction rate was unaffected by r.h. $k = 1.7 \times 10^{-5}$ min^{-1} equivalent noonday sunlight
Wilson, Levy	56		0 - 65	black fluo-rescent light GE F40BL	pyrex jar	SO_2=0.05-0.75 ppm	reaction rate strongly depend on water vapor concentration
Quon, et al.	61	3.3×10^{-3}	13 - 77	GE black light F 20 T12-BLB	Saran bag	SO_2=0.20-0.65 ppm	
Katz, Gale	58	4.7×10^{-5} in dry air 1.7×10^{-4} in 50%r.h.	0 - 50	u.v. light 3200 - 4000 Å	borosilicate glass	SO_2=3.2 - 6.6 ppm	reaction rate increase with increasing light intensity and relative humidity
Cox, Penkett	59	1.1×10^{-4}	64	natural sunlight	aluminium perspex sheet	SO_2=0.1 - 0.5 ppm	from aerosol measure-ment
Allen	49	5.8×10^{-5}		super-press. mercury arc lamp	quartz cell	SO_2=19 - 100 torr	
Clark	62	0.63 - 1.7×10^{-4}		flourescent u.v. lamp	Teflon bag	SO_2=.049-2.88 ppm	value of k is for equivalent noonday sunlight

2.4 Photochemical Reaction in the System of Sulfur Dioxide and Other Substances

2.4.1 Mechanism of Reactions

A few researches on the mechanism of photochemical reaction of SO_2 in the system existing other chemicals such as hydrocarbons and nitrogen oxides have been reported. But, not only the chemical nature of the products, but also the mechanism of reaction of SO_2 in the NO_x - hydrocarbon photolises are known unsufficiently. Badcock et al. [63] and Sidebottom et al. [43] investigated the photochemical reaction mechanism of SO_2 - hydrocarbon mixtures and estimated the triplet sulfur dioxide ($^3SO_2$) quenching rate constants for the paraffin and aromatic hydrocarbons, respectively.

Daiton and Ivin [64,65] studied the photochemical formation of sulfuric acid from SO_2 with hydrocarbons, both paraffins and olefins, They [64] suggested that the over-all reaction $RH + SO_2 \longrightarrow R{\cdot}SO{\cdot}OH$, where RH is an olefin or paraffin, occurs with a quantum yield of about 10^{-2} in the presence of u.v. light, and olefins were less active than paraffins. They [65] also suggested that excitation of SO_2 molecules is followed by competitive processes: 1) addition to hydrocarbon, 2) quenching by hydrocarbon, and 3) internal deactivation. And they showed the possible steps of the mechanisms of both the uninhibited n-butane reaction and 1-butene reaction.

The schemata of several photochemical reaction processes which may occur in SO_2, NO and hydrocarbon mixtures were proposed by Renzetti and Doyle [54] and that in SO_2 and saturated hydrocarbon mixtures by Penzhorn et al. [66] and Ogata et al. [67].

2.4.2 Photochemical Reaction in Homogeneous Mixtures

Studies on the photochemical reaction in homogeneous (gas-phase) mixtures are divided into two groups. One of them is on

the effect of other substances, such as hydrocarbons and nitrogen oxides, than SO_2 in homogeneous mixture on the aerosol formation and the photochemical oxidation rate of SO_2 to SO_3, and the other is on the effect of SO_2 on the photochemical aerosol formation in homogeneous mixtures.

(1) Effect of other substances on the aerosol formation and photochemical reaction rate of SO_2

Renzetti and Doyle [54] examined the effect of hydrocarbon and NO_x on the aerosol formation by photo-oxidation of SO_2. In the separate presence of NO_x or hydrocarbon, although the aerosol formation is hindered by NO, the presence of NO_2 can enhance the oxidation of SO_2. The addition of olefins has a strong suppressive effect on the production of light-scattering aerosol. On the other hand, in the simultaneous presence of NO_x and hydrocarbon called co-photo-oxidation, the aerosol formation and SO_2 photo-oxidation are enhanced by co-photo-oxidation. The olefinic hydrocarbons, however, are the only important aerosol forms in contrast to the paraffinic and aromatic hydrocarbons.

Kopczynski and Altshuller [68] reported that photochemical reaction of SO_2 in the presence of saturated hydrocarbon at the concentrations found in the atmosphere does not contribute significantly to the formation of aerosol in air pollution situations, in comparison with aerosol results from other reactions involving SO_2 in combination with NO and olefins.

Wilson and Levy [56] reported that the rate of decay of SO_2 concentration is greatly increased in the presence of photochemical smog, and then a light-scattering aerosols are produced in both dry and humid systems.

Cox and Penkett [69] found that conversion rate of SO_2, based on the rate of aerosol formation, ranges between 0.04 and 0.06%

hr^{-1} ($0.7 - 1.0 \times 10^{-5}$ min^{-1}) for SO_2 concentration of 0.07 - 0.7 ppm and that it increases markedly when NO and olefinic hydrocarbons are present.

Studies about the effect of addition of substances other than SO_2 on the aerosol formation of sulfuric acid are summarized in Table 2-2. Studies about that on the photochemical reaction rate of SO_2 are simultaneously summarized for reference.

(2) Effect of SO_2 on the photochemical aerosol formation

In the studies on the effect of SO_2 on photochemical reaction or aerosol formation in the homogeneous gas mixtures, Schuck et al. [72] reported that the addition of SO_2 to automobile exhaust - air mixture leads to the dramatic increase in the rate of aerosol formation. Prager et al. [73] studied the reactions of hydrocarbon and NO_2 with or without SO_2. In photochemical NO_2 - olefin reaction, only highly substituted or cyclic olefins and diolefins form aerosol particles. But when SO_2 is added, all types of olefins produce particulates. And the present of SO_2 enhanced aerosol formation in a handredfold to thousandfold. They concluded that aerosol particles are produced by reaction of SO_2 with an intermediate in the NO_2 - olefin photolysis. Also Stevenson et al. [74] found that the addition of SO_2 into air mixtures containing NO_2 and unsaturated hydrocarbon increases extremely aerosol production.

Jaffe and Klein [75] studied the photolysis of NO_2 in the presence of SO_2 at the wavelength of 3660 Å. Since SO_2 does not absorb light at 3660 Å, no excited sulfur dioxide is formed. And SO_2 reacts with atomic oxygen produced by photo-dissociation of NO_2 to form SO_3. A second order rate constant for $SO_2 + O \longrightarrow SO_3^*$ is $(1.1 \pm 0.1) \times 10^9$ l/mole/sec.

Wilson and Levy [56] studied the effect of the SO_2 and water vapor concentration in the 1-butene - NO_x - SO_2 system. The presence

Table 2-2. Summary of photochemical reaction in homogeneous mixtures

1. Effect of the addition of other substances than SO_2 on the photochemical reaction rate of SO_2 and aerosol formation of sulfuric acid

Workers	Ref.	System				Effect[b]	Remarks
		SO_2	NO_2	NO_x	HC[a]		
Gerhard, Johnstone	51	*	*			A 0	
Haagen-Smit	70	*	*		*	A -	
Renzetti, Doyle	54	*		*		B -	NO_x = NO
		*			*	B -	HC = butadiene or pentene-1
		*	*			B +	
		*		*	*	B +	HC = olefinic HC
		*		*	*	B 0	HC = paraffinic & aromatic HC
Kopczynski, et al.	68	*			*	B 0	HC = saturated HC
		*		*	*	B +	HC = olefinic HC
Harkins, Nicksic	71	*			*	A +	
Urone, et al.	55	*	*		*	A +	HC = sat., unsaturated HC water vapor had no effect (except 100% r.h. where +)
Katz, Gale	58	*	*			A +	
		*			*	A -	HC = olefinic HC
		*	*		*	A -	HC = olefinic HC
Wilson, Levy	56	*		*	*	A,B +	HC = 1-butene
Cox, Penkett	69	*		*	*	A,B +	HC = olefinic HC, NO_x = NO
Friend, et al.	47	*	+ NH_3			B +	

a : HC = hydrocarbon

b : Effect 0 = addition of other substances than SO_2 had no effect on the reaction rate of SO_2 (A) and on the aerosol formation of sulfuric acid (B).

\- = addition of the other substances than SO_2 enhanced the reaction rate of SO_2 (A) and on the aerosol formation of sulfuric acid (B).

\+ = addition of the other substances than SO_2 inhibited the reaction rate of SO_2 (A) and on the aerosol formation of sulfuric acid (B).

of SO_2 results to a general slowing down of the photochemical smog reactions. The maximum concentration of oxidant produced by the photochemical smog reactions is significantly influenced by the SO_2 concentration added and relative humidity. Wilson et al. [76] also studied the influence of SO_2 on photochemical smog reaction sequence in several diverse system of SO_2 - NO_2 - hydrocarbons (olefin, paraffin, aromatic or olefin - aromatic) mixtures, and found that the effects of SO_2 on oxidant production depends on the concentrations of water vapor, and initial NO_2 and SO_2 concentrations.

Cox and Penkett [77] found that large amounts of aerosol are produced when SO_2 is added to the O_3 - olefin mixture, and calculated the rate of aerosol formation for various kinds of olefin.

In Table 2-3, studies on the effect of addition of sulfur dioxide on photochemical aerosol formation in homogeneous mixtures are summarized. But we can not assert a systematical tendency of the effect of sulfur dioxide on photochemical aerosol formation from those results.

2.4.3 Photochemical Reaction in Heterogeneous Mixtures

Although a few studies on the photochemical reaction in heterogeneous (gas phase containing initially particulate matters) mixtures containing SO_2 have been investigated, studies on the photochemical reaction and on the interaction of SO_2 with solid particles are just beginning.

Gerhard and Johnstone [51] reported that the presence of sodium chloride nuclei has no effect on the reaction rate of SO_2 to sulfuric acid aerosols.

Goetz and Pueschel [78] studied the effects of SO_2, humidity, and order of mixing of reactants on the photochemical production of aerosol particles from 1-octen and NO_2 in air. In the absence of reaction centers, namely homogeneous mixture, the aerosol formation rate is strongly influenced by the SO_2 fractional concentration

Table 2-3. Summary of photochemical reaction in homogeneous mixtures

II. Effect of addition of SO_2 on the photochemical aerosol formation in homogeneous mixtues

Workers	Ref.	System				Effect[b]	Remarks
		SO_2	NO_2	NO_x	HC[a]		
Schuck, et al.	72	*	automobile exhaust			+	
Prager, et al.	73	*	*		*	+	HC = olefinic HC
Stevenson, et al.	74	*	*		*	+	HC = unsaturated HC
Harkins, Nicksic	71	*			*	+	HC = exhaust gas from fuel
Goetz, Pueschel	78	*	*		*	-	as low SO_2 concentration ($SO_2 / NO_2 = 10^{-2}$)
						-	as high SO_2 concentration ($SO_2 / NO_2 = 1$)
						+	and at high r.h.
							and at low r.h.
Altshuller, et al.	79	*		*	*	0	rate of consumption of NO_x and propylene
						+	sulfate levels with increasing SO_2 concentration
							HC = propylene
Wilson, Levy	56	*		*	*	-	photochemical smog reaction (inhibiting effect for NO to NO_2) in dry system
						0	in moist system
							HC = 1-butene
Wilson, et al.	76	*	*		*	-	oxidation production, but
						+	if HC = toluene
Cox, Penkett	77	*			*	+	SO_2 / olefinic HC / O_3 system

a : HC = hydrocarbon

b : Effect 0 = addition of SO_2 had no effect on photochemical aerosol formation in homogeneous mixtures.

- = addition of SO_2 enhanced photochemical aerosol formation in homogeneous mixtures.

+ = addition of SO_2 inhibited photochemical aerosol formation in homogeneous mixtures.

and relative humidity. And the presence of reaction centers, namely heterogeneous mixture, supplied by nebulizing highly diluted aqueous suspensions of polystylene latex particles (diameter = 0.36 μm) does not alter the effect of initial reduction by SO_2, nor the strong influence of humidity.

Urone et al. [55] found the photochemical reaction rate of SO_2 to be 0.1% hr^{-1} in equivalent noonday sunlight. In the presence of saturated and unsaturated hydrocarbon, and of NO_2, but of no particulates (homogeneous mixture), it becomes faster and is 1 to 3% hr^{-1}. The heterogeneous reaction rates of SO_2 with powdered oxides such as iron and aluminum are several orders of magnitude greater than the homogeneous reaction rates of SO_2. However, as particulates are inert solids such as sodium chloride and calcium carbonate, the difference between heterogeneous and homogeneous reaction is small.

Johnstone and Moll [80] and Kimura et al. [81] studied the rate of sulfuric acid formation from SO_2 in the atmosphere without u.v. irradiation. According to their results, the particulate matters lead to significant production of sulfuric acid mist. But when only sodium chloride particles are present, no significant sulfuric acid formation is observed.

In Table 2-4, the studies on photochemical reaction in heterogeneous mixtures are summarized. In those studies, it is verified that the presence of particulate matters enhances generally the sulfuric acid formation in heterogeneous mixtures containing SO_2, other gaseous contaminants and particulate matters, but the presence of NaCl, $CaCO_3$ particulates has no effect.

2.4.4 Reactions of Sulfur Dioxide in Ambient Air

Katz [82] suggested from a field measurement of the concentrations of SO_2 and total sulfur contaminants in a nickel-smelter area that the reaction, of SO_2 to SO_3 and to sulfuric acid aerosols,

Table 2-4. Summary of photochemical reaction in heterogeneous mixtures

Workers	Gerhard et al.	Goetz & Pueschel	Urone, et al.	Johnstone & Moll	Kimura, et al.
Ref.	51	78	55	80	81
Studies on	effect of particulate on sulfuric acid formation	effect of SO_2 on aerosol formation in heterogeneous mixture	effect of particulate on photochemical reaction of SO_2	effect of paticulate on the sulfuric acid formation	effect of particulate on the sulfuric acid formation
Particulate used	NaCl	polystylene latex particles (d = 0.36 μm)	powdered oxides of Al, Ca, Cr, Fe, Pb and V; NaCl; $CaCO_3$	$MnSO_4$, $FeSO_4$ NaCl	carbon particulate
System	SO_2, particulate	SO_2, hydrocarbon, NO_2, particulate	SO_2, particulate	SO_2, particulate	SO_2, NO_2, particulate
r.h.(%)	32 - 91	15 - 70	50	77 - 96	
Results	presence of NaCl had no effect (0) on sulfuric acid formation	presence of SO_2 1) at low SO_2 conc., reduced aerosol formation (-) especially, high r.h., 2) with increasing SO_2 concentration, inhibitory effect reversed	powdered oxide of Al, Ca, Cr, Fe, Pb and V enhanced heterogeneous reaction rate of SO_2 (+), $CaCO_3$, NaCl = 0	presence of $FeSO_4$ and $MnSO_4$ enhanced aerosol formation (+), NaCl = 0	particulate promoted sulfuric acid formation (+)
Remarks				no irradiation	no irradiation

In Table, 0 means what there was no effect on the reaction rate and aerosol formation.

\+ means the effect that the reaction rate and aerosol formation is enhanced.

\- means the effect that the reaction rate and aerosol formation is inhibited.

is catalyzed by sunlight and fine dust particles, especially by minute metallic oxide particles found in smelter smoke. These sulfur components, especially sulfuric acid aerosol, give rise to a tremendous number of condensation nuclei in the air.

According to Shirai et al. [57], the rate of disappearance of SO_2 in mine smelter area obtained in a field experiment is 1.95 x 10^{-3} sec^{-1} (0.12 min^{-1}). The value of 0.12 min^{-1} is quite higher than the values reported by other investigators. One factor probably contributing to this high rate is an amount of light intensity in a shorter range than 3300 Å of solar radiation.

From measurement of SO_2 and sulfuric acid aerosol concentration in Los Angeles, Thomas [83] found that when the base of the inversion ceiling and wind speeds are low and oxidants are high, the oxidation of SO_2 to sulfuric acid is maximal, and also found that percentage oxidation of SO_2 decreases with the increasing SO_2 concentration.

Gartrell et al. [22] reported that the atmospheric photooxidation rate of SO_2 varies from 0.0003 to 0.018 min^{-1} and then moisture in ambient air is the main factor causing the increase in oxidation rate.

The results of studies on the photochemical reaction of sulfur dioxide in ambient atmosphere are summarized in Table 2-5.

2.5 Aerosol Formation from Photochemical Reaction of SO_2

According to Urone and Schorender [10], Roddy [84] studied the formation of condensation nuclei in city air by irradiation with u.v. light of greater than 2900 Å wavelength. Nuclei production is proportional to the ambient SO_2 concentration. No nuclei is produced when the SO_2 concentration is less than 0.02 ppm. Many nuclei are formed when air containing SO_2 is filtered through either cotton, wool or millipore filter.

Table 2-5. Summary of photochemical oxidation in atmosphere

Investigators	Katz	Shirai, et al.	Thomas	Gartrell, et al.
Reference	82	57	83	22
Location	nickel - smelter area (Sudburg, Canada)	mine smelter area (Zaoh, Japan)	Los Angeles	near large coal-burning power plant
Results of concentration measurements	SO_2/total sulfur contaminants = 82 - 87 %	SO_2/total sulfur oxides = 3 - 36 %	sulfuric acid / total sulfur = 5 - 20 %	
Reaction rate (min^{-1})	3.5×10^{-4} oxidation rate of SO_2 to SO_3 was catalyzed by sunlight and fine dust particles, especially minute metallic oxide	0.12	decreased with the increase of concentration of sulfur dioxide	0.0003 at low r.h. to 0.018 at high r.h. oxidation rate increased with increasing moisture

Quon et al. [61] investigated the particle formation from the photo-oxidation of SO_2. They found that particle concentration is proportional to the third power of irradiation time for a given SO_2 concentration and proportional to the third power of the SO_2 concentration for a given irradiation time. They also found that the number concentration of particles formed is greater at high humidity than at low humidity. At the condition of 0.65 ppm of SO_2 and 50% r.h., nuclei concentration ranges from 10^6 cm^{-3} for an irradiation time of 30 seconds to 3×10^6 cm^{-3} for an irradiation time of 3 minutes. They showed that a slope of log-log plots of nuclei concentration versus irradiation time or SO_2 concentration indicates a number of molecules in an embryo or particle, denoted by i. And they found the value of i to be 3 to 5 in their experimental conditions and does not depend on relative humidity strongly.

Clark [62], Cox and Penkett [59], Renzetti and Doyle [54] and Bricard et al. [85] observed the variation of particle number concentration of aerosols with time of irradiation. From those observation, it is found that after some period from the onset of irradiation during which no aerosol is detected, the particle number concentration of aerosols formed by photochemical reaction of SO_2 increases rapidly, reaches a maximum value, and then decays uniformly by coagulation. According to Clark, the maximum number concentration attained is in general greater for condition with higher volumetric conversion rates and ranges from 4.9×10^4 for 0.0491 ppm of SO_2 to 1.2×10^6 cm^{-3} for 1.94 ppm of SO_2.

Cox [86] measured the particle number concentration and the mass of the sulfuric acid aerosols, which formed photochemically in the u.v. photolysis of wide range of SO_2 concentration (5 - 625 ppm) in pure nitrogen and in nitrogen - oxygen mixtures. Particle formation is remarkably dependent on relative humidity and SO_2 concentration.

Harkins and Nicksic [71] investigated the effect of relative humidity and temperature on SO_2 - induced aerosol. There is an inverse correlation between relative humidity and SO_2 - induced aerosols, and an inverse correlation also exists between chamber temperature and aerosol formation.

Wilson et al. [87] investigated the effect of stirring rate on aerosol formation in the photochemical smog. Aerosol formation is decreased by stirring, and the faster the chamber contents are stirred, the greater the reduction in aerosol formation is observed. The differences in aerosol formation between stirred and nonstirred chamber operation were dependent on the type of system being studied and on the stirring rate.

Cox and Penkett [88] suggested that although $SO_2 - O_3$ gas mixture does not form aerosols at appreciable rate, the presence of olefins results in the formation of a large number of aerosols ($> 10^6$ cm^{-3}) without irradiation. Vohra [89] also suggested that there is no formation of aerosols between SO_2 and water without irradiation. On the other hand, Cox and Penkett [59] and Bricard et al. [85] suggested that aerosol particles are formed in the dark when SO_2 is added in air and that this phenomenon is thought to be due to the interaction of SO_2 with trace impurities in air.

The results of studies on formation and evolution of aerosol particles (particle number concentration change with time) and the physical properties of photochemically formed aerosols will be discussed in the following section, and are summarized in Table 2-6.

2.6 Properties of Particles Formed by Photochemical Reaction

Studies on properties of aerosol particles formed by photochemical reaction are classified into two groups. The first group

Table 2-6. Summary of physical properties of photochemical particles

Investigators	Ref.	System					Properties of particle radius, r and light-scattering	Properties of particle concentration, N
		SO_2	NO_2	NO_x	HC[a]	PM[b]		
Gerhard, Johnstone	51	*					particle size distribution = log-normal function having radius 0.1 to 0.2 μm, and σ_g = 1.1 to 1.3	N = 0.19×10^6 to 0.47×10^6 cm^{-3}
Renzetti, Doyle	54	*					if SO_2 consumption > .05 ppm light-scattering ∝ r^2 if SO_2 consumption < .05 ppm light scattering ∝ (r^2 r^6) sulfuric acid content = 1.24×10^{-15} g/particle light-scattering decrease as r.h. decrease	variation of N with time
Endow, Doyle, Jones	90	*	*		*		law dr^2/dt = constant	
Stevenson, et al.	74	*	*		*		average radius = 0.15 μm (HC = trans-2-butene)	
Harkins, Nicksic	71	*	fuel exhaust gas					effect of temperature and r.h. on SO_2 induced aerosol
Wilson, et al.	87	*		*	*			effect of stirring rate on aerosol formation
Cox, Penkett	59	*					mass mean radius = 0.0035 μm (11 min irradi'n) 0.01 μm (100 min irradi'n)	variation of N with time
Quon, et al.	61	*					radius of photochemical oxidation products = 0.0005 μm (5Å)	relation between N, and initial SO_2 concentration and irradiation time
Bricard, et al.	85	*	*					aerosol formation is different with order of mixing
		*		+NH_3			addition of NH_3 lead to rapidly increase of radius r = 0.003 to 0.012 μm	variation of N with time
Clark	62	*					particle size distribution log-normal function having σ_g = 1.2 to 1.8 volume mean radius ∝ volumetric conversion rate	variation of N with time
Friend, et al.	47	*		+NH_3			addition compound of NH_3 and SO_2 enhance photochemical aerosol formation and follow to rapid growing of aerosols	
Cox	86	*		in N_2			radius = 0.0012 - 0.01 μm	relations between N, and r.h. and SO_2 concentration
Kimura, et al.	81	*	*		*		radius = 0.1 to few μm	
		(no irradiation)						
Matteson, et al.	60	*					radius = 3.18 μm	
		(corona discharge oxidation)						

a : HC means hydrocarbons
b : PM means particulate matters

is the study on identification of aerosol particles formed, and the second is the study on physical and chemical properties of aerosol particles formed by photochemical reaction of sulfur dioxide.

2.6.1 Identification of Photochemical Aerosol Particles

Johnston and Dev Jain [35] examined aerosols, which formed by photochemical reaction in the SO_2 - n-butane - O_2 (air) system, by means of Tyndall beam of light. Light aerosols were formed with SO_2 and butane or with SO_2 and air, and heavy aerosols were formed only when all these components were present. Chemical and elemental analysis for the liquid aerosol formed showed that the liquid has pH less than 2 and was an average empirical formula of $C_2H_5SO_5$.

Endow et al. [90] examined the properties, such as absorption spectra, particle size distribution and elemental composition, of the aerosols derived from photochemical reaction of the gas mixtures of SO_2 - NO_2 - olefin hydrocarbon. The evidence from infrared spectra of aerosols formed indicated that the principal constituent of the aerosol is sulfuric acid. In addition to sulfuric acid, aerosols contain a smaller concentration of nitrate type material.

Harkins and Nicksic [71] used a radio-tracer technique to test a hypothesis that SO_2 could produce nuclei for the growth of organic aerosols. Although SO_2 consistently causes the formation of aerosols, those aerosols do not contain any organic compounds. Those experiments showed that SO_2 does not provide condensation nuclei for organic aerosol particles. This result is consistent with Doyle's study [91] in which the aerosol is shown to be predominantly sulfuric acid.

Altshuller et al. [79] concluded that since sulfuric acid aerosol can be formed without any significant change in the yield of the other products associated with the photo-oxidation, the aerosol formed from photo-oxidation of the propylene - NO_x - SO_2

system at higher relative humidity are sulfuric acid aerosol.

Cox and Penkett [88] also found that sulfur containing aerosol formed in SO_2 - O_3 - olefin mixtures is sulfuric acid.

In Table 2-7, the results of studies on the identification of aerosol particles formed by photochemical reaction are summarized. Those studies verified the principal constituent of aerosols formed by photochemical reaction in the gas mixtures containing sulfur dioxide, nitrogen oxide and hydrocarbons is sulfuric acid.

2.6.2 Physical Properties of Photochemical Aerosol Particles

The determination of particle size, particle size distribution and light scattering properties of photochemical aerosols have been performed in the both systems of only SO_2 in air and of gas mixtures of SO_2, NO_x and hydrocarbons etc.

For the determination of those properties of photochemical aerosol particles in the SO_2 - air system, Gerhard and Johnstone [51] suggested that the particle size distribution of sulfuric acid aerosols produced by photo-oxidation of SO_2 might be represented by a log-normal distribution function. They reported that since the geometric standard deviation is usually 1.1 to 1.3, the aerosols are rather homogeneous, and that the particle size of sulfuric acid aerosols produced photochemically is very small, varying from 0.2 to 0.4 μm in diameter.

Renzetti and Doyle [54] investigated the light scattering properties of particles formed by photo-oxidation of SO_2 by an aerosol counter photometer. They also measured the particle size distribution of aerosols larger than 0.25 μm diameter and reported that a considerable number of optically significant particles are present. In a separate experiment, both light scattering concentration and condensation nuclei are followed as a function of irradiation time, and a great number of particles appear immedeately and then decay to an intermediate value while the light

Table 2-7. Summary of identification of photochemical particles

Workers	Ref.	System					Aerosol particles identified	Remarks
		SO_2	NO_2	NO_x	HC[a]	PM[b]		
Johnston, Dev Jain	35	* * *			 * *		light aerosol light aerosol heavy aerosol	in air HC = n-butane in air liquid products : empirical formula = $C_2H_5SO_5$, and pH < 2
Endow, Doyle, Jones	90	*	*		*		sulfuric acid	HC = olefin
Harkins, Nicksic	71	* + fuel exhaust gas					SO_2 causes formation of aerosols	aerosol did not contain any organic compounds
Doyle, Jones	91	*			*		sulfuric acid	HC = ethylene
Altshuller, et al.	79	*		*	*		sulfuric acid	HC = propylene
Kimura, et al.	81	*	*			*	sulfuric acid	no irradiation

a : HC means hydrocarbons.

b : PM means particulate matters.

scattering increases steadily. They also reported that a sulfuric acid content is 1.24×10^{-15} g per particle and that particle diameter, d, becomes approximately $(\overline{d^3})^{1/3} = 0.16$ μm.

Beside, the particle size of aerosols formed by photochemical oxidation of SO_2 was measured using diffusion method by Quon et al. [61], and Cox [86] (SO_2 in N_2) who obtained the particle diameter to lie in the order of 0.001 μm and in the range from 0.0025 to 0.02 μm, respectively.

Clark [62] investigated in detail the particle size distribution of aerosols produced photochemically in SO_2 - air system using Whitby Aerosol Analyzer. As the aerosol grows by condensation and coagulation, the approximately log-normal size distributions shift to larger sizes and spread over an increasingly greater range of sizes. The geometric standard deviation of the volume distribution ranges from 1.2 to 1.8. The volume mean diameter is found to increase linearly at a rate which correlated strongly with the volumetric conversion rate. From the calculation of the volume concentration, it is found to increase linearly with time indicating a steady condensation of material from the vapor to the condensed phase. Volumetric conversion rate ranges from 0.389 to 22.9 $\mu m^3/cm^3/hr$.

According to Matteson et al. [60], a mean diameter of particles formed by corona discharge oxidation of sulfur dioxide was 6.36 μm.

For the particle size distribution of photochemical aerosols in the system of gas mixture of SO_2 - (NO_x and hydrocarbon) etc., Renzetti and Doyle [54] showed the particle size distribution of aerosols formed by photolysis of gas mixtures of methylbutene, NO and SO_2 both in dry and in humid air. They noted that as the humidity decreases, light scattering decreases and the particle size distribution changes, and the standard deviation of the distribution in dry air is larger than that in humid air.

Endow et al. [90] determined the particle size distribution of aerosols, of which principal constituent is sulfuric acid, formed by photo-oxidation of olefin - NO_2 - SO_2 mixtures. They verified a theoretical assumption that the particle size distribution from a stirred-flow reactor of diffusion controlled growth would obey the law dr^2/dt = constant, where r is the radius of an aerosol particle, suggested by Schuck et al. [92].

Stevenson et al. [74] measured the particle size of photochemical aerosol formed in the unsaturated hydrocarbon - NO_2 - SO_2 system. The average size of aerosols is in the range of 0.3 - 0.5 μm. The size of aerosol particle, however, depends upon the conditions of the experiment.

Bricard et al. [85] found that the addition of NH_3 to air nucleated by SO_2 leads to the brisk reduction in the particle number concentration from 10^5 to 2×10^4 cm^{-3} and the increase in their diameter from 0.006 to 0.024 μm.

According to Cox and Penkett [88], SO_2 and O_3 do not react at an appreciable rate, but in the presence of olefins a rapid oxidation of SO_2 occurs and forms a large number of particles which subsequently coagulate to form a droplet aerosol of fairly uniform size of about 0.1 μm diameter. Also Friend et al. [47] suggested that the addition of NH_3 in SO_2 - air mixtures enhances photochemical aerosol formation and follows rapid growing of aerosols.

According to Kimura et al. [81], electron-micrograph of the particulate matter, sulfuric acid mist, produced by the reaction of SO_2 and NO_2 without irradiation showed that the particles are sphere and particle diameters are ranged from 0.2 to several microns.

2.7 Theoretical Studies on Aerosol Formation

The theory of the condensation of supersaturated vapor into

liquid and of nucleation by chemical interaction in the gas phase such as sulfuric acid mist from SO_3 and water vapor has received much attention recently.

2.7.1 Homogeneous nucleation

The classical theory of homogeneous nucleation (phase transition in one component systems) was developed by Volmer, Becker and Döring, Zeldovich, and Frenkel (the references are given in Reiss's study [93]). In these theories, two basic assumptions were used : 1) it is an equilibrium rate theory, and 2) the equilibrium concentration of embryos is obtained by assuming that the free energy of cluster is equal to the bulk free energy plus the free energy due to the embryo surface [94]. The classical nucleation theory has been accepted as correct on the basis of experimental nucleation rate studies by Katz and Ostermier [95], Jaeger et al. [96], Dawson et al. [97], and Katz [98].

On the oter nand, Frenkel [99] and Kuhrt [100] pointed out that the translation and rotation of the droplet contribute to the free energy (thermodynamic properties) of embryo formation, and Lothe and Pound [101] discussed first quantitatively rotational and translational contributions. They concluded that numerical nucleation rates increase by 10^{17} as compared to that of the classical theory. In some systems, the experimental results showed that the nucleation rate agreed with Lothe and Pound's predictions [97].

Reiss et al. [102] have criticized this " translation and rotation paradox" and proposed a new model. The calculation for the nucleation rate by this model decreases the pre-exponential factor of Lothe and Pound by $10^{-10} - 10^{-12}$. Reiss [103] has also improved the nucleation theory by using a new treatment of the partition function.

Burton [104] examined the difference between the classical

theory and the exact results which was obtained using the exact thermodynamic properties, and found that the ratio of homogeneous vapor phase nucleation rates in exact results to those by classical theory varies from 10^{-2} to 10^{7} and depends strongly on temperature and supersaturation.

2.7.2 Nucleation in Binary Homogeneous System

The kinetic model of phase transition in two component system, such as sulfuric acid mist from SO_3 and water vapor, has been first presented by Reiss [93]. In this theory, the nucleation rate I from a binary vapor system is given by an equation of the form,

$$I = C \exp (-\Delta G / \kappa T) \quad , \tag{2.10}$$

where, ΔG is the free energy of formation of embryo consisting of two reactant gas molecules, κ is the Boltzmann's constant, T is the absolute temperature, and C is a frequency factor meaning the probability of capture of molecule of vapor by the critical embryo. The evaluation of C can only be accomplished by means of a kinetic approach and Reiss [93] and Kiang et al. [105] evaluated C for such systems.

The quasi-thermodynamic approach was tried to Reiss theory by Doyle [106], and the free energy of formation of an embryo was given by Eq.(6.2). Doyle calculated the self-nucleation rate for the sulfuric acid and water system for typical case of 50% relative humidity at 25°C, and concluded that rapid nucleation would take place at sulfuric acid partial pressures in the range $10^{-8} - 10^{-10}$ mmHg. He pointed out the problem that the considerable uncertainty is principally due to lack of data on the partial pressure of sulfuric acid above its aqueous solutions.

Kiang et al. [105, 107] calculated the nucleation rate of embryo from a binary mixtures of $H_2SO_4 - H_2O$ and $HNO_3 - H_2O$ in air as

functions of relative humidities up to 99 per cent. Mirabel and Katz [108] also calculated the nucleation rate of liquid aerosols from the gaseous mixtures of $H_2SO_4 - H_2O$ and $HNO_3 - H_2O$ at 25°C for various relative humidities (10 to 100%) and various activities of acid vapor. They calculated simultaneously the growth curves for $H_2SO_4 + H_2O$ droplets (radius versus composition of droplet) at various relative humidities from the critical size radius up to a 0.1 μm radius. And they showed the limitations of the binary homogeneous nucleation theory.

Heist and Reiss [109] calculated the free energy surfaces required to form a droplet from sulfuric acid - water vapor for various relative humidities up to 300% and H_2SO_4 vapor concentrations, and displayed these surfaces as three dimensional perspective plots. They suggested from the results of calculation that virtually all the H_2SO_4 present exists in hydrate form, and that hydrate formation can exert an appreciable effect on the processes of vapor phase nucleation in $H_2SO_4 - H_2O$ mixtures and must be considered in any theory of nucleation rate.

Hirschfelder [110] developed the Reiss's kinetic model of homogeneous nucleation in a system containing two components to many component systems.

Walter [111] and Stauffer et al. [112] calculated the growing process of aqueous droplets formed by heteromolecular nucleation. Walter calculated the changes of concentration and size distribution of condensation aerosols with time when there is a constant rate of production of primary particles of uniform size. And the model is extended to include the production of particles of two different size. Stauffer et al. calculated the growth of sulfuric acid droplets originating from the binary homogeneous system of sulfuric acid and water vapor. The particle growth and the final particle size were calculated as functions of relative humidity.

The studies on the nucleation theory has been reviewed by Kiang et al. [94] and Stauffer et al. [113].

References

[1] Haagen-Smit, A. J. (1963) : Photochemistry and Smog, J. Air Poll. Contr. Assoc., Vol.13, pp.444-446, 454.

[2] Junge, C. (1963) : Air chemistry and radioactivity, Academic Press, New York.

[3] Thomas, M. D. (1964) : Review of recent studies of sulfur oxides as air pollutants, J. Air Poll. Contr. Assoc., Vol.14, pp.517-520.

[4] Stern, A. C. (1968) : Air pollution, Vol.I, II and III, Academic Press, New York.

[5] Cadle, R. D. and Allen, E. R. (1970) : Atmospheric photochemistry, Science, Vol.167, pp.243-249.

[6] Leighton, P. A. (1961) : Photochemistry of air pollution, Academic Press, New York.

[7] Altshuller, A. P. and Bufalini, J. J. (1965) : Photochemical aspects of air pollution : A review, Photochem. Photobiol., Vol.4, pp.97-146.

[8] Altshuller, A. P. and Bufalini, J. J. (1971) : Photochemical aspects of air pollution : A review, Environ. Sci. Tech., Vol.5, pp.39-64.

[9] Wagman, J. (1966) : Current problems in atmospheric aerosol research, Int. J. Air Water Poll., Vol.10, pp.777-782.

[10] Urone, P. and Schroeder, W. H. (1969) : SO_2 in the atmosphere: A wealth of monitoring data, but few reaction rate studies, Environ. Sci. Tech., Vol.3, pp.436-445.

[11] Bufalini, M. (1971) : Oxidation of sulfur dioxide in polluted atmosphere - A review, Environ. Sci. Tech., Vol.5, pp.685-700.

[12] Kasahara, M. and Takahashi, K. (1971) : Aerosol formation from photochemical oxidation of sulfur dioxide (review in Japanese), Kogai to Taisaku (J. Environ. Poll. Contr.), Vol.7, pp.997-1001 & 1151-1160.

[13] U.S. Department of Health, Education, and Welfare (1969) : Air quality criteria for sulfur oxides, NAPCA No.AP-50.

[14] U.S. Department of Health, Education, and Welfare (1969) : Control techniques for sulfur oxide air pollutants, NAPCA No.AP-52.

[15] American Chemical Society (1969) : Cleaning our environment, American Chemical Society.

[16] Administration of Japan (every year) : Kankyo hakusho and Kogai hakusho (White papers on environmental Pollution).

[17] Oshio, T. (1968) : Air pollution problems in Japan (in Japanese), Kogai to Taisaku (J. Environ. Poll. Contr.), Vol. 4, pp.197-208.

[18] Oshio, T. (1968) : Air pollution problems in Japan (in Japanese), ibid., Vol.4, pp.547-556.

[19] Ministry of Health and Welfare (1971) : Air pollution by SO_2 in Japan (in Japanese), ibid., Vol.7, pp.117-122.

[20] Fujiwara, M. (1971) : Status of air pollution by sulfur dioxide in Japan (in Japanese), ibid., Vol.7, pp.325-332.

[21] Rohrman, F. A. and Ludwig, J. H. (1965) : Sources of sulfur dioxide pollution, Chem. Eng. Progr., Vol.61, pp.59-63.

[22] Gartrell, F. E., Thomas, F. W. and Carpenter, S. B. (1963) : Atmospheric oxidation of SO_2 in coal-burning power plant plumes, Amer. Ind. Hyg. Assoc. J., Vol.24, pp.113-120.

[23] Kasahara, M. and Takahashi, K. (1973) : Ultraviolet irradiation on photochemical reaction of air pollutants (in Japanese), Taikiosen Kenkyu (J. Japan Soc. Air Poll.), Vol.8, pp.645-653.

[24] Toyo Rika Instruments (1971) : Solar energy (in Japanese), Technical News, No.61 1971-6.

[25] Tsuruta, H. (1973) : Attenuation of solar u.v. radiation by lower atmosphere (in Japanese), Taikiosen Kenkyu (J. Japan Soc. Air Poll.), Vol.8, pp.303.

[26] Okita, T. (1972) : Measurements of u.v. radiation in the atmosphere (in Japanese), Special Report for Analysis of Photochemical Smog, pp.8-35.

[27] Kankyo-cho, private communication.

[28] Volz, F. E. (1970) : Spectral skylight and solar radiance measurements in the caribbean, maritime aerosols and Sahara dust, J. Atmos. Sci., Vol.27, pp.1041-1047.

[29] Chisaka, F., Yanagisawa, S. and Shimada, I. (1974) : U.V. energy distribution in MEL smog chamber (in Japanese), Taikiosen Kenkyu (J. Japan Soc. Air Poll.), Vol.9, pp.152.

[30] Shettle, E. P. and Weinman, J. A. (1970) : The transfer of solar irradiance through inhomogeneous turbid atmospheres evaluated by Eddington's approximation, J. Atmos. Sci., Vol.27, pp.1048-1055.

[31] Shettle, E. P. (1972) : The transfer of near ultraviolet irradiances through smog over Los Angeles, Atmos. Environ., Vol.6, pp.165-180.

[32] Unsworth, M. H. and Monteith, J. L. (1972) : Aerosol and solar radiation in Britain, Quart. J. Roy. Met. Soc., Vol.98, pp. 778-797.

[33] Kubo, T. (1973) : Solar radiation and air pollution (in Japanese), Kankyo Gijutsu (Environ. Conservation Eng.), Vol.2, pp.396-398.

[34] Twomey, S. (1972) : The effect of cloud scattering on the absorption of solar radiation by atmospheric dust, J. Atmos. Sci., Vol.29, pp.1156-1159.

[35] Johnston, H. S. and Dev Jain, K. (1960) : Sulfur dioxide sensitized photochemical oxidation of hydrocarbons, Science, Vol.131, pp.1523-1524.

[36] Hall, T. C. (1953) : Photochemical studies of nitrogen dioxide and sulfur dioxide, Ph.D. Thesis, Univ. of California at Los Angeles.

[37] Blacet, F. E. (1952) : Photochemistry in the lower atmosphere, Ind. Eng. Chem., Vol.44, pp.1339-1342.

[38] Rao, T. N., Collier, S. S. and Calvert, J. G. (1969) : Primary photophysical processes in the photochemistry of sulfur dioxide at 2875 Å, Amer. Chem. Soc. J., Vol.91, pp.1609-1615.

[39] Rao, T. N., Collier, S. S. and Calvert, J. G. (1969) : The quenching reactions of the first excited singlet and triplet states of sulfur dioxide with oxygen and carbon dioxide, Amer. Chem. Soc. J., Vol.91, pp.1616-1621.

[40] Brand, J. C. D., Lauro, C. and Jones, V. T. (1970) : Structure of the $^3B_1$ state of sulfur dioxide, J. Amer. Chem. Soc., Vol.92, pp.6095-6096.

[41] Collier, S. S., Morikawa, A., Slater, D. H. and Calvert, J. G. (1970) : The lifetime and quenching rate constant for the lowest triplet state of sulfur dioxide, J. Amer. Chem. Soc., Vol.92, pp.217-218.

[42] Sidebottom, H. W., Badcock, C. C., Calvert, J. G., Reinhardt, G. W., Rabe, B. R. and Damon, E. K. (1971) : A study of the decay processes in the triplet sulfur dioxide molecule excited at 3828.8 Å, J. Amer. Chem. Soc., Vol.93, pp.2587-2593.

[43] Sidebottom, H. W., Badcock, C. C., Calvert, J. G., Rabe, B. R. and Damon, E. K. (1971) : Mechanism of the photolysis of mixtures of sulfur dioxide with olefin and aromatic hydrocarbons, J. Amer. Chem. Soc., Vol.93, pp.3121-3128.

[44] Jackson, G. E. and Calvert, J. G. (1971) : The triplet sulfur dioxide - carbon monoxide reaction excited within the SO_2 ($^1A_1$) $\longrightarrow$ ($^3B_1$) "forbidden" band, J. Amer. Chem. Soc., Vol. 93, pp.2593-2599.

[45] Otsuka, K. and Calvert, J. G. (1971) : Decay mechanism of triplet sulfur dioxide molecules formed by intersystem crossing in the flash photolysis of sulfur dioxide (2400 - 3200 Å), J. Amer. Chem. Soc., Vol.93, pp.2581-2587.

[46] Sidebottom, H. W., Badcock, C. C., Jackson, G. E., Calvert, J. G., Reinhardt, G. W. and Damon, E. K. (1972) : Photo-oxidation of sulfur dioxide, Environ. Sci. Tech., Vol.6, pp.72-79.

[47] Friend, J. P., Leifer, R. and Trichon, M. (1973) : On the formation of stratospheric aerosols, J. Atmos. Sci., Vol. 30, pp.465-479.

[48] Sethi, D. S. (1971) : Photo-oxidation of sulfur dioxide, J. Air Poll. Contr. Assoc., Vol.21, pp.418-420.

[49] Allen, E. R., McQuigg, R. D. and Cadle, R. D. (1972) : The photooxidation of gaseous sulfur dioxide in air, Chemosphere, Vol.1, pp.25-32.

[50] Cox, R. A. (1972) : Quantum yields for the photooxidation of sulfur dioxide in the first allowed absorption region, J. Phys. Chem., Vol.76, pp.814-820.

[51] Gerhard, E. R. and Johnstone, H. F. (1955) : Photochemical oxidation of sulfur dioxide in air, Ind. Eng. Chem., Vol.47, pp.972-976.

[52] Blacet, F. E., Private communication to Leighton, P. A.

[53] Vohra, K. G., Nair, P. V. N. and Muraleedharan, T. S. (1972) : Possible role of singlet oxygen in an ion-induced reaction mechanism of nucleus formation by sulfur dioxide, Aerosol Sci., Vol.3, pp.225-236.

[54] Renzetti, N. A. and Doyle, G. J. (1960) : Photochemical aerosol formation in sulfur dioxide - hydrocarbon systems, Int. J. Air Poll., Vol.2, pp.327-345.

[55] Urone, P., Lutsep, H., Noyes, C. M. and Parcher, J. F. (1968) : Static studies of sulfur dioxide reactions in air, Environ. Sci. Tech., Vol.2, pp.611-618.

[56] Wilson, Jr. W. E. and Levy, A. (1970) : A study of sulfur dioxide in photochemical smog, I. Effect of SO_2 and water vapor concentration in the 1-butene/NO_x/SO_2 system, J. Air Poll. Contr. Assoc., Vol.20, pp.385-390.

[57] Shirai, T., Hamada, S., Takahashi, H., Ozawa, M., Ohmuro, T. and Kawakami, T. (1962) : Photo-oxidation of sulfur dioxide in air (in Japanese), Kogyo-kagaku Zasshi, Vol.65, pp.1906-1911.

[58] Katz, M. and Gale, S. B. (1970) : Mechanism of photooxidation of sulfur dioxide in atmosphere, 2nd Int. Clean Air Congress, Washington, D. C., CP1E pp.336-343.

[59] Cox, R. A. and Penkett, S. A. (1970) : The photo-oxidation of sulfur dioxide in sunlight, Atmos. Environ., Vol.4, pp.425-433.

[60] Matteson, M. J., Stringer, H. L. and Busbee, W. L. (1972) : Corona discharge oxidation of sulfur dioxide, Environ. Sci. Tech., Vol.6, pp.895-901.

[61] Quon, J. E., Siegel, R. P. and Hulburt, H. M. (1970) : Particle formation from photolysis of sulfur dioxide in air, 2nd Int. Clean Air Congress, Washington, D. C., CP1D pp.330-335.

[62] Clark, W. E. (1972) : Measurements of aerosol produced by the photochemical oxidation of SO_2 in air, Ph.D. Thesis, Univ. Minnesota.

[63] Badcock, C. C., Sidebottom, H. W., Calvert, J. G., Reinhardt, G. W. and Damon, E. K. (1971) : Mechanism of the photolysis of sulfur dioxide - paraffin hydrocarbon mixtures, J. Amer. Chem. Soc., Vol.93, pp.3115-3121.

[64] Daiton, F. S. and Ivin, K. J. (1950) : The photochemical formation of sulphinic acids from sulphur dioxide and hydrocarbons, Trans. Faraday Soc., Vol.46, pp.374-381.

[65] Daiton, F. S. and Ivin, K. J. (1950) : The kinetics of the photochemical gas phase reactions between sulphur oxide and n-butane and 1-butene respectively, ibid., Vol.46, pp.382-394.

[66] Penzhorn, R, D., Stieglitz, L, Filby, W. G. and Günther, K. (1973) : A combined MS - GC study of the photoreaction of SO_2 with hydrocarbons, Chemosphere, No.3, pp.111-118.

[67] Ogata, G., Izawa, Y. and Tsuda, T. (1956) : The photochemical sulphoxidation of n-hexane, Tetrahedron, Vol.21, pp.1349-1356.

[68] Kopczynskii, S. L. and Altshuller, A. P. (1962) : Photochemical reaction of hydrocarbons with sulfur dioxide, J. Air and Water Poll., Vol.6, pp.133-135,

[69] Cox, R. A. and Penkett S. A. (1971) : Photo-oxidation of atmospheric SO_2, Nature, Vol.229, pp.486-488.

[70] Haagen-Smit, A. J. (1956) : Atmospheric reactions of air pollutants, Ind. Eng. Chem., Vol.48, pp.65A-66A, 68A, 70A.

[71] Harkins, J. and Nicksic, S. W. (1965) : Studies of the role of sulfur dioxide in visibility reduction, J. Air Poll. Contr. Assoc., Vol.15, pp.218-221.

[72] Schuck, E. A., Ford, H. W. and Stephens, E. R. (1958) : Air pollution effects of irradiated automobile exhaust as related to fuel composition, Rept. No.26, Air Poll. Foundation.

[73] Prager, M. J., Stephens, E. R. and Scott, W. E. (1960) : Aerosol formation from gaseous air pollutants, Ind. Eng. Chem., Vol.52, pp.521-524.

[74] Stevenson, H. J. R., Sanderson, D. E. and Altshuller, A. P. (1965) : Formation of photochemical aerosols, Int. J. Air and Water Poll., Vol.9, pp.367-375.

[75] Jaffe, S. and Klein, F. S. (1966) : Photolysis of NO_2 in the presence of SO_2 at 3660 Å, Trans. Faraday Soc., Vol.62, pp.2150- 2157.

[76] Wilson, Jr. W. E., Levy, A. and Wimmer, D. B. (1972) : A study of sulfur dioxide in photochemical smog, II. Effect of sulfur dioxide on oxidant formation in photochemical smog, J. Air Poll. Contr. Assoc., Vol.22, pp.27-32.

[77] Cox, R. A. and Penkett, S. A. (1971) : Oxidation of atmospheric SO_2 by Products of the ozone - olefin reaction, Nature, Vol. 230, pp.321-322.

[78] Goetz, A. and Pueschel, R. (1967) : Basic mechanisms of photochemical aerosol formation, Atmos. Environ., Vol.1, pp.287-306.

[79] Altshuller, A. P., Kopczynski, S. L., Lonneman, W. A., Becker, T. L. and Wilson, D. L. (1968) : Photooxidation of propylene with nitrogen oxide in the presence of sulfur dioxide, Environ. Sci. Tech., Vol.2, pp.696-698.

[80] Johnstone, H. F. and Moll, A. J. (1960) : Formation of sulfuric acid in fogs, Ind. Eng. Chem., Vol.52, pp.861-863.

[81] Kimura, K., Tada, O., Kimotsuki, K. and Nakaaki, K. (1965) : On the generation of sulfuric acid mist from sulfur dioxide in the atmospheric air (in Japanese), J. Sci. Labour, Vol.41, pp.501-511.

[82] Katz, M. (1950) : Photoelectric determination of atmospheric sulfur dioxide, Anal. Chem., Vol.22, pp.1040-1047.

[83] Thomas, M. D. (1962) : Sulfur dioxide, sulfuric acid aerosol and visibility in Los Angeles, Int. J. Air and Water Poll., Vol.6, pp.443-454.

[84] Roddy, A. F. (1967) : The formation of condensation nuclei in city air by ultraviolet radiation of wavelength greater than 2900 Å, Ph.D. Thesis, Univ. of Edinburgh, Scotland.

[85] Bricard, J., Cabane, M., Madelaine, G. and Vigla, D. (1972) : Formation and properties of neutral ultrafine particles and small ions conditioned by gaseous impurities of the air, J. Colloid Interface Sci., Vol.39, pp.42-58.

[86] Cox, R. A. (1973) : Some experimental observations of aerosol formation in the photo-oxidation of sulfur dioxide, Aerosol Sci., Vol.4, pp.473-483.

[87] Wilson, Jr. W. E., Merryman, E. L., Levy, A. and Taliaferro, H. R. (1971) : Aerosol formation in photochemical smog, I. Effect of stirring, J. Air Poll. Contr. Assoc., Vol.21, pp. 128-132.

[88] Cox, R. A. and Penkett, S. A. (1972) : Aerosol formation from sulfur dioxide in the presence of ozone and olefinic hydrocarbons, Faraday Trans. I, Vol.68, pp.1735-1753.

[89] Vohra, K. G. and Nair, P. V. N. (1970) : Recent thinking on the chemical formation of aerosols in the air by gas phase reactions, Aerosol Sci., Vol.1, pp.127-133.

[90] Endow, N., Doyle, G. J. and Jones, J. L. (1963) : The nature of some model photochemical aerosol, J. Air Poll. Contr. Assoc., Vol.13, pp.141-147.

[91] Doyle, G. J. and Jones, J. L. (1963) : Automobil exhaust-gas aerosols, J. Air Poll. Contr. Assoc., Vol.13, pp.365-367.

[92] Schuck, E. A., Doyle, G. J. and Endow, N. (1960) : A progress report on the photochemistry of polluted atmospheres, Stanford Research Inst., prepared for Air Poll. Foundation, San Marino, Cal., and U.S. Public Health Service, Washington, D.C., by Stanford Research Inst.

[93] Reiss, H. (1950) : The kinetics of phase transitions in binary systems, J. Chem. Phys., Vol.18, pp.840-848.

[94] Kiang, C. S., Stauffer, D., Walker, G. H., Puri, O. P., Wise, Jr. J. D. and Patterson, E. M. (1971) : A reexamination of homogeneous nucleation theory, J. Atmos. Sci., Vol.28, pp. 1222-1232.

[95] Katz, J. L. and Ostermier, B. J. (1967) : Diffusion cloud-chamber investigation of homogeneous nucleation, J. Chem. Phys., Vol.47, pp.478-487.

[96] Jaeger, H. L., Wilson, E. J. and Hill, P. G. (1969) : Nucleation of supersaturated vapors in nozzles. I. H_2O and NH_3, J. Chem. Phys., Vol.51, pp.5380-5388.

[97] Dawson, D. B., Wilson, E. J., Hill, P. G. and Russell, K. C. (1969) : Nucleation of supersaturated vapors in Nozzles. II. C_6H_6, $CHCl_3$, CCl_3F, and C_2H_5OH, J. Chem. Phys., Vol.51, pp. 5389-5397.

[98] Katz, J. L. (1970) : Condensation of a supersaturated vapor. I. The homogeneous nucleation of the n-alkanes, J. Chem. Phys., Vol.52, pp.4733-4748.

[99] Frenkel, J. (1939) : A general theory of heterophase fluctuations and pretransition phenomena, J. Chem. Phys., Vol.7, pp.538-547.

[100] Kuhrt, F. (1952) : Troepfchen Modell (uebersaettigter) realer Gase, Z. Phys., Vol.131, pp.185-204, 205-214.

[101] Lothe, J. and Pound, G. M. (1962) : Reconsiderations of nucleation theory, J. Chem. Phys., Vol.36, pp.2080-2086.

[102] Reiss, H., Katz, J. L. and Cohen, E. R. (1968) : Translation rotation paradox in the theory of nucleation theory, J. Chem. Phys., Vol.48, pp.5553-5560.

[103] Reiss, H. (1970) : Treatment of droplike clusters by means of the classical phase integral in nucleation theory, J. Statist. Phys., Vol.2, pp.83-104.

[104] Burton, J. J. (1973) : On the validity of homogeneous nucleation theory, Acta Metallurgica, Vol.21, pp.1225-1232.

[105] Kiang, C. S. and Stauffer, D. (1973) : Chemical nucleation theory for various humidities and pollutants, Preprint for the Faraday Symposium of the Chemical Society.

[106] Doyle, G. J. (1961) : Self-nucleation in the sulfuric acid-water system, J. Chem. Phys., Vol.35, pp.795-799.

[107] Kiang, C. S., Stauffer, D., Mohnen, V. A., Bricard, J. and Vigla, D. (1973) : Heteromolecular nucleation theory applied to gas-to-particle conversion, Atmos. Environ., Vol.7, pp. 1279-1283.

[108] Mirabel, P. and Katz, J. L. (1974) : Binary homogeneous nucleation as a mechanism for the formation of aerosols, J. Chem. Phys., Vol.60, pp.1138-1144.

[109] Heist, R. H. and Reiss, H. (1974) : Hydrates in supersaturated binary sulfuric acid - water vapor, J. Chem. Phys., Vol.21, pp.573-581.

[110] Hirschfelder, J. O. (1974) : Kinetics of homogeneous nucleation on many-component systems, J. Chem. Phys., Vol.61, pp.2690-2694.

[111] Walter, H. (1973) : Coagulation and size distribution of condensation aerosols, Aerosol Sci., Vol.4, pp.1-15.

[112] Stauffer, D., Mohnen, V. A. and Kiang, C. S. (1973) : Heteromolecular condensation theory applied to particle growth, Aerosol Sci., Vol.4, pp.461-471.

[113] Stauffer, D., Walker, G. H., Brown, G. R., Wise, Jr. J. D. and Kiang, C. S. (1974) : Nucleation literature review 1972, Aerosol Sci., Vol.5, pp.157-173.

Chapter 3

3. Ultraviolet and Photochemical Reaction of Air Pollutants

3.1 Introduction

Photochemical smog which is injurious to the human life is formed by receiving solar radiation in the atmosphere. Therefore, it is desirable that the investigation on photochemical reaction is performed under natural sunlight in the atmosphere. There are, however, many technical difficulties in such a investigation. Because the reaction must be influenced by environmental factors in the atmosphere, such as chemical compounds, degree of humidity, temperature, intensity of solar radiation and so on, which change momentarily. In this study, as well as many other investigations, smog chamber tests have been performed using an artificial light. The experimental result obtained by smog chamber test is finally required to be converted into the case of reaction under the natural sunlight in the atmosphere. Or at least, the effective intensity of the artificial light for substances in question should be estimated and compared with that of the natural sunlight.

For this purpose, the following examinations are considered to be useful; to analyze composition of wavelength of light which is effective in photochemical reaction; to evaluate specific absorption rate constant of both the sunlight and the artificial light by the absorbing substances in question. In this chapter, the following subjects were treated to obtain the basic data which are essential to these examinations;

1) Calculation of the ultraviolet intensity of solar radiation at the earth's surface for various values of environmental factors which have effect on the transmittance of the sunlight,

2) Measurement of the direct and scattered ultraviolet intensities

of solar radiation,

3) Proposition of estimation of specific absorption rate constant of the artificial radiation in the system used in the experimental studies of photochemical reaction,

4) Calculation of specific absorption rate constant of solar radiation by sulfur dioxide.

3.2 Solar Irradiance in the Lower Atmosphere [1]

In the problem with respect to photochemical reaction of air pollutants, solar spectral light intensity is one of the most important factors as well as the amount of radiation. The photochemically active wavelength of light is invisible and near ultraviolet regions of the solar spectrum. Spectral light intensity outside the atmosphere, denoted by $I_{o\lambda}$ hereafter, in these regions has been obtained by a number of investigators [2,3]. Spectral light intensity curve shown by a dotted line in Fig.3-2 is taken from Johnson's data [4], and it was used as the values of $I_{o\lambda}$ in this study. Where the value of $I_{o\lambda}$ is averaged solar spectral light intensity over band width $\Delta\lambda$ Å centered at the wavelength λ per unit cross section, and the unit of $I_{o\lambda}$ is such as (m watt/cm$^2\Delta\lambda$) or (photons/cm^{2}sec $\Delta\lambda$).

3.2.1 Absorption and Scattering of Solar Radiation in Atmosphere

Solar radiation is weakened by absorption and scattering during the pass through the atmospheric air. And in the lower atmosphere, 50 per cent of the total radiation lies in the visible region, and less than 5 per cent is in the ultraviolet. Solar intensity received in the lower atmosphere depends on a number of factors, such as time of day, time of year, latitude, elevation above sea level, atmospheric turbidity and thickness of the ozone layer. A common denominator for the first four factors is the air mass m and it means the ratio of the length of path of the direct solar radiation through the

atmosphere relative to the vertical path length of atmosphere. For a solar zenith angle z less than 60°, m is approximately proportional to secant z. At larger zenith angles, corrections are necessary for near the horizontal factors such as the curvature of the atmosphere and the refraction. The relation between m and z is shown graphicall in Fig.3-1. The solar zenith angle for any specific location and any time can be calculated by substituting the latitude of location (lat), the local hour angle (lha) and declination angle (dla) to the following equation [5].

$$\cos z = \cos(\text{lat}) \times \cos(\text{lha}) \times \cos(\text{dla}) + \sin(\text{lat}) \times \sin(\text{dla}) \qquad (3.1)$$

Fig.3-1 shows the solar zenith angle calculated for various times of the day throughout the year in Kyoto (N 35°, E 136°).

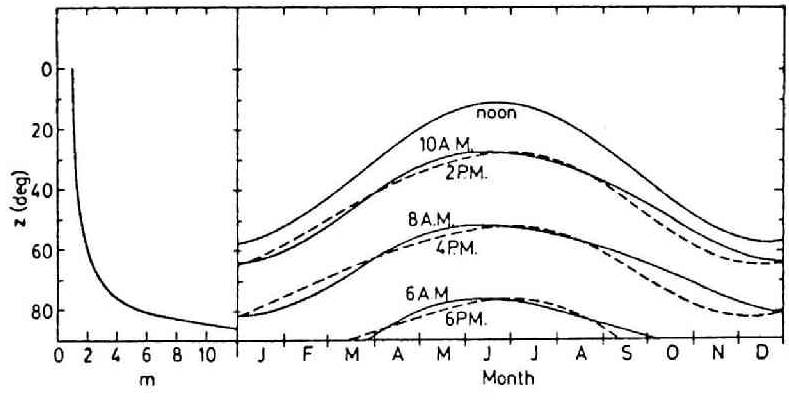

Fig.3-1. Solar zenith angle z in Kyoto, and relation between z and air mass m.

Several factors such as molecular scattering, particulate diffusion and absorption are considered to contribute to the attenuation of solar irradiance in the atmosphere. Where particulate diffusion refers to the over-all effects of particulate matters in the

atmosphere on the attenuation of the direct solar radiation. The transmissivities relative to above three factors (T_m, T_p and T_a) are functions of air mass, m, the amount of precipitable water vapor in the atmosphere, W, the amount of dust content in the atmosphere, D and the thickness of equivalent layer of pure ozone, (O_3), and are given, respectively, by the following equations;

$$\log T_{m\lambda} = -4.54 \times 10^{20} \ (\eta_{o\lambda} - 1)^2 \ \lambda^{-4} \ m \tag{3.2}$$

$$\log T_{p\lambda} = -(3.75 \times 10^5 \ \lambda^{-2} \ W + 3.5 \times 10 \ \lambda^{-0.75} D) \ m \tag{3.3}$$

$$\log T_{a\lambda} = -\alpha_g{}'_\lambda \ (O_3) \ m \tag{3.4}$$

where, $\eta_{o\lambda}$ is the index of refraction of air at wavelength λ and at the pressure and temperature chosen, and $\alpha_g{}'_\lambda$ is the absorption coefficient of ozone (base 10).

3.2.2 Direct and Scattered Intensity

The solar irradiance outside the atmosphere $I_{o\lambda}$ is scattered and absorbed in the atmosphere, and then on a cloudless day the direct ($I_{d\lambda}$) and scattered spectral light intensity ($I_{s\lambda}$) per unit horizontal cross section in the lower atmosphere may be expressed by

$$I_{d\lambda} = I_{o\lambda} \ T_{a\lambda} \ T_{m\lambda} \ T_{p\lambda} \cos z \tag{3.5}$$

$$I_{s\lambda} = I_{o\lambda} \ T_{a\lambda} \ (1 - T_{m\lambda} \ T_{p\lambda}) \ g \cos z \tag{3.6}$$

where, g is a fraction determined by the directional distribution of the scattered radiation and by the amount of multiple scattering. And $g = 0.5$ may be adopted as useful approximation for all conditions.

3.2.3 Numerical Calculation and Results

The direct and scattered spectral light intensities which are expressed approximately by Eqs.(3.5) and (3.6) were calculated for $\lambda \leq 8000$ Å. Beside, the sum of spectral light intensities for the wavelength less than 4000 Å is considered as ultraviolet irradiance in this study. The values of parameters, such as z, (O_3), W and D adopted in the numerical calculation were varied within the following ranges, respectively.

a) $z = 0°$ ($m = 1.0$) - $85°$ ($m = 10.4$)

b) $(O_3) = 2.0 - 3.4$ mm

(O_3) is the thickness of equivalent layer of pure ozone in the atmosphere. According to Dobson [7], the amount of ozone increases with latitude and varies with the season, that is, with the maximum in spring and the minimum in fall. For N 35° latitude, (O_3) lies between 2.2 and 2.8 mm.

c) $W = 1.0 - 4.5$ cm

The coefficient W is the thickness of equivalent layer of precipitable water vapor in the atmosphere, measured vertically above the point of observation, and is expressed in cm. The values of W calculated for Kyoto area lie between 1.0 (January) and 4.5 cm (August) with anual average of 2.1 cm [8].

d) $D = 0 - 10$

The coefficient D is a function of dust content in the atmosphere. It is defined here to be the ratio of particle number concentration, d_n, of rather large aerosols (order of 1 μm diameter) in the atmosphere directly above the observation point to the standard number concentration of 800 particles/cm^3, i.e. $D = d_n/800$. The value of D ranges normally from 0 for clean atmosphere to 1 or considerably greater for urban area [2]. However, it is thought that the particle diameter contributing to the particulate diffusion of light is smaller than 1 μm. Take the particle diameter of about

0.1 μm for instance, the light scattering by particulate matters decreases by about 10^{-2} times and the particle number concentration in the atmosphere increases by about 10 times [9], so that the value of D may ranges from 0 to 10.

The distributions of the total (I_λ), direct ($I_{d\lambda}$) and scattered ($I_{s\lambda}$) intensity in the solar spectrum at the earth's surface were calculated for various atmospheric conditions and are illustrated in Figs.3-2a to 3-2d. In those figures, the condition of z=0° (m=1.0), (O_3)=2.4 mm, W=2.0 cm and D=1.0 was chosen as the standard state, and the effects of z, (O_3), W and D on the spectra of the solar radiation are shown, respectively.

From those figures the following deductions may be drawn;

1) The transmitted light intensity at the earth's surface decreases as z increases, and then the ratio of $I_{s\lambda}$ to I_λ increases with the increase of z, namely m, and reaches almost 1 at z=85°,
2) When the value of W and D increase, $I_{d\lambda}$ decreases rapidly and $I_{s\lambda}$ increases, and I_λ, which is the sum of them, decreases slightly,
3) It is due to the increases of absorption and scattering of solar irradiance in the atmosphere that I_λ and $I_{d\lambda}$ decrease and $I_{s\lambda}$ increases as the value of the factors such as z, W and D increases. Absorption and scattering of solar irradiance in the atmosphere is not uniform with respect to the wavelength of light and is strong at the shorter wavelength. Therefore, even as the values of z, W and D are relatively small and then $I_{d\lambda}$ is much greater than $I_{s\lambda}$ at the longer wavelength, $I_{d\lambda}$ is less than $I_{s\lambda}$ at the region of shorter wavelength.

The total (I), direct (I_d) and scattering (I_s) ultraviolet intensities per unit horizontal cross section at the earth's surface were calculated for the various values of (O_3), W and D, and are illustrated as a function of z in Figs.3-3a to 3-3c, respectively.

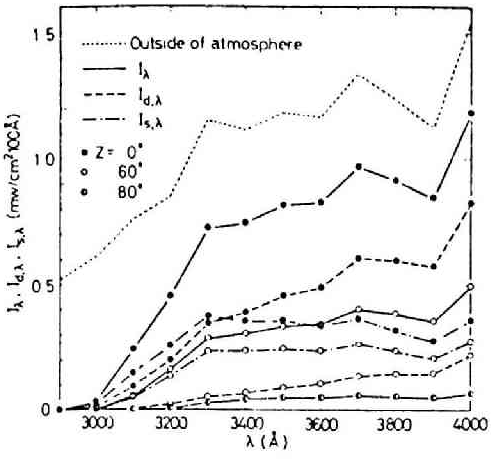

a. For various value of z, at D=1.0, W=2.0 cm and (O_3)=2.4 mm.

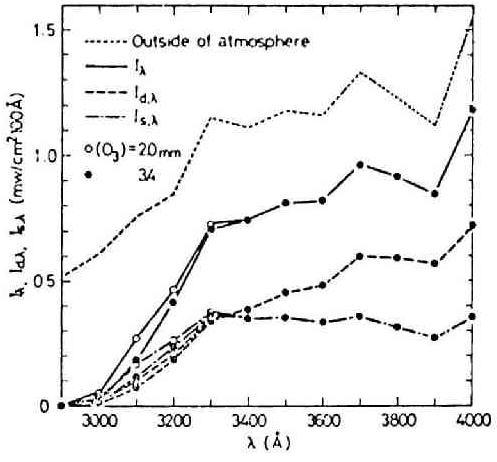

b. For various value of (O_3), at z=0°, D=1.0 and W=2.0 cm.

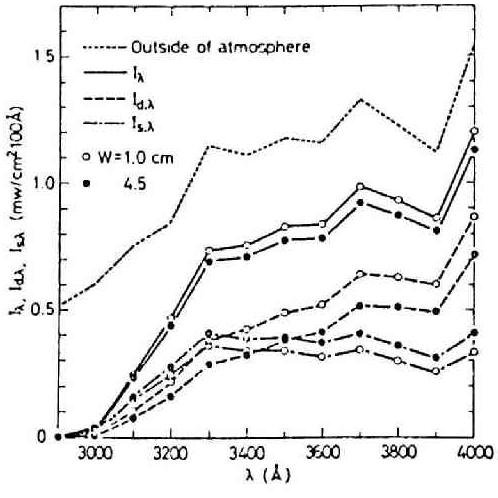

c. For various value of W, at z=0°, D=1.0 and (O_3)=2.4 mm.

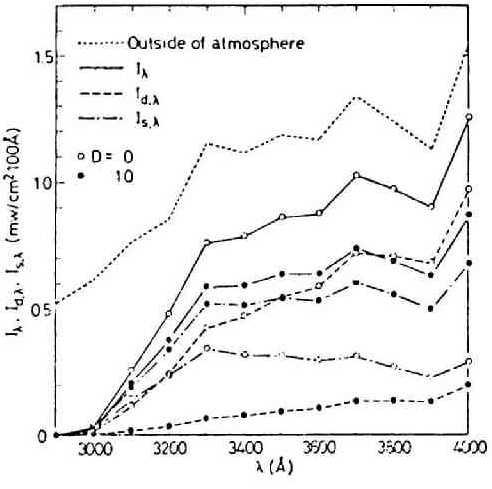

d. For various value of D, at z=0°, W=2.0 cm and (O_3)=2.4 mm.

Fig. 3-2. Total, direct and scattering radiation spectra in the lower atmosphere.

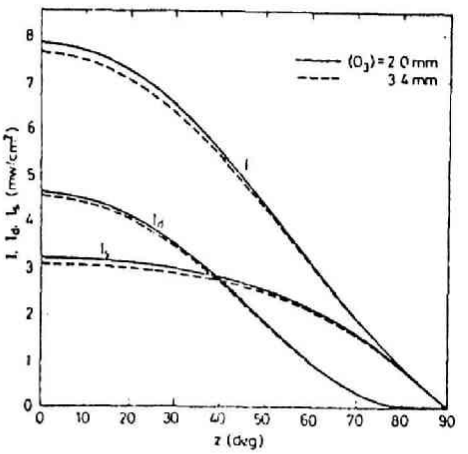

a. For various value of (O_3), at D=1.0 and W=2.0 cm.

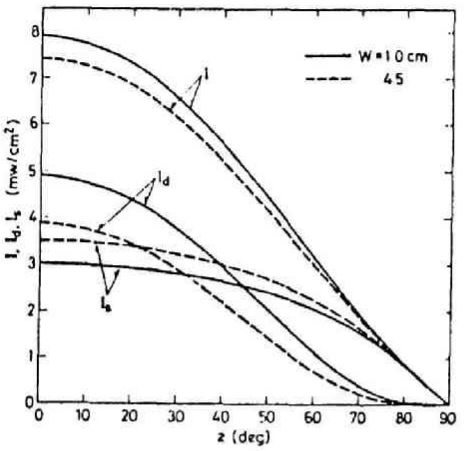

b. For various value of W, at D=1.0 and (O_3)=2.4 mm.

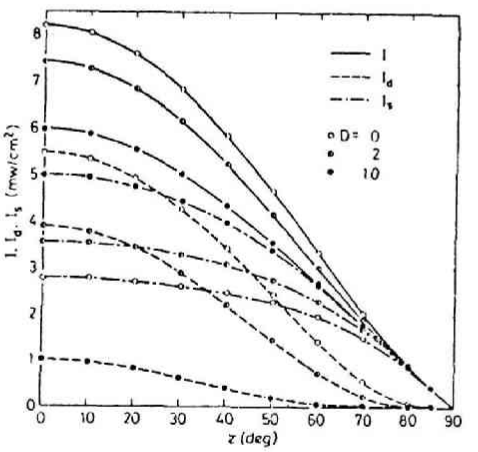

c. For various value of D, at W=2.0 cm and (O_3)=2.4 mm.

Fig. 3-3. Total, direct and scattering ultraviolet radiation in the lower atmosphere.

Where the ultraviolet intensity means one in the region of wavelength less than 4000 Å, that is, $I = \sum_{\lambda \leq 4000} I_\lambda$.

The calculated results are summarized as follows;

1) Existence of dust and water vapor in the atmosphere reduces the direct intensity but increases the scattered intensity. On the other hand, existence of ozone decreases both the direct and scattered intensities because light is absorbed by ozone.

2) In these phenomena, the influence of D is the most severe and that of (O_3) is pretty small within the calculation range of this study.

3.3 Measurement of Ultraviolet Intensity in Solar Radiation

3.3.1 Measurement of Ultraviolet Intensity

The ultraviolet (u.v.) intensity (3000 - 4000 Å) in solar radiation was measured by Toshiba UV meter Type PI - 1 UV installing a collimator of which solid angle ($\Delta\omega$) was 0.0165 steradian. The spectral response curve of the meter is supplied by the manufacturer and shown in Fig.3-4 [10]. The u.v. intensity was measured for θ and ϕ ranging from (-90°) or 0° to 90° and from 0° to 360°, respectively. Where θ is an angle of elevation from horizontal plane and ϕ is an angle from base direction within horizontal plane as shown in Fig.3-5. Measurement interval ($\Delta\theta$,$\Delta\phi$) for θ and ϕ direction was generally taken to be $\Delta\theta$=15° and $\Delta\phi$=30°.

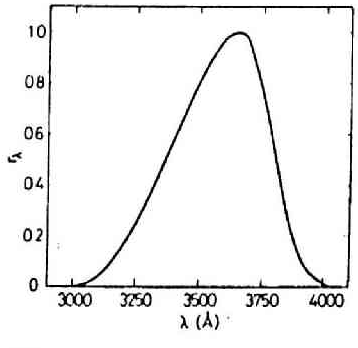

Fig.3-4. Response curve of UV meter.

Let the u.v. intensity per unit cross section which is perpendicular with an axis of direction (θ,ϕ) denote

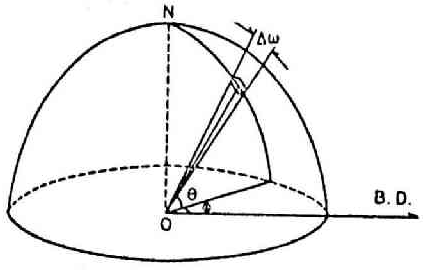

Fig.3-5. Measured direction
θ : angle of elevation from horizontal plane,
φ : angle from base direction (B.D.) within horizontal plane.

by $i(\theta,\phi)$ m watt/cm^2. The u.v. intensity at sun direction, namely at an azimuth angle (θ_o,ϕ_o), is the sum of direct intensity (i_d) and scattered intensity (i_s) in the direction (θ_o,ϕ_o). Therefore, $i(\theta_o,\phi_o) = i_d + i_s(\theta_o,\phi_o)$. When a detector does not receive the direct radiation, the u.v. intensity measured comes from the scattered light only. That is, $i(\theta,\phi) = i_s(\theta,\phi)$. Fig.3-6 shows an example of directional distribution of the scattered intensity measured at the earth's surface.

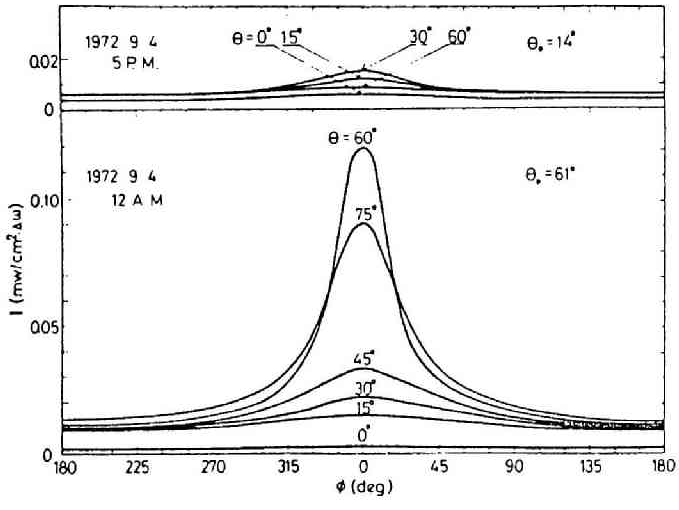

Fig.3-6. Spacial distribution of scattering u.v. radiation.

3.3.2 Analyses of Measured Values

(1) Direct u.v. intensity per unit horizontal cross section

The direct u.v. intensity per unit horizontal cross section ($I_{d,mea}$) is estimated from the measured values by the following equation;

$$I_{d,mea} = [i(\theta_0,\phi_0) - i_s(\theta_0,\phi_0)] \sin\theta_0 \tag{3.7}$$

It is impossible, however, to measure directly $i_s(\theta_0,\phi_0)$. The value of $i_s(\theta_0,\phi_0)$ is approximated with a value obtained by extrapolating to azimuth angle (θ_0,ϕ_0) on the $i_s(\theta,\phi)$ curve as shown in Fig.3-6.

(2) Scattered u.v. intensity per unit horizontal cross section

The scattered u.v. intensity per unit horizontal cross section ($I_{s,mea}$) is estimated by the following equation;

$$I_{s,mea} = \frac{1}{2\,\Delta\omega} \int_0^{2\pi} \int_0^{\pi/2} i_s(\theta,\phi) \sin 2\theta \, d\theta d\phi$$

$$= \frac{1}{2\,\Delta\omega} \sum_{\Delta\theta} \sum_{\Delta\phi} i_s(\theta,\phi) \sin 2\theta \, \Delta\theta\Delta\phi \tag{3.8}$$

3.3.3 Results

The direct and scattered u.v. intensities per unit horizontal cross section can be estimated by Eqs.(3.7) and (3.8) from the measured values of $i(\theta,\phi)$. On the other hand, the theoretical direct and scattered intensity of solar radiation can be calculated by Eqs.(3.5) and (3.6), respectively. Assuming that solar radiation is measured with a UV meter whose spectral response is r_λ, the direct ($I_{d,theo}$) and scattered ($I_{s,theo}$) intensities which must

be observed at the earth's surface are given by,

$$I_{d,theo} = \int I_{o\lambda}\, T_{a\lambda}\, T_{m\lambda}\, T_{p\lambda}\, r_{\lambda} \cos z \, d\lambda \qquad (3.9)$$

$$I_{s,theo} = \int I_{o\lambda}\, T_{a\lambda}\, (1 - T_{m\lambda}\, T_{p\lambda})\, g\, r_{\lambda} \cos z \, d\lambda \qquad (3.10)$$

The direct and scattered u.v. intensities measured in Uji city are plotted as a function of z for the various air polluted levels in Figs.3-7 and 3-8, and the theoretical values of those intensities calculated by Eqs.(3.9) and (3.10) are simultaneously shown by solid lines. The direct u.v. intensities measured coincided with the theoretical values. As for the scattered part, observed values have the same qualitative tendencies with the calculated, but the values are one and half as much as the calculated. It is considered to be due to the method of measurement of $i(\theta,\phi)$ around azimuth

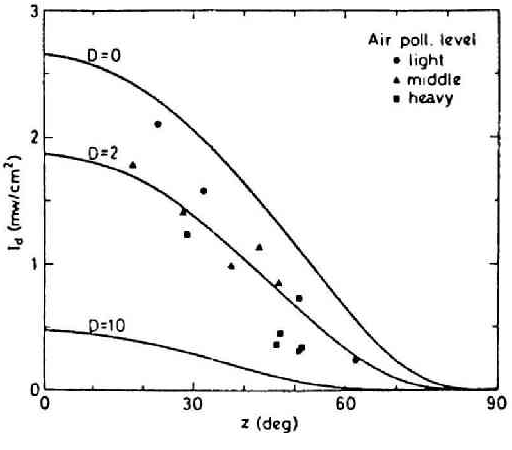

Fig.3-7. Theoretical and measured direct u.v. intensity at the earth's surface.

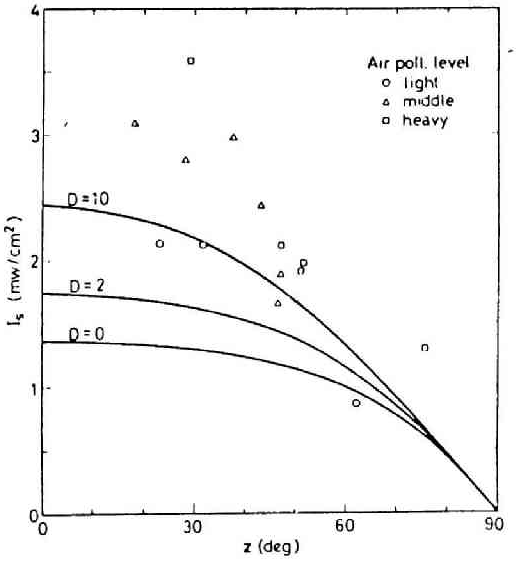

Fig.3-8. Theoretical and measured scattered u.v. intensity at the earth's surface.

angle (θ_0,ϕ_0) and to the change of the spectrum for the large scattering angle, etc. As for the mean of settling those problems, it is required to use a collimator of which solid angle is as small as possible for the former, and to measure the spectral intensities at the various azimuth angle for the latter.

3.4 Absorption of Radiation in Photochemical Reaction

3.4.1 Photochemical Reaction in Polluted Air

Some of the polluted substances discharged into the atmosphere absorb the energy of solar radiation and react photochemically to produce the second polluted substances. In photochemical reaction, only the energy absorbed by a system can proceed the reaction. Average fraction receiving photons per unit time, namely from the law of photochemical equivalence the ratio of the number of molecules absorbing energy to that of the absorbing substances, is called the specific absorption rate constant and is denoted by k_a hereafter. The quantum yield Φ meaning the efficiency of photochemical reaction is defined as follows;

$$\Phi = \frac{\text{number of molecules which absorb energy and react}}{\text{number of molecules which absorb energy}}$$

From the definition of the quantum yield, the product of k_a and Φ is equal to the molecular number of substance which react photochemically. Therefore, the changes of them per unit time are also equal mutually, that is,

$$k_a\Phi = k \tag{3.11}$$

where k is a reaction rate constant.

3.4.2 Absorption of Light Energy

Although photochemical reaction of substances in the polluted air proceed by receiving the solar radiation in the atmosphere, most of the investigations on photochemical smog as well as this study have been performed using the artificial light. In this section, k_a is adopted as an index for evaluating the effective u.v. intensity in photochemical reaction. The estimation method of k_a of the solar radiation in the atmosphere is reviewed, and a method is proposed for estimating the value of k_a of the artificial irradiation in the experimental system for photochemical reaction study.

(1) For solar radiation [1]

For weak absorption, the spectral average rate of absorption per unit volume, $I_{a\lambda}$, is given approximately by the following equation;

$$I_{a\lambda} = 2.30\ \alpha_{g\lambda}\ c\ (I_{d\lambda}\ \sec z + I_{s\lambda}\ \xi) \tag{3.12}$$

Where, $\alpha_{g\lambda}$ is decadic absorption coefficient, c is the concentration of absorbing substances in the atmosphere and ξ is a factor relative to the path length of the scattered radiation. If the values of I_d and I_s are given in the unit of [photons/cm^{2}sec] and the units of α_g and c are optional on condition that be compatible, k_a is given by I_a / jc. Where j is a conversion factor such that the unit of jc is [molecules/cm^3]. The total absorption rate per unit volume I_a and the specific absorption rate constant k_a by the substance in question are given by the following forms;

$$I_a = \sum_{\lambda} I_{a\lambda} = \sum_{\lambda} 2.30\ \alpha_{g\lambda}\ c\ J_{\lambda} \tag{3.13}$$

$$k_a = \sum_{\lambda} k_{a\lambda} = \sum_{\lambda} 2.30\ \alpha_{g\lambda}\ J_{\lambda} / j \tag{3.14}$$

where

$$J_\lambda = I_{o\lambda}\, T_{a\lambda}\, [T_{m\lambda}\, T_{p\lambda} + g\, \xi\, (1 - T_{m\lambda}\, T_{p\lambda})\, \cos z] \qquad (3.15)$$

(2) For artificial radiation

An experimental system consisting of the reaction chamber which is setted in the irradiation chamber is often used in the experimental work of photochemical reaction. Then it is desirable that light intensity is measured in the reaction chamber. The measurement of light intensity in the reaction chamber, however, is difficult in most actual cases.

In the case that the measurement of light intensity at point P in the reaction chamber is impossible but is possible at point P by taking away the reaction chamber, k_a at the point P can be estimated as follows ;

Expressing the spectral intensity at the azimuth angle (θ,ϕ) by $i_\lambda(\theta,\phi)$ m watt/cm^{2}100Å·sterad similarly in Section 3.3, $k_{a\lambda}$ at the point P is given by

$$k_{a\lambda} = \frac{2.52\times10^{11}\lambda}{2\ jc}\int_0^{2\pi}\int_{-\pi/2}^{\pi/2} i_\lambda(\theta,\phi)\, \sin 2\theta\, t_{c\lambda}^{\,y(\theta,\phi)}\, (1 - 10^{-\alpha_{g\lambda}\, c\, \sec\theta})\, d\theta d\phi \qquad (3.16)$$

where t_c is the transmissivity of light per unit length of the reaction chamber and $y(\theta,\phi)$ is path length of light within the reaction chamber wall in the direction of (θ,ϕ). For weak absorption substances, Eq.(3.16) is approximated by

$$k_{a\lambda} = \frac{1.16\times10^{12}}{j}\, \lambda\, \alpha_{g\lambda} \int_0^{2\pi}\int_{-\pi/2}^{\pi/2} i_\lambda(\theta,\phi)\, \sin\theta\, t_{c\lambda}^{\,y(\theta,\phi)}\, d\theta d\phi \qquad (3.17)$$

Although $y(\theta,\phi)$ is given as a function of the wall thickness and

shape of the reaction chamber and of the position of point P in the reaction chamber, it is generally difficult to estimate the magnitude of $y(\theta,\phi)$. If $t_{c\lambda}$ is nearly equal to 1, that is, the reaction chamber wall is highly transmissible and/or extremely thin, $t_{c\lambda}^{y}$ is also approximately 1 and then an error caused by $y(\theta,\phi)$ is less. Beside, if the measurement of $i_\lambda(\theta,\phi)$ is possible in the reaction chamber, $k_{a\lambda}$ ia given by substituting 1 into $t_{c\lambda}$ in Eq. (3.17).

An instrument which can not measure the spectral intensity but the total intensity is often used. In this case, i_λ is estimated by the following equation;

$$i_\lambda = \frac{\zeta_\lambda}{\Sigma\ \zeta_\lambda\ r_\lambda} \cdot M \tag{3.18}$$

where M (m watt/cm^{2}sterad) is the total light intensity measured and ζ_λ is a spectral distribution of relative intensity of the artificial light. In a case that the light intensity is isotropic and that the reaction chamber is spherical, $k_{a\lambda}$ around the center of the reaction chamber is given from Eq.(3.17) as follows;

$$k_{a\lambda} = 1.45 \times 10^{13}\ \alpha_{g\lambda}\ i_\lambda\ t_{c\lambda}^{\ Y} / j \tag{3.19}$$

Where, Y is the thickness of the reaction chamber wall. On the other hand, as the total intensity is measured instead of i_λ, $k_{a\lambda}$ is given by

$$k_{a\lambda} = 1.45 \times 10^{13}\ \alpha_{g\lambda}\ \zeta_\lambda\ M\ t_{c\lambda}^{\ Y} / j\ (\Sigma\ \zeta_\lambda\ r_\lambda) \tag{3.20}$$

Beside, it is possible to estimate $k_{a\lambda}$ of the solar radiation from the measured values of solar intensity $i_\lambda(\theta,\phi)$ by substituting 1

into $t_{c\lambda}$ in Eq.(3.17).

3.4.3 Specific Absorption Rate Constant by Sulfur Dioxide

In this section, the specific absorption rate constant k_a in the photochemical reaction of sulfur dioxide, SO_2 which is one of the most common air pollutants is considered.

Sulfur dioxide found in the community atmosphere absorbs solar radiation between 2900 and 4000 Å, and molecules are excited electrically. Some of them are oxidized and become sulfur trioxide which combines with water to form sulfuric acid mist.

The over-all photochemical reaction of sulfur dioxide to sulfuric acid mist is schematized as follows;

$$SO_2 \xrightarrow{h\nu} SO_2^* \xrightarrow{O_2} SO_3 \xrightarrow{H_2O} H_2SO_4 \longrightarrow$$

sulfuric acid aerosols

The sulfur trioxide formation [11] or the sulfuric acid formation [12] obeys first order reaction with respect to SO_2, and then the following equation is concluded.

$$-\frac{d\,(SO_2)}{dt} = \frac{d\,(SO_3)}{dt} = k\,(SO_2) \tag{3.21}$$

$$= k_a\,\Phi\,(SO_2) \tag{3.22}$$

The specific absorption rate constants of the solar and artificial radiation are calculated by Eqs.(3.14) and (3.17), respectively. Although the absorption spectra of SO_2 gas [11,13] and of the aqueous solutions of SO_2 [14,15] have been examined, the studies on the ultraviolet absorption spectra of SO_2 gas were rare. The

spectral absorption coefficients in Table 3-1, averaged over 100 Å intervals, have been estimated by Hall [11], and these values are used in this study.

Table 3-1. Spectral absorption coefficient of SO_2

λ(Å)	$\alpha_{g\lambda}$(1/mole cm)	λ(Å)	$\alpha_{g\lambda}$(1/mole cm)
2900	156	3200	13
3000	121	3300	3.7
3100	46	3400	1.1

The spectral specific absorption rate of the solar radiation by SO_2 were calculated as functions of z, (O_3), W and D. Fig.3-9 illustrates the spectrum of k_a for various values of z at (O_3)=2.4 mm, W=2.0 cm and D=1.0. And Fig.3-10 shows k_a as a function of z for various values of (O_3) at W=2.0 cm and D=1.0 (solid line), and

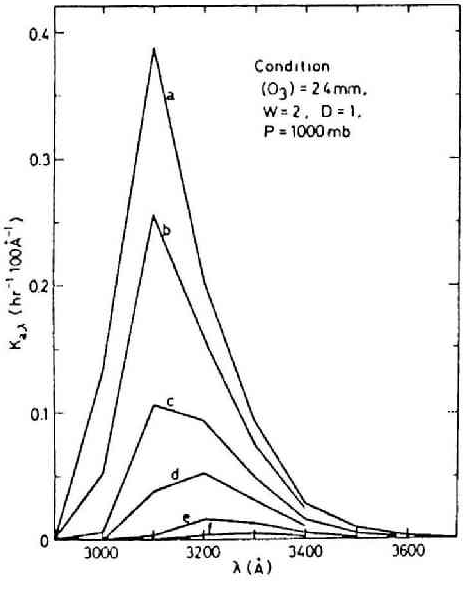

Fig.3-9. Spectral absorption of solar radiation by SO_2 for various values of z, z : a=0°, b=40°, c=60° d=70°, e=80°, e=85°.

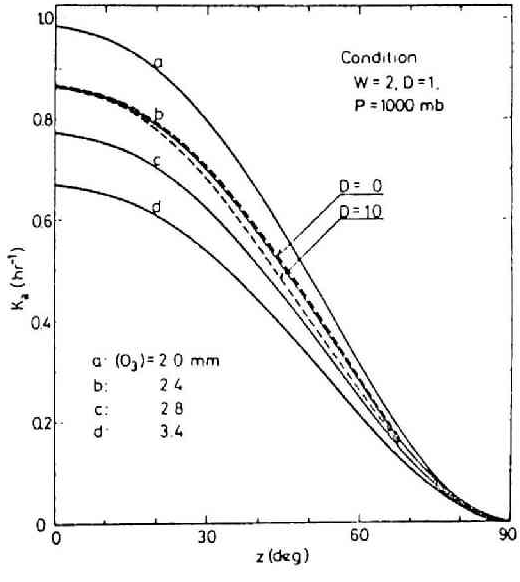

Fig.3-10. Absorption of solar radiation by SO_2.

for various values of D at (O_3)=2.4 mm and W=2.0 cm (broken line). From these calculations, the following deductions can be drawn;

1) For $z < 60°$, the spectrum of k_a has peak in the region of 3100 Å, and the wavelength at peak shifts to the longer when the value of z increases as well as the values of (O_3), D and/or W increase. Because the absorption and scattering of the solar radiation in the atmosphere increase with the increasing z, and those phenomena are remarkable at the shorter wavelength,

2) The factor of (O_3) influences most significantly on the absorption of solar radiation by SO_2. Because the most significant factor having effects on u.v. intensity at the earth's surface is (O_3) in the region of 3100 Å,

3) The specific absorption rate constant of solar radiation by SO_2 ranges from 0.31 to 0.85 hr^{-1} as shown in Table 3-2 at noon in Kyoto (N 35°).

Table 3-2. k_a by SO_2 in lower atmosphere at N 35°

Month	(O_3) (mm)	z at noon (deg.)	k_a (hr^{-1})
1	2.7	56	0.31
6	2.5	10	0.82
7	2.3	13	0.85
8	2.2	21	0.84

3.5 Results and Discussion

In this study, the specific absorption rate constant k_a is considered as an index for evaluating effective u.v. intensity of sunlight and artificial light in photochemical reaction of air pollutants. The direct and scattered intensities at the earth's surface were calculated theoretically and were measured under the

various environmental conditions. For the photochemical reaction of air pollutants by solar radiation in the atmosphere, k_a by SO_2 were calculated for various environmental conditions. And for the photochemical reaction by artificial radiation in a popular system used in the experimental studies, the equation to estimate k_a is introduced. As a result,

1) Ultraviolet intensity of solar radiation measured by UV meter almost coincided with the theoretical value. And Eqs.(3.5) and (3.6) can be used to evaluate the solar intensity in the lower atmosphere.

2) In the problem of irradiation for the photochemical reaction of polluted air, the information of spectral intensity, especially of spectral intensity within the absorption band of substance in question, is more important than the information of total intensity. Although a few measurements of the spectral u.v. intensity of solar radiation have been performed in Japan [16,17], still it is strongly desired to measure systematically the spectral u.v. intensity under the various environmental conditions.

3) The direct and scattered intensities in the lower atmosphere are influenced significantly by D and W. Therefore, in the problem such as diffusion and transportation of polluted substances which react photochemically during the travel in the atmosphere, the vertical distribution of solar intensity introducing D and W have to be considered.

4) The specific absorption rate constant of the solar radiation by SO_2 influenced most significantly by (O_3). It is, however, presumed from the results of section 3.2.2 that k_a by the substance whose absorption band lies in rather long wavelength such as NO_2 [18], is affected more significantly by factors of D and W than factor of (O_3). Therefore, it is necessary to investigate quantitatively the influence of D, which will become a wide variable with degree of air pollution, on the solar irrdiance in the atmosphere.

Beside, some investigations relative to the influence of particulate matter on the solar irradiance have been reported as reviewed in Chapter 2 [19-23].

5) In the irradiation system whose light source is setted outside of the reaction chamber, radiation is weakened during the pass through the reaction chamber wall, especially weakened at shorter wavelength as shown in Fig.3-11. Therefore, it is necessary to measure the spectral transmittance of the reaction chamber wall in order to evaluate the effective light intensity in the reaction chamber or specific absorption rate constant. Koller [24] reviewed the measured values of the spectral transmittance for various materials and thicknesses.

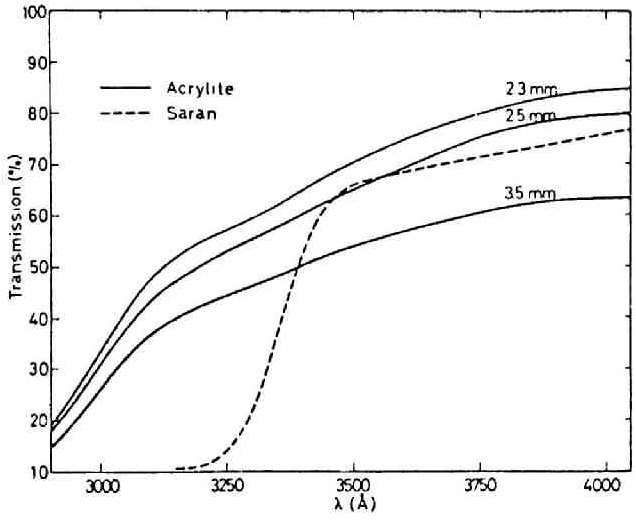

Fig.3-11. Spectral transmittance of various thicknesses of acrylite and of saran.

6) The calculation and measurement in this study were performed under the condition without cloud. In the future, it is required to consider the existence of cloud in these problems.

List of Symbols in Chapter 3

c : concentration of gaseous matter, (ppm, etc.)

D : factor with respect to the amount of dust content of the atmosphere, (-)

g : factor with respect to scattered radiation, (-)

I : light intensity per unit horizontal cross section in the lower atmosphere, (m watt/cm^2 or photons/cm^2sec)

I_a : absorption rate of radiation per unit volume of air, (photons/cm^2sec)

I_o : light intensity outside the atmosphere, (m watt/cm^2 or photons/cm^2sec)

$i(\theta,\phi)$: light intensity per unit cross section which is perpendicular to axis of direction (θ,ϕ), (m watt/cm^2)

j : conversion factor

k : reaction rate constant, (sec^{-1})

k_a : specific absorption rate constant, (sec^{-1})

M : total light intensity, (m watt/cm^2sterad)

m : air mass, (-)

(O_3) : thickness of the equivalent layer of pure ozone, (mm)

r : response of UV meter, (-)

T_a : transmissivity by absorption, (-)

T_m : " by molecular scattering, (-)

T_p : " by particulate diffusion, (-)

t_c : transmissivity of light per unit length of the reaction chamber, (-)

W : thickness of the equivalent layer of precipitable water vapor in the atmosphere, (cm)

y : path length of light within the reaction chamber wall, (cm)

z : zenith angle, (deg)

α : absorption coefficient of gaseous polluted matter, (1/mole cm)

α_g' : absorption coefficient of ozone, (mm^{-1})

ζ : relative intensity of the artificial light, (-)

λ : wavelength, ($\mathring{A}$)

ξ : factor relative to the path length of scattered radiation, (-)

θ : angle of elevation from horizontal plane, (deg)

ϕ : angle from base direction within horizontal plane, (deg)

Φ : over-all quantum yield, (-)

suffix λ : spectral

suffix d : direct

suffix s : scattered

References

[1] Leighton, P. A. (1961) : Photochemistry of air pollution, 1st ed., Academic Press, New York.

[2] Moon, P. (1940) : Proposed standard solar - radiation curves for engineering use, J. Franklin Inst., Vol.230, pp.583-618.

[3] Hulburt, E. O. (1947) : The upper atmosphere of the earth, J. Opt. Soc. Am., Vol.37, pp.405-415.

[4] Johnson, F. S. (1954) : The solar constant, J. Meteorology, Vol.11, pp.431-439.

[5] Benford, F. (1947) : Duration and intensity of sunshine, Illumi. Eng., Vol.42, pp.527-544.

[6] Penndorf, R. (1957) : Tables of the refractive index for standard air and the Rayleigh scattering coefficient for the spectral region between 0.2 and 20.0 μ and their application to atmospheric optics, J. Opt. Soc. Am., Vol.47, pp.176-182.

[7] Dobson, G. M. B. (1930) : Observations of the amount of ozone in the earth's atmosphere, and its relation to other geophysical conditions, Proc. Roy. Soc. of London, Vol.A129, pp.411-433.

[8] Tokyo Tenmondai (1972) : Rikanenpyō, Vol.45, Maruzen, Tokyo.

[9] Takahashi, K. (1972) : Kiso Aerosol Kōgaku, 1st ed., pp.140, Yokendō, Tokyo.

[10] Toshiba, Catalogue No.60106 - 1.

[11] Hall, T. C. (1953) : Photochemical studies of nitrogen dioxide and sulfur dioxide, Ph.D. thesis, Univ. of California at Los Angeles.

[12] Gerhard, E. R. and Johnstone, H. F. (1955) : Photochemical oxidation of sulfur dioxide in air, Ind. End. Chem., Vol.47, pp.972-976.

[13] Deslandres, H. (1925) : Recherches complementaires sur la structure et la distribution des spectres de bandes, Comptes Rendus Hebdomadaires des Seances de l'Academie des Sciences, Vol.181, pp.387.

[14] Wright, R., (1914) : The absorption spectra of sulphurous acid and sulphites, J. Chem. Soc., Vol.105, pp.696, 2907.

[15] Ratkowsky, D. A. and McCarthy, J. L. (1962) : Spectrophotometric evaluation of activity coefficients in aqueous solutions of sulfur dioxide, J. Phys. Chem., Vol.66, pp.516-519.

[16] Okita, T. (1972) : Measurements of u.v. radiation in the atmosphere (in Japanese), Special Report for Analysis of Photochemical Smog, pp.8-35.

[17] Kankyo-cho, private communication.

[18] Beattie, I. R. and Vosper, A. J. (1961) : Dinitrogen trioxide, J. Chem. Soc., Vol.163, pp.2106.

[19] Shettle, E. P. and Weinman, J. A. (1970) : The transfer of solar irradiance through inhomogeneous turbid atmospheres evaluated by Eddington's approximation, J. Atmos. Sci., Vol.27, pp.1048-1055.

[20] Shettle, E. P. (1972) : The transfer of near ultraviolet irradiances through smog over Los Angeles, Atmos. Environ. Vol.6, pp.165-180.

[21] Volz, F. E. (1970) : Spectral skylight and solar radiance measurements in the caribbean : maritime aerosols and Sahara dust, J. Atmos. Sci., Vol.27, pp.1041-1047.

[22] Twomey, S. (1972) : The effect of cloud scattering on the absorption of solar radiation by atmospheric dust, J. Atmos. Sci., Vol.29, pp.1156-1159.

[23] Unsworth, M. H. and Monteith, J. L. (1972) : Aerosol and solar radiation in Britain, Quart. J. Roy. Meteor. Soc., Vol.98, pp.778-797.

[24] Koller, L. R. (1952) : Ultraviolet radiation (Chap. 5 : Transmission), pp.140-177, 1st ed., Wiley, New York.

Others

Fleagle, R. G. and Businger, J. A. (1963) : An introduction to atmospheric physics, Academic Press, New York.

Nader, J. S. (ed.) : Pilot study of ultraviolet radiation in Los Angeles October 1965, U.S. Dept. of H. E. W., PHS No. 999-AP-38.

Robinson, N. (1966) : Solar radiation, Elsevier Pub. Co., Amsterdam.

Kikuchi, S. and Hamano, Y. (1970) : Kokagaku (Photochemistry), Corona-sha, Tokyo.

Chapter 4

4. Aerosol Formation by Photochemical Oxidation of Sulfur Dioxide

It is generally understood that the photochemical oxidation of sulfur dioxide in air leads to sulfuric acid mist formation. In this chapter, the effects of the environmental factors on formation and evolution processes of aerosol particles produced by photochemical oxidation of sulfur dioxide in pure air are investigated experimentally, and the number formation rates of aerosol particles are determined under various environmental conditions.

4.1 Introduction

Sulfur dioxide absorbs near-ultraviolet radiation energy and molecules are electrically excited. Some of those excited molecules react chemically to become sulfur trioxide which combines with water in the atmosphere to form sulfuric acid embryos. Embryos grow to large aerosol particles through the condensation of sulfuric acid, sulfur trioxide, sulfur dioxide and water molecule and through the coagulation with other particles. The formation processes of sulfuric acid aerosols can be schematized as,

$$SO_2 \xrightarrow{h\nu,\ O_2} SO_3 \xrightarrow{H_2O} H_2SO_4 \quad \text{(vapor)} \qquad (4.1)$$

(photo-oxidation and hydration)

$$\xrightarrow{H_2SO_4,\ H_2O} (H_2SO_4)_n(H_2O)_m \quad \text{(embryo)} \qquad (4.2)$$

(nucleation)

$$\xrightarrow{H_2SO_4,\ H_2O,\ SO_2,\ SO_3,\ \text{particle}} \text{particle} \qquad (4.3)$$

(growth)

The aerosol formation from photochemical oxidation of sulfur dioxide in air has been studied by a number of investigators as mentioned in Chapter 2.

One of the topics of those studies is on the aerosol formation and evolution, i.e. variation of the number concentration of aerosol particles with environmental factors, and on the properties of aerosol particles produced by photochemical oxidation of sulfur dioxide [1-9].

In the studies on the aerosol formation and evolution, Renzetti and Doyle [2], Cox and Penkett [5], Clark [6] and Bricard et al.[10] observed the variation of number concentration of aerosol particles with irradiation time. From those observations, it was found that after some period from the onset of irradiation, the particle number concentration of aerosols increases rapidly, reaches the maximum value, and then decays almost uniformly. Quon et al. [4] found that particle number concentration is proportional to the third power of irradiation time for a given SO_2 concentration and is proportional to the third power of SO_2 concentration for a given irradiation time. Cox [9] showed that aerosol formation is evidently dependent on relative humidity and SO_2 concentration. The above refered experimental studies have been made for the different purposes or under various environmental conditions. Therefore, those experimental results can neither be evaluated in the systematic way nor be compared mutually.

This chapter presents some experimental results for the effects of the environmental factors such as SO_2 concentration, relative humidity, u.v. light intensity and irradiation time on the formation and evolution of aerosol particles produced by photochemical oxidation of sulfur dioxide in pure air, and on the number formation rate of particles at the early stage of formation process, in which it is considered that aerosol formation dominates rather than aerosol growth.

4.2 Experimental Equipment and Procedure

4.2.1 Photochemical Reaction Chamber and Related Facilities

(1) General description of the system

An experimental system was designed to use under controlled reproducible conditions. A schematic flow diagram of the system is shown in Fig.4-1. Ambient air drawn through a compressor was passed through a bed of silicagel to remove most moisture, and then introduced to an air purification system to remove gaseous impurities and atmospheric particulate matters. The air purification system consisted of a glasswool filter, a bed of activated charcoal and a high efficiency particulate filter in series. The filter column of glasswool and charcoal were approximately 8 cm in diameter and 50 cm in depth. The high efficiency particulate filter used was one of the cartridge type filter with 0.45 μm in pore size, $2\frac{1}{4}$ inches in diameter and 31 inches in length from the Nihon Millipore Ltd. Performance of the purification system was sufficient to reduce the background particle concentration to less than 100 per cm^3, and sulfur dioxide and nitrogen oxides concentrations to less than the least measurable concentrations by West Gaeke method and Saltzman method, respectively. And it was also confirmed that no detectable particle was formed by irradiation of pure air under any environmental conditions applied in this experiments.

The gaseous impurities with regards to hydrocarbons contained in pure air or sulfur dioxide - air mixture were examined by means of gas chromatograph (Shimadzu, Type GC - 1C). Hydrocarbons, such as ethane [C_2H_6], iso-butylene [$(CH_3)_2 C = CH_2$], acetaldehyde [CH_3CHO] and methyl-ethyl-ketone [$CH_3COC_2H_5$], were analyzed on a SF96 column and detected by a flame ionization detector (FID). Fig.4-2 shows the relation between the sample volume of these

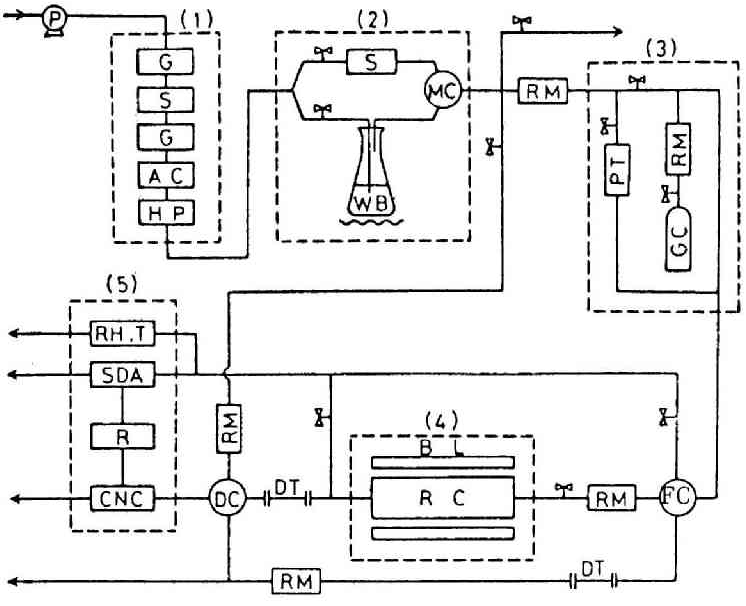

Fig.4-1. Schematic flow diagram of the experimental system

(1) Air purification system; G = glass wool filter, S = silica-gel filter, AC = activated charcoal filter, HP = high efficiency particulate filter.

(2) Humidity control system; WB = water bath, MC = mixing chamber.

(3) Sulfur dioxide supplying system; GC = sulfur dioxide gas cylinder, PT = sulfur dioxide permeation tube.

(4) Illumination system and reaction chamber; BL = blacklight, RC = reaction chamber.

(5) Measuring instrument; CNC = condensation nuclei counter, SDA = sulfur dioxide analyzer, RH,T = hygrometer, R = recorder.

(6) Others; P = pump, RM = rotor meter, FC = flow controlled valve, DT = diffusion tube, DC = dilution chamber.

hydrocarbon gases and the chart integrater readings by a certain condition (sensitivity=10^3, range=0.1 V). In this condition, these compounds can be quantitatively determined as far as about $10^{-2}\mu l$, and also can be qualitatively determined as far as about $10^{-3}\mu l$. No hydrocarbon was detected with 4 ml of pure air and traces of hydrocarbons were detected with 4 ml of 50 ppm SO_2 gas. And so, it was confirmed that the amount of these impurities were less than 0.5% of sulfur dioxide in sulfur dioxide - air mixture. The effect of gaseous impurities of such hydrocarbons on aerosol formation is qulitatively discussed in Appendix 1.

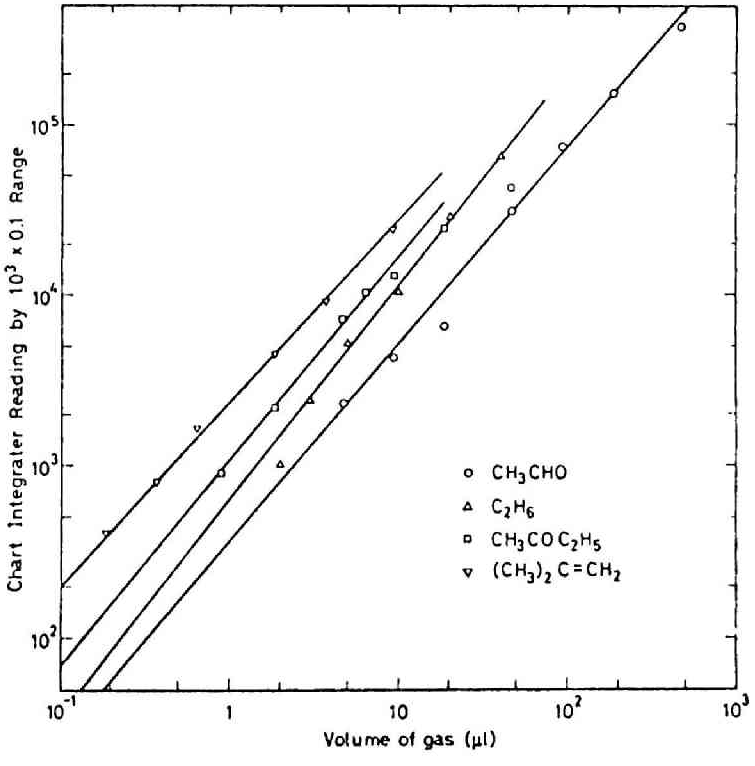

Fig.4-2. Calibration of some hydrocarbons by gas chromatograph : Relation between sample volume of hydrocarbon gases and chart integrater readings by 10^3 X 0.1 range. column = SF96, detector = FID.

Dry pure air from the purification system was divided into two flows. They were mixed again after one of them was humidified by bubbling through a constant temperature water bath. The relative humidity was controlled by the flow rates of both dry and wet pure air. The relative humidity and temperature in the experimental system was checked across the reaction chamber by Ace Sensitive Hygrometer, Type AH-2S.

The sulfur dioxide - air mixture was prepared either by adding about 50 ppm sulfur dioxide gas from gas cylinder obtained from Seitetsu Kagaku Co., Ltd. into the air stream, or by metering a known rate of air flow through a mixing chamber containing a sulfur dioxide permeation tube obtained from Kimoto Denshi Co., Ltd. The temperature of the permeation tube was kept constant within $\pm$ 1°C (within the range from 25 to 30°C) with cooling fan and/or hot wire fan. SO_2 concentration of gas mixture was measured with the Sulfur Dioxide Analyzer (Koritsu - Kiki Inc., Model KS-5S) in the exhaust flow from a flow controlled valve placed before the reaction chamber.

The sulfur dioxide - pure air mixture was introduced into a reaction chamber and irradiated by blacklights. The particle number concentration of aerosols formed was measured using a condensation nuclei counter (CNC, Environment/One condensation nuclei monitor, Model Rich 100). A sampling line from the reaction chamber to the CNC consisted of about 90 cm Teflon tube of 6 mm in inner diameter. The flow rate through the sampling tube was 50 cc/sec. It was confirmed experimentally that the diffusion loss in the sampling line was negligible.

(2) Irradiation system and reaction chamber

Blacklights (Toshiba, FL 20S BLB) were used as the light source. The energy spectrum of the blacklights given by the manufacturer is shown in Fig.4-3. In an irradiation box, four blacklights were set symmetrically with respect to the reaction chamber. The inside wall

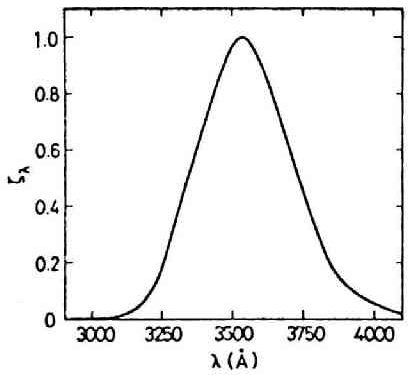

Fig.4-3. Energy spectrum of blacklight.

of the box was lined with aluminum foil as a light reflector. Average u.v. intensity at the center of the irradiation box was measured by the UV meter (Toshiba, Type PI - 1UV) with a collimater of solid angle 0.283 steradian, and it was 0.15 m watt/cm^{2}sterad. The spectrum response curve of the UV meter from manufacturer is shown in Fig.3-4. A fan was used to ventilate and prevent the reaction chamber from temperature rise by irradiation with blacklights. And then, the temperature and relative humidity differences across the reaction chamber were negligible.

The reaction chamber was of an Acrylite cylinder whose inside wall was coated with Teflon thin film in order to prevent neither adsorption nor desorption of sulfur dioxide onto the wall surface [11,12]. The size of the cylinder was 7.5 cm in inner diameter, 56.6 cm in length and 2.5 liter in volume. The fraction of light penetrated into inside of the reaction chamber through the wall whose thickness was 2.5 mm was measured by a spectrophotometer (Shimadzu, Type QV-50), and its result is shown in Fig.3-11. As shown in Table 4-1, the effective light intensity in the reaction chamber is estimated from Eq.(3.20) to be approximately 0.05 per hour of the specific absorption rate constant of sulfur dioxide.

In the experiment on the effect of light intensity on aerosol formation, light intensity was changed in the range from 0.15 to 0.015 m watt/cm^{2}sterad by shielding the light partially with a cover. The adequate numbers of small hole were distributed uniformly on the cover in order to obtain the u.v. intensity required. In this study, u.v. intensity is presented by a relative intensity, the ratio to 0.15 m watt/cm^{2}sterad, and denoted by I_r.

Table 4-1. Effective light intensity in reaction chamber

λ (Å)	α_λ (1/mole cm)	$t_{c\lambda}^{Y}$	ζ_λ	r_λ	$k_{a\lambda}$ (sec^{-1})
					$x10^{-5}$
3000	121	0.31	0.003	0.003	0.04
3100	46	0.44	0.03	0.04	0.22
3200	13	0.50	0.14	0.17	0.35
3300	3.7	0.56	0.36	0.36	0.31
3400	1.1	0.61	0.78	0.58	0.22
3500	(0.32)	0.65	1.00	0.81	0.09
3600	(0.10)	0.70	0.89	0.98	0.02

$$k_a = \Sigma\, k_{a\lambda} = 0.05\ hr^{-1}$$

$$k_{a\lambda} = 1.45 \times 10^{13} \lambda\ \alpha_\lambda\, \zeta_\lambda\, t_{c\lambda}^{Y} M / \Delta\omega\, j\, (\Sigma\, \zeta_\lambda r_\lambda)$$

$j = 6.02 \times 10^{20}$ (c = mole / 1 at 1 atm and 25°C)

$\Sigma\, \zeta_\lambda r_\lambda = 2.91$

$(M / \Delta\omega) = 0.15$ m watt / cm^2sterad

4.2.2 Measurement Instrument

(1) Condensation nuclei counter (CNC) [13]

An Environment/One condensation nuclei monitor (Model Rich 100) was used to measure the total number concentration of particles. It responds to atmospheric particles with diameters of 0.0025 μm and larger*, and it covers a concentration range of 300 to 10^7 particles per cubic centimeter. Air sample is drawn at a rate of

---

***** The smallest particle radius detectable in the CNC has been determined from measurement of gas-to-particle conversion in connection with coagulation process by Walter and Jaenicke [14], and from measurement of the diffusional decay of spontaneously produced aerosol particles by Pedder [15].

50 cc/sec and the total measurement cycle time is approximately once per second. An examination of the accuracy of the CNC using a Pollack type counter made by our laboratory indicated that the factory calibration for the CNC was good within a factor of about two.

The counter has been described in detail by Skala [16]. Briefly, the principles of operation is as follows; The counter operates on the principle of a cloud chamber in which water is condensed upon submicro scopic particles to produce micron sized droplets. A constant flow air sample is periodically diverted through a humidifier and then into a cloud chamber where a fixed volume expansion of the sample occurs, providing a supersaturation of at least 300%, which produced a cloud. The formation of the cloud causes a decrease in light, which results finally in a change of a DC signal. The DC signal is displayed on a panel indicator and is also available for operation of a recorder. After expansion, the cloud chamber is pressurized and flushed out.

Dunham [17] proved that condensation nuclei technique could be used in a qualitative way in the determination of the predominating reaction and that the CNC is highly sensitive to the presence of sulfuric acid particles in the air.

(2) Sulfur dioxide analyzer

A Koritsu - Kiki Inc. Model KS-5S Sulfur dioxide analyzer was used to measure the concentration of SO_2. It covers a concentration range of 0 - 10 ppm and has accuracy of ± 2% of full scale, a response time of 90% of full scale in less than 60 seconds and a recovery time of 90% of full scale in less than 20 seconds [18]. The analyzer is a similar type of Dynasciences Air pollution monitors which is characterized by a electrochemical tranducer capable of selectively monitoring SO_2 and NO_x through at the 0 - 5000 ppm range.

The typical electron transfer reactions occuring in the electrochemical tranducer for SO_2 is as follows;

$$SO_2 + 2H_2O \longrightarrow SO_4^{=} + 4H^{+} + 2e^{-}, \quad E^{\circ}_{298^{\circ}K} = 0.17 \text{ volts} \tag{4.4}$$

The tranducers selectivity toward a particular pollutant is obtained by unique membrane/electrolyte/electrodes combinations. In operation, the pollutant gas (SO_2) diffuses through the membrane and thin electrolytic layer to become absorbed at the sensing electrode where it undergoes electro-oxidation. The direct electro-oxidation of absorbed gas molecules at a sensing electrode results in a current directly proportional to the partial pressure of the pollutant gas. The transducer's electrical output is associated with a solid-state amplification and read out electronic circuit by way of ppm unit. More detailed description for the analyzer has been given by Chand and Marcote [19].

The analyzer was calibrated using the sulfur dioxide permeation tube whose permeation rate was determined by measuring the weight loss over a period of two weeks at daily intervals.

(3) Hygrometer [20]

Ace sensitive hygrometer, Type AH-2S was used to measure relative humidity in the system. It consists of a indicator and four detectors which respond to 10 - 30%, 20 - 40%, 40 - 70% and 70 - 100% relative humidity. Accuracy of the hygrometer is better than 2% and response time is shorter than that of other type of hygrometer such as hair hygrometer, psychrometer and dew-point hygrometer.

4.2.3 Experimental Procedure

The number concentration of aerosol particles formed by photochemical oxidation of sulfur dioxide in pure air were measured for

various combinations of environmental factors such as SO_2 concentration, relative humidity, ultraviolet light intensity and irradiation time. The ranges of those environmental factors used in this study are shown in Table 4-2.

Table 4-2. Ranges of environmental factors used in this study

SO_2 concentration	: 0.1 - 10 ppm
relative humidity	: Dry[1] - 80 %
u.v. light intensity	: 0.15(I=1) - 0.015(I=0.1) m watt/cm²sterad at outside of the reaction chamber wall
" as k_a[2]	: 0.05 - 0.005 hr^{-1}
irradiation time	: 0 - 750 sec

1) : Dry means the degree of relative humidity under the condition that dry pure air is sufficiently flowed further after the hygrometer indicates zero (<10% r.h.).

2) : k_a is the specific absorption rate constant of sulfur dioxide.

The experiment was performed in a dynamic flow system. The reaction chamber was first cleaned at least for 30 minutes with pure air before starting experiments. And at least 30 liters of sample gas, 12 times of the volume of the reaction chamber, were flowed through the reaction chamber before each run in order to flush out the particles and sulfur dioxide vapor from the previous experiment and also to pre-condition to minimize the adsorption and deposition losses. An average residence time in the reaction chamber was considered to be the irradiation time τ. That is,

$$\tau = \frac{\text{volume of reaction chamber}}{\text{flow rate in reaction chamber}} \qquad (4.5)$$

The irradiation time, therefore, was practically regulated in the

range from 15 to 750 sec by changing the flow rate of sample gas passing through the reaction chamber. After u.v. lights were turned on, the particle number concentration of aerosols formed attained an equilibrium at about three times as long as the average residence time. The equilibrium value was considered to be the particle number concentration for the irradiation time of τ. At least three separate measurements were performed under the same environmental conditions on different day. The average value of them was adopted as the experimental value.

The advantages of the dynamic flow system are in easy operation and good reproducibility. The other advantage of this system facilitates the determination of particle radius by diffusion method. The irradiation time, however, was restricted by the lower limit of flow rate, accordingly irradiation for very long time was unsuitable in this system.

4.3 Results and Discussion

4.3.1 Variation with Irradiation Time

Several series of experimental runs were made to study effects of environmental factors on aerosol formation and evolution of sulfuric acid aerosols. The environmental factors and those ranges taken up in this study are shown in Table 4-2. The variation of particle number concentration N with irradiation time τ under the environmental condition, such as the initial sulfur dioxide concentration of s ppm, relative humidity of h % and the relative u.v. intensity of I_r, is represented by Run $N\tau(s,h,I_r)$.

(1) Data analysis

Fig.4-4 shows the variation of particle number concentration, n, with real time, t, for Run $N\tau(1,60,1)$, where t is the subsequent time from the onset of u.v. irradiation. And in Appendix 5-1, the

original experimental data of n - t curves at τ of 50, 200 and 750 sec for Run Nτ(1,60,1) are illustrated. Detectable particles for the CNC were formed after some period t_o from the onset of irradiation, and n was increased rapidly. When the average residence time was short, n reached an equilibrium concentration after rapid increase. While, when the average residence time was rather long, it reached a maximum value at first, and decreased gradually to an equilibrium concentration at the time of t_e. In this example, the equilibrium concentration was 4.3×10^5 and 2.1×10^5 cm^{-3} for the irradiation time of 50 and 750 sec, respectively, and these values were adopted as the particle number concentration N for each irradiation time. Fig.4-5 shows an example of the experimental results. Each point and the vertical line on it represent an average particle number concentration and standard deviation obtained from at least three runs for the same experimental conditions. The number concentration N increased rapidly after some threshold time τ_o, reached the maximum value and decreased; And then in the majority of cases

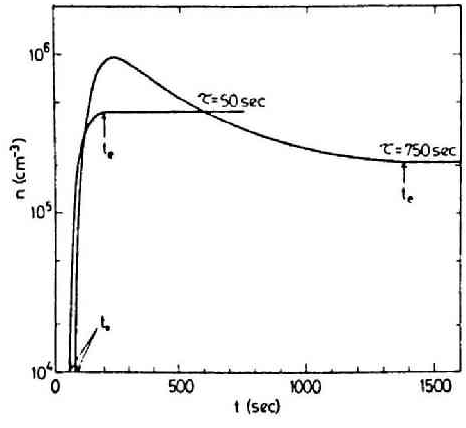

Fig.4-4. Variation of particle number concentration with extended time from onset of irradiation. Average residence time τ=50 and 750 sec, s=1 ppm, 60% r.h., I_γ=1.

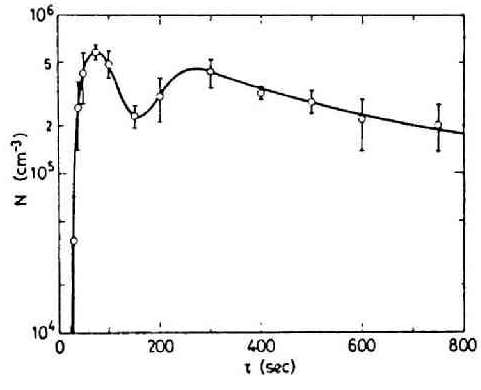

Fig.4-5. Average value and standard deviation of particle number cocentrations obtained in four separate measurements for Run Nτ(1,60,1).

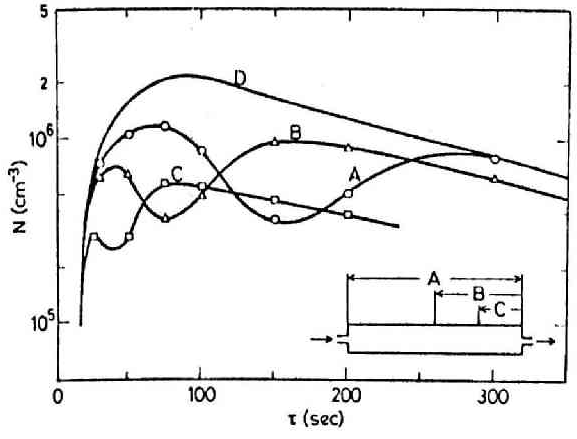

Fig.4-6. Effects of the flow condition and the corrected curve for Nτ(1,60,1). A is for the whole of reaction chamber. B and C are for a half and a quater in the outlet side of reaction chamber, respectively.

N increased again, reached the second peak value and decreased gradually. From observing the curve in Fig.4-4 or from referring the experimental results obtained separately using batch system and also the results reported by other investigators (Renzetti and Doyle [2], Bricard *et al.* [10], Clark [6]), it is unexpected that N - τ curve may have two peak values. The experimental examinations for possible errors in flow rate and dilution rate and for possible effects of flow condition have been performed in order to clarify this phenomenon. It is consequently concluded that the phenomenon is due to effect of flow condition and that effects of the rest causes are negligibly small. Fig.4-6 shows one of the results of the examinations for effect of flow condition on the variation of particle number concentration with irradiation time. Curves A, B and C were obtained using the whole of the reaction chamber, a half and a quarter part in the outlet side of the reaction chamber, respectively. It was found that every curves have two peaks and then the bottoms and the second peaks in three curves appear at about same flow rate, respectively, and that the slopes of N - τ curves after the second peak are almost same. Although the mechanism of this phenomenon is remained still unexplained, the curve A was corrected in the following manner; the curve A was extrapolated

to shorter period than irradiation time at the second peak with keeping the equal slope to the curves B and C, and the maximum particle number concentration N_m was equated to the maximum value of n - t curve. Observation of flow using incense stick smoke showed that smoke was flowing rather uniformly through the reaction chamber, and neither strong mixing nor short cut current was observed. Thus, the estimation of N_m from n - t curve is considered to be acceptable, because the peak value on n - t curve seems very close to the real peak value in the case of perfectly uniform flow. The corrected curve was further checked by comparing with n - t curve. In the subsequent discussions, values corrected in the same manner as described above are used as the final data.

(2) Effect of sulfur dioxide concentration and relative humidity

The particle number concentration N in Run Nτ(s,h,1) was measured for irradiation time τ ranged from 0 to 750 sec. Figs.4-7a and 4-7b

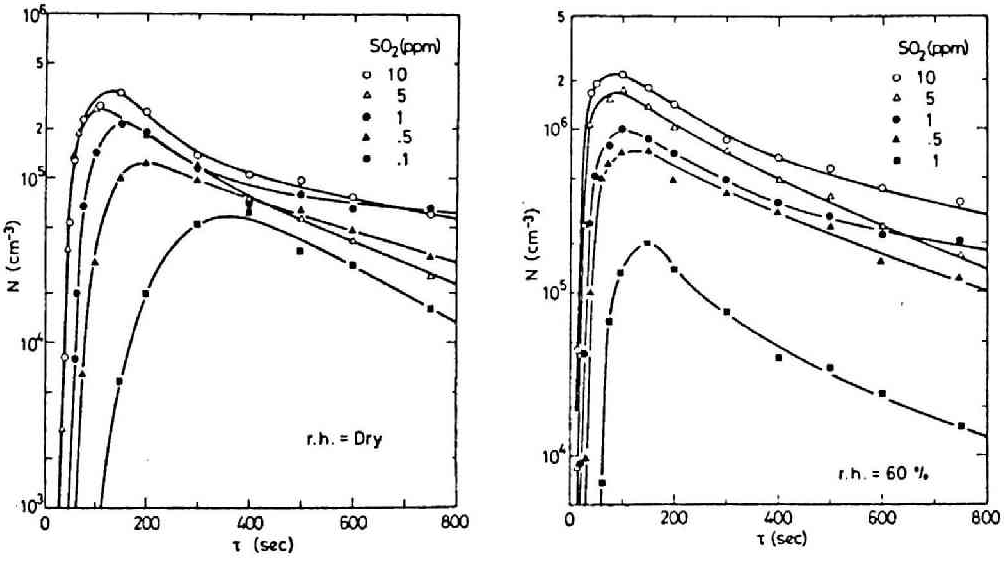

a). Run Nτ(s,Dry,1). *b). Run Nτ(s,60,1).*

Fig.4-7. Variation of the particle number concentration with irradiation time for various SO_2 concentrations.

show the variations of N with τ for various values of SO_2 concentration at Dry and 60% r.h., respectively. Figs.4-8a to 4-8d also show the variations of N with τ for various values of relative humidity at SO_2 concentration of 0.1, 1, 5 and 10 ppm, respectively.

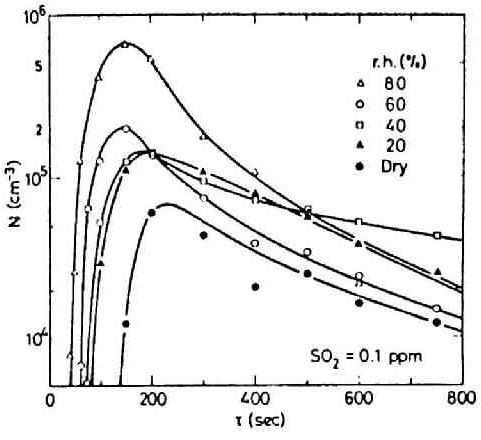

a). Run Nτ(0.1,h,1).

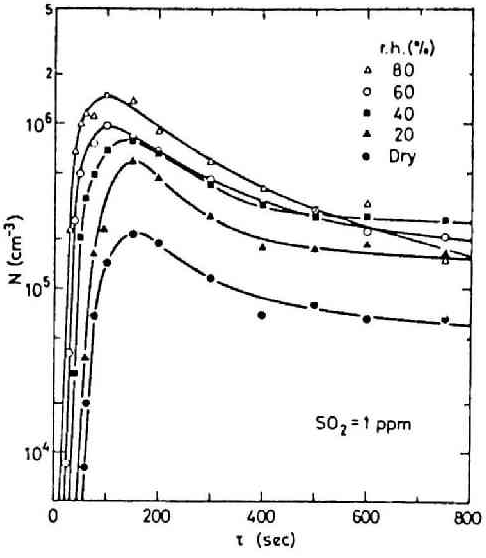

b). Run Nτ(1,h,1).

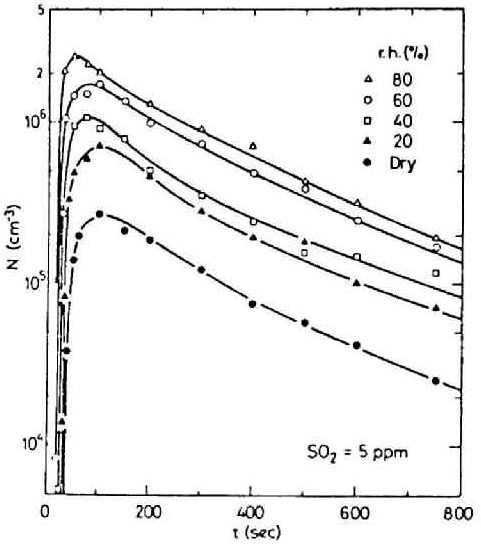

c). Run Nτ(5,h,1).

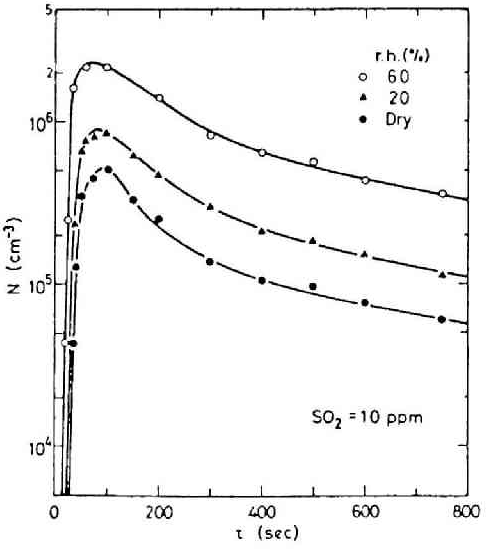

d). Run Nτ(10,h,1).

Fig.4-8. Variation of the particle number concentration with irradiation time for various relative humidities.

In any Runs, N increased rapidly after some period during which no particle was detectable, reached the maximum value N_m at irradiation time τ_m, and then decreased gradually.

Here, "the early stage of reaction" denotes the process from the start of reaction to the end of rapid increase of N, in which particle formation is considered to be dominant rather than growth. In the early stage of reaction, N for some fixed τ was high as SO_2 concentration and/or relative humidity was higher. Some properties in the early stage of aerosol formation process such as the threshold time and the formation rate are influenced very sensitively by irradiation time, SO_2 concentration and relative humidity, and shall be discussed in detail later.

For long period of τ, the relation between N and SO_2 concentration or relative humidity is various. It is, however, generally found that for higher SO_2 concentration N increases with relative humidity and for higher relative humidity N increases with SO_2 concentration. The various variations of N with environmental conditions in long period of τ is considered to be caused by the difference of growth mechanism of particles. As SO_2 concentration and/or relative humidity are higher, the more molecules of sulfur dioxide and water vapor are absorbed by already formed particles, and then the particles may grow faster.

Cox [9] showed the particle number concentrations as a function of SO_2 concentration or relative humidity at fixed residence time of 2.5 minutes. The investigation is imagined to have been made in the early stage of reaction, because the results show rapid variations with SO_2 concentration and relative humidity. Therefore, the shapes of N - SO_2 concentration curves and N - relative humidity curves obtained by Cox probably vary with even slight change of the residence time.

The relations between N_m and relative humidity and between τ_m

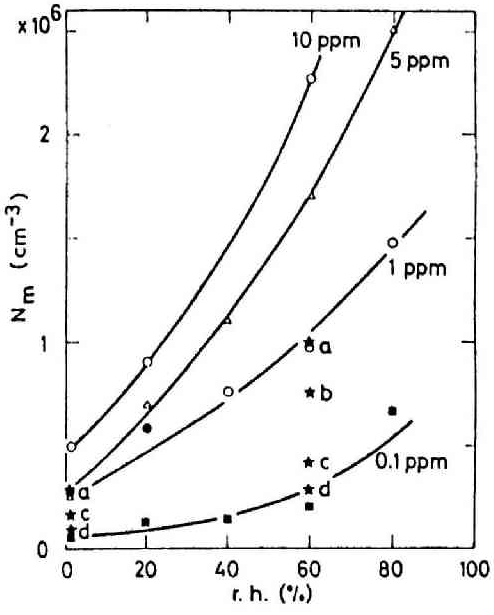

Fig.4-9. Effects of SO_2 concentration, relative humidity and relative u.v. intensity on the maximum number concentration. Symbols a, b, c and d are for relative u.v. intensity of 1, 0.5, 0.2 and 0.1, respectively, in Run $N\tau(1,60,I_r)$ and Run $N\tau(1,Dry,I_r)$.

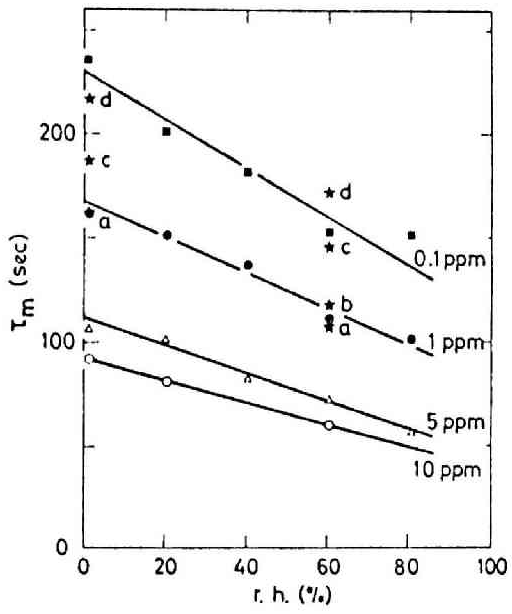

Fig.4-10. Effects of SO_2 concentration, relative humidity and relative u.v. intensity on irradiation time when particle number concentration reaches maximum. Symbols a, b, c and d are for relative u.v. intensity of 1, 0.5, 0.2 and 0.1, in Run $N\tau(1,60,I_r)$ and Run $N\tau(1,Dry,I_r)$.

and relative humidity are shown for various SO_2 concentrations in Figs.4-9 and 4-10, respectively. The values of N_m and τ_m are strongly dependent on SO_2 concentration and relative humidity. It is concluded that N reaches a maximum value fast and the value of N_m is high as SO_2 concentration and relative humidity are higher.

(3) Effect of u.v. intensity

The u.v. intensity is also an important factor on aerosol formation from photochemical reaction of sulfur dioxide. Fig.4-11a and 4-11b show the curves of $N\tau(1,Dry,I_r)$ and $N\tau(1,60,I_r)$, respectively.

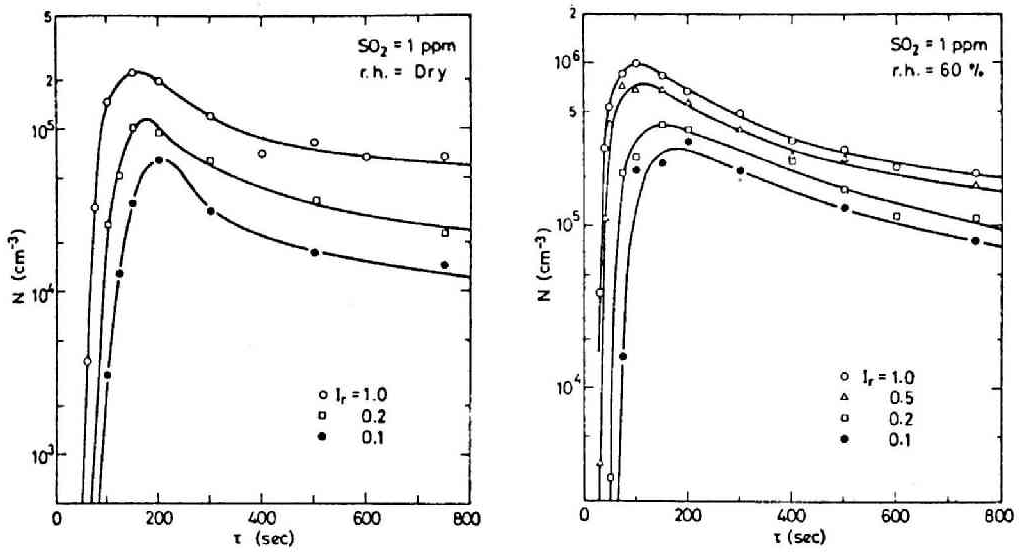

a). Run Nτ(1,Dry,I_r). *b). Run Nτ(1,60,I_r).*

Fig.4-11. Variation of the particle number concentration with irradiation time for various relative u.v. light intensities.

The curve of Run Nτ(1,60,0.5) is almost similar to that of Run Nτ (0.5,60,1) in Fig.4-7b. On the other hand, the curve of Run Nτ(1, 60,0.1) is almost similar to that of Run Nτ(0.1,60,1) in the early stage of reaction, but is different in long period of τ. These similarities in the early stage of reaction are considered to be due to the fact that particle formation dominated rather than growth in the early stage of reaction and also that the formation rate of aerosol particles depends on the amount of excited sulfur dioxide molecules, i.e. on the product of SO_2 concentration and u.v. intensity. The values of N_m and τ_m for I_r = 1, 0.5, 0.2 and 0.1 in Run Nτ(1,Dry and 60,I_r) are plotted in Figs.4-9 and 4-10. These values, especially N_m, for I_r = 0.1 are close to those for 0.1 ppm SO_2 concentration at I_r = 1.

4.3.2 Effects of Environmental Conditions in the Early Stage of Reaction

More detailed investigation in the early stage of reaction is necessary in order to clarify the aerosol formation mechanism. Figs.4-12a and 4-12b show the particle number concentration changes with irradiation time in the early stage of reaction for Runs $N\tau$ (s,60 and Dry,1) and Runs $N\tau$(1,60 and Dry,I_r), respectively.

Here, we define the number formation rate by the amount of particles formed newly per unit time per unit volume. In the early

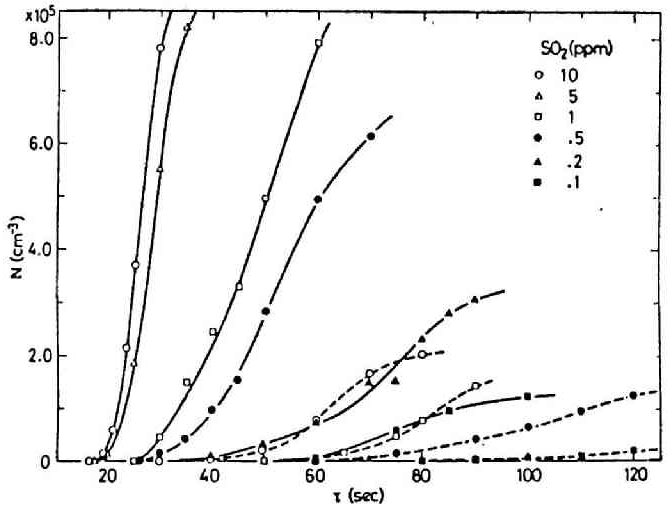

a). For various SO_2 concentration and relative humidities. Solid lines are for Runs $N\tau(s,60,1)$ and broken lines are for Runs $N\tau(s,Dry,1)$.

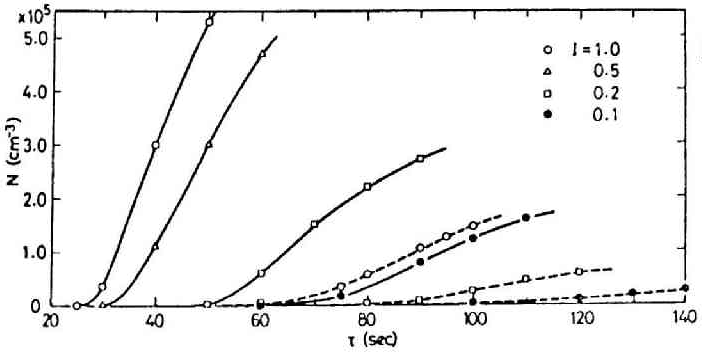

b). For various relative humidities and relative u.v. intensities. Solid lines are for Runs $N\tau(1,60,I_r)$ and broken lines are for Runs $N\tau(1,Dry,I_r)$.

Fig.4-12. Variation of the particle number concentration with irradiation time in the early stage of reaction.

stage of reaction, the number formation rate is approximated by the change of the particle number concentration per unit time, because disappearance of particles can be neglected in comparison with formation. And the maximum number formation rate F is given by the maximum tangential slope of N - τ curve. The values of F were determined graphically for various environmental conditions, and are tabulated in Table 4-3 and shown in Fig.4-13. The maximum number formation rate is in the first order with respect to SO_2 concentration in lower SO_2 concentration. It, however, become lower degree than the first order with the increase of SO_2 concentration. It is considered to be caused by the fact that at higher SO_2 concentration, more part of gas molecules or embryos of sulfuric acid is absorbed by aerosol particles formed already than at lower SO_2 concentration. Also F is dependent strongly on relative humidity, and increases rapidly with the increase of relative humidity.

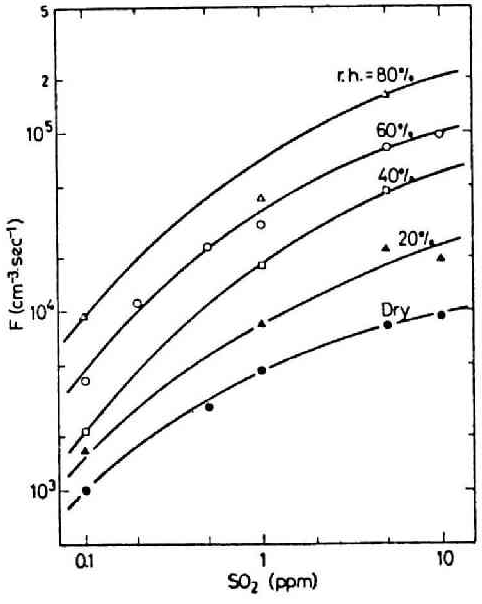

Fig.4-13. Effects of SO_2 concentration and relative humidity on the maximum number formation rate.

To investigate the effect of u.v. intensity on aerosol formation in the early stage of reaction, the values of F for Run Nτ (1,60,I_r) and Run Nτ(1,Dry,I_r) were determined from Fig.4-12b and are tabulated in Table 4-4. Also in the table, the values for Run Nτ(s,60,1) and Run Nτ(s,Dry,1) are shown for reference. It is found that if the products, s(ppm) x I_r, are same, the values of F are very close each other. It is supported experimentally from

Table 4-3. Properties in formation and evolution processes of sulfuric acid mist under various environmental conditions.

Run $N\tau(s, h, I_r)$	τ_o (sec)	τ_m (sec)	N_m (cm^{-3})	F ($cm^{-3}sec^{-1}$)
			x 10^6	x 10^4
10, 60, 1	16	60	2.25	9.7
10, 20, 1		80	0.90	1.9
10,Dry, 1	30	90	0.50	0.90
5, 60, 1	17	70	1.7	8.2
5, 40, 1		80	1.1	4.7
5, 20, 1		100	0.70	2.2
5,Dry, 1	30	105	0.26	0.77
1, 80, 1		100	1.45	4.2
1, 60, 1	24	110	0.95	3.0
1, 40, 1		135	0.76	1.8
1, 20, 1		150	0.58	0.85
1,Dry, 1	55	160	0.22	0.46
0.5, 60, 1	27	125	0.74	2.3
0.5,Dry, 1	60	200	0.13	0.30
0.2, 60, 1	35			1.1
0.1, 80, 1		150	0.68	0.95
0.1, 60, 1	50	150	0.21	0.40
0.1, 40, 1		180	0.14	0.21
0.1, 20, 1		200	0.13	0.17
0.1,Dry, 1	80	235	0.08	0.10
1, 60, 1	25	105	0.97	2.6
1, 60,.5	29	115	0.74	1.9
1, 60,.2	49	143	0.41	0.90
1, 60,.1	59	170	0.29	0.45
1,Dry, 1	57	160	0.25	0.48
1,Dry,.2	77	185	0.15	0.20
1,Dry,.1	90	215	0.09	0.09

Table 4-4. Maximum number formation rate as a function of product, s x I_r.

r.h.	F x 10^{-4} $cm^{-3}sec^{-1}$				Remarks
	s(ppm) x I_r =				
	1.0	0.5	0.2	0.1	
60 %	2.6	1.9	0.90	0.45	Run Nτ(1,60,I_r) I_r=variable
	3.0	2.3	1.1	0.40	Run Nτ(s,60,1) s =variable
Dry	0.48	-	0.20	0.09	Run Nτ(1,Dry,I_r) I_r=variable
	0.46	0.30	-	0.10	Run Nτ(s,Dry,1) s =variable

those results that F is dependent on the amount of excited sulfur dioxide molecules, i.e. the product of SO_2 concentration and u.v. intensity. The maximum number formation rate at 60% r.h. is roughly in direct proportion to the value of s x I_r. But at Dry, the increase of F with the value of s x I_r is much smaller than directly proportional order, especially for large value of s x I_r. This phenomenon is explained by Reaction (4.2). When the amount of molecules of water vapor is sufficiently large as compared with that of sulfuric acid vapor which is dependent on the value of s x I_r, Reaction (4.2) must be in proportion to the value of s x I_r.

The number formation rate at irradiation time τ_m can be estimated by following way; The amount of aerosol particles formed is equated to that disappeared at τ_m. Assuming that the disappearance of particles is due to coagulation and diffusional deposition onto the reaction chamber wall, the number formation rate at τ_m is given by

$$F_m = K N_m^2 + \beta N_m \qquad (4.6)$$

Where F_m is the number formation rate of aerosol particles at τ_m, K and β are coagulation coefficient and deposition rate to the wall

surface, respectively. The number formation rate decreases after reaching the maximum value F, and if $10^{-9}cm^3/sec$ and $10^{-4}sec^{-1}$ are taken as the values of K and β, respectively, it drops under 10 % of F at τ_m. The decrease of number formation rate must be caused by the following change in formation and evolution processes of aerosol particles. Particle number concentration increases rapidly in the early stage of reaction, and aerosol particles formed grows by absorbing molecules of sulfur dioxide, sulfur trioxide, sulfuric acid vapor and water vapor, and embryos, and by coagulating with other aerosol particles formed already. The fraction of non-excited sulfur dioxide molecules reduced by Reaction (4.1) is negligibly small even after several hundred seconds irradiation, and so the number formation rate of excited sulfur dioxide does not vary with time. While, since the absorption of excited sulfur dioxide, sulfur trioxide, and sulfuric acid vapor and embryos onto the already formed aerosol particles increases with the growth of aerosol particles, the amount effective to form particles newly through Reaction (4.2) decreases.

In the case of practical application, it is useful to express effects of the environmental factors on the formation and evolution processes of aerosol particles in experimental equations. The maximum particle number concentrations for various environmental conditions are plotted against the maximum number formation rate on log-log scale in Fig.4-14. They give approximately a straight line with a slope of 0.75, and the relation between N_m and F is expressed by

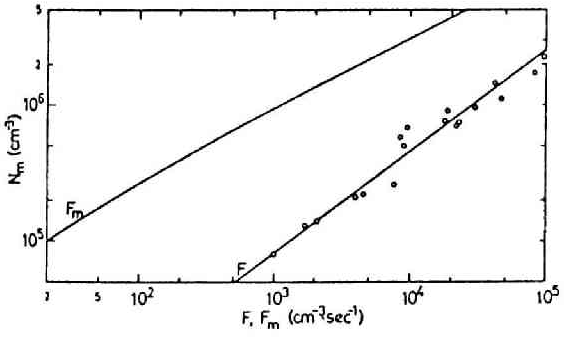

Fig.4-14. Relation between the maximum number formation rate and the maximum particle number concentration.

$$N_m = 4.6 \times 10^2 \, F^{0.75} \quad . \tag{4.7}$$

Also in Fig.4-14, the relation between N_m and F_m given by Eq.(4.6) is simultaneously illustrated for k of 10^{-9} cm^3/sec and β of 10^{-4} sec^{-1}.

The irradiation time τ_m is strongly dependent on SO_2 concentration, relative humidity and relative u.v. intensity as shown in Fig.4-15. And then the relation between τ_m and F is expressed by

$$\tau_m = 8.0 \times 10^2 \, F^{-0.27} \quad . \tag{4.8}$$

Similarly, as the threshold irradiation time τ_o is plotted against F on log-log scale, it gives also the straight line with a slope of -0.37. Therefore, τ_o is expressed as a function of F by

$$\tau_o = 4.8 \times 10^2 \, F^{-0.37} \tag{4.9}$$

The properties of F, N_m, τ_m, and τ_o in the formation and evolution processes of aerosol particles are strongly influenced by the environmental factors such as irradiation time, u.v. intensity, SO_2 concentration and relative humidity as mentioned before. The properties of latter three factors can be expressed as a function of F by Eqs.(4.7), (4.8) (4.9) through taking

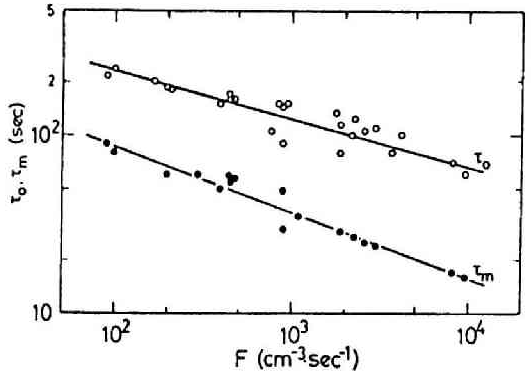

Fig.4-15. Relation between the maximum number formation rate and irradiation times when the particle number concentration reaches maximum and when detectable particles are first formed.

into acount of all effects of various environmental factors in F. Considering practical application of the results obtained in this study, the maximum number formation rate of aerosol particles in the atmosphere is estimated by measuring or by forecasting SO_2 concentration, relative humidity and u.v. intensity. And then the maximum particle number concentration and times when particles are first formed and the particle number concentration reaches the maximum can be further estimated by Eqs.(4.7), (4.8) and (4.9). Besides, in order to protect N_m from exceeding the maximum acceptable concentration in environment, the maximum permissible number formation rate can be estimated by Eq.(4.7), and followingly we can determine the maximum permissible SO_2 concentration.

List of Symbols in Chapter 4

F : maximum number formation rate of particles, ($cm^{-3}sec^{-1}$)

F_m : number formation rate of particles at τ_m, ($cm^{-3}sec^{-1}$)

h : relative humidity (r.h.) in the system, (%)

I_r : relative u.v. intensity, (-)

K : coagulation constant of particle, (cm^3/sec)

N : particle number concentration at irradiation time of τ, (cm^{-3})

N_m : maximum particle number concentration, (cm^{-3})

n : particle number concentration at time of t, (cm^{-3})

s : initial sulfur dioxide concentration, (ppm)

t : real time after u.v. irradiation is turned on under fixed residence time, (sec)

t_e : real time when particle number concentration reaches the equilibrium concentration, (sec)

t_o : real time when detectable particles are first formed, (sec)

β : diffusional deposition rate of particle to the chamber wall, (sec^{-1})

τ : irradiation time, i.e. average residence time in the reaction chamber, (sec)

τ_m : time when particle number concentration, N, reaches the maximum number concentration, (sec)

τ_o : threshold time when detectable particles are first formed, (sec)

References

[1] Gerhard, E. R. and Johnstone, H. F. (1955) : Photochemical oxidation of sulfur dioxide in air, Ind. Eng. Chem., Vol.47, pp.972-976.

[2] Renzetti, N. A. and Doyle, G. J. (1960) : Photochemical aerosol formation in sulfur dioxide - hydrocarbon systems, Int. J. Air Poll., Vol.2, pp.327-345.

[3] Wilson, Jr., W. E. and Levy. A. (1970) : A study of sulfur dioxide in photochemical smog. I. Effect of SO_2 and water vapor concentration in the 1-butene/NO_x/SO_2 system, J. Air Poll. Contr. Assoc., Vol.20, pp.385-390.

[4] Quon, J. E., Siegel, R. P. and Hulburt, H. M. (1970) : Particle formation from photolysis of sulfur dioxide in air, 2nd Int. Clean Air Congress, Washington, D. C., U.S.A., pp.330-335.

[5] Cox, R. A. and Penkett, S. A. (1970) : The photo-oxidation of sulfur dioxide in sunlight, Atmos. Environ., Vol.4, pp.425-433.

[6] Clark, W. E. (1972) : Measurements of aerosol produced by the photochemical oxidation of SO_2 in air, Ph.D. thesis, University of Minnesota.

[7] Bricard, J., Cabane, M., Madelaine, G. and Vigla, D. (1972) : Formation and properties of neutral ultrafine particles and small ions conditioned by gaseous impurities of the air, J. Colloid Interface Sci., Vol.39, pp.42-58.

[8] Friend, J. P., Leifer, R. and Trichon, M. (1973) : On the formation of stratospheric aerosols, J. Atmos. Sci., Vol.30, pp. 465-479.

[9] Cox, R. A. (1973) : Some experimental observations of aerosol formation in the photo-oxidation of sulfur dioxide, Aerosol Sci., Vol.4, pp.473-483.

[10] Bricard, J., Billard, F. and Madelaine, G. (1968) : Formation and evolution of nuclei of condensation that appear in air initially free of aerosols, J. Geophys, Res., Vol.73, pp. 4487-4496.

[11] Conner, W. D. and Nader, J. S. (1964) : Air sampling with plastic bags, Am. Ind. Hyg. Assoc. J., Vol.25, pp.291-297.

[12] Wohlers, H. C., Trieff, N. M., Newstein, H. and Stevens, W. (1967) : Sulfur - dioxide adsorption on - and desorption from Teflon, Tygon, glass, stainless steel and aluminium tubing, Atmos. Environ., Vol.1, pp.121-130.

[13] Environment/One Co. (1972) : Instrument instruction manual for condensation nuclei monitor, Model Rich 100.

[14] Walter, H. and Jaenicke, R. (1973) : Remarks about the smallest particle size detectable in condensation nuclei counters, Atmos. Environ., Vol.7, pp.939-944.

[15] Pedder, M. A. (1974) : Note on the smallest particles detected by condensation nucleus counters, Atmos. Environ., Vol.8, pp.1061-1062.

[16] Skala, G. F. (1963) : A new instrument for the continuous measurement of condensation nuclei, Anal. Chem., Vol.35, pp. 702-706.

[17] Dunham, S. B. (1960) : Detection of photochemical oxidation of sulphur dioxide by condensation nuclei techniques, Nature, Vol.188, pp.51-52.

[18] Koritsu-Kiki Inc. (1971) : SO_2 analyzer manual.

[19] Chand, R. and Marcote, R. V. (1971) : Evaluation of portable electrochemical monitors and associated stack sampling for stationary source monitoring, Am. Inst. Chem. Eng., 68th national meeting, Texas, U.S.A.

[20] Yamato Kogaku-Kiki Co. : Ace sensitive hygrometer manual.

Chapter 5

5. Physical and Chemical Properties of Photochemical Aerosols from Sulfur Dioxide

Size distribution and concentration of particles are probably the most fundamental and important factors for chemical, physical and physiological phenomena, such as formation mechanism of aerosol particles, reduction of visibility and toxicity of aerosol contaminants. In this chapter, the effects of environmental factors on the properties of sulfuric acid aerosols formed by photochemical oxidation of sulfur dioxide are investigated. The basic technique used in this investigation is diffusion tube method.

5.1 Introduction

The photochemical oxidation of sulfur dioxide leads to formation of aerosol particles which are identified to be sulfuric acid mist [1,2]. The formation mechanisms of sulfuric acid aerosols generally held are shown in Reaction (4.1) to (4.3), in Section 4.1.

A number of studies on the properties of sulfuric acid aerosols formed photochemically have been made as shown in Table 2-6. There is an apparent disagreement in particle size obtained from these experiments as shown in the table. The reaction rate for the oxidation or aerosol formation processes has been determined by considerable number of investigators (Hall [3], Gerhard and Johnstone [4], Renzetti and Doyle [5], Urone et al. [6], Cox et al. [7], Katz and Gale [8], Allen et al. [9] and others). There is also considerable disagreement in the reaction rate, and the values of reaction rate scatter in the range over several orders. These disagreements are considered to be due to the differences in the experimental conditions, such as temperature, degree of humidity, reactants,

reactant concentration, type of irradiation source, irradiation time, irradiation intensity and type of reaction chamber in the laboratory experiments. Therefore, it is difficult to interpret or to compare mutually these results.

Only a few studies has been performed on the chemical properties of photochemical aerosols (Endow et al. [1], Altshuller et al. [2], Renzetti and Doyle [5], and Doyle and Jones [10]). Endow et al. reported that sulfuric acid droplets formed in slightly humid atmosphere (10 to 20% r.h.) and 50% r.h. would be around 64% and 44% sulfuric acid by weight, respectively.

In this chapter, the effect of environmental factors on the properties of aerosol particles formed by photochemical oxidation of sulfur dioxide in air were investigated systematically, and sulfuric acid concentration of particles was determined. Beside, the volumetric formation rate was calculated from the data of the variation of particle size of aerosols with irradiation time, and then the reaction rate from sulfur dioxide to aerosols was determined.

5.2 Theory and Numerical Calculation on Diffusion Tube Method

5.2.1 General

Diffusion tube (D.T.) method is utilized for the determination of diffusion coefficient of gaseous and small particulate matter. This method can also be applied to the characterization of gaseous multi-component system as well as to the determination of particle size distribution of aerosols. Moreover, the contamination of tube due to the deposition of gaseous or particulate matter can be evaluated by calculating the deposited amount of those matter inside the tube.

Pollak and Metnieks [11] proposed first the "exhaustion method" for the determination of size distribution of polydisperse aerosols.

Fuchs [12], and Sansone and Weyel [13] calculated the penetration of polydisperse aerosols with log-normal particle size distribution through a parallel-wall channel and a circular tube, respectively. And they proposed a method for determining the size distribution of polydisperse aerosols assuming log-normal size distribution of aerosols. On the other hand, Twomey [14], Thomas [15] and Ikebe [16,17] proposed mathematical method for determining the size distribution of aerosols without any assumption concerning the form of particle size distribution.

For example of practical use of the diffusion tube or diffusion battery, Fuchs et al. [18] determined the particle size of aerosols by the diffusion tube method. Meagaw [19] determined the diffusion coefficient and particle diameter of nuclei in the reactor shell atmosphere by the diffusion battery method. And Browning and Ackley [20], and Takahashi [21,22] evaluated the amount of each compound in a multi-component system and the adsorption of iodine vapor on fume particles by means of diffusion tube method and radioactive technique.

5.2.2 Theory and Numerical Calculation

When submicron aerosol particles are suspended in a gaseous medium flow through a channel, some of them are brought into contact with the channel wall to deposit by random Brownian movement, or by diffusion of particles and the remains are penetrated through the channel.

Several equations for the penetration of aerosol passing through a circular tube as laminar flow were derived by various authors [23,24]. The deposition of aerosol particles onto the

inside wall surface of a tube is a function of the particle size r, flow rate Q, tube length X and the condition of the wall surface. In this study, assuming a perfect sink for the deposition surface, the equation of Gormley and Kennedy [24] is applied to the calculation, that is,

$$\frac{n}{n_o}\left(r, \frac{X}{Q}\right) = 0.819e^{-3.657y} + 0.097e^{-22.3y} + 0.032e^{-57y} \qquad (5.1)$$

at $n / n_o \leq 0.8$ $(y \geq 0.0312)$ and

$$\frac{n}{n_o}\left(r, \frac{X}{Q}\right) = 1 - 2.56\, y^{2/3} + 1.2\, y - 0.177\, y^{4/3} \qquad (5.2)$$

at $n / n_o \geq 0.8$ $(y \leq 0.0312)$.

Here, n / n_o is the number fraction of monodisperse particles leaving the tube to those entering the tube, and $y = \pi D X / Q$, where D is the diffusion coefficient of the aerosol particles. For spherical particle, the diffusion coefficient is given by Millikans equation [25] as a function of particle radius.

The number and mass fractions, denoted by N / N_o and M / M_o, respectively, of a monodisperse aerosol through the circular tube are given by Eq.(5.1) or (5.2). That is, for the monodisperse aerosols,

$$\frac{N}{N_o} = \frac{M}{M_o} = \frac{n}{n_o}\left(r, \frac{X}{Q}\right) \qquad (5.3)$$

The number and mass fractions of a polydisperse aerosol, of which particle size distribution is assumed to be log-normal, through the circular tube are given by the following equations.

$$\frac{N}{N_o}\left(r_g, \sigma_g, \frac{X}{Q}\right) = \int_{-\infty}^{\infty} \frac{n}{n_o}(r)\ f(r_g, \sigma_g)\ d(\log r) \qquad (5.4)$$

and

$$\frac{M}{M_o}\left(r_g,\sigma_g,\frac{X}{Q}\right)=\frac{\int_{-\infty}^{\infty}\frac{n}{n_o}(r)\ f(r_g,\sigma_g)\ r^3\,d(\log r)}{\int_{-\infty}^{\infty}f(r_g,\sigma_g)\ r^3\,d(\log r)} \tag{5.5}$$

where r_g is the geometric mean particle radius and σ_g is the geometric standard deviation, and $f(r_g,\sigma_g)$ is the log-normal distribution function expressed as,

$$f(r_g,\sigma_g)=\frac{1}{\sqrt{2\pi}\log\sigma_g}\exp\left(-\frac{(\log r-\log r_g)^2}{2(\log\sigma_g)^2}\right) \tag{5.6}$$

On the other hand, the number and mass fractions of deposited aerosol particles inside the circular tube are given by $1-N/N_o$ and $1-M/M_o$, respectively.

The numerical calculations of Eqs.(5.4) and (5.5) were carried out for the following ranges of r_g, $\log\sigma_g$ and X/Q.

r_g (μm) = 0.001 (0.0005) 0.010 (0.001) 0.015
$\log\sigma_g$ = 0, 0.05 (0.025) 0.15 (0.05) 0.30, 0.40
X / Q (sec/cm^2) = 5, 10, 20 (20) 100 (50) 300 (100) 1000

Some examples of the computational results of N/N_o and M/M_o are tabulated numerically in Appendix 4. In the table, LS and X/Q mean the values of $\log\sigma_g$ and X/Q (sec/cm^2) and the value of 0.642E-01, for example, means 0.642×10^{-1}. The whole data are tabulated elsewhere [Publication 3 in page ii]. Some of the results are also illustrated by diagrams as shown in Figs.5-1a, 5-1b and 5-1c.

5.2.3 Determination of Particle Size Distribution

As seen from the illustrated figures, a coupled value of

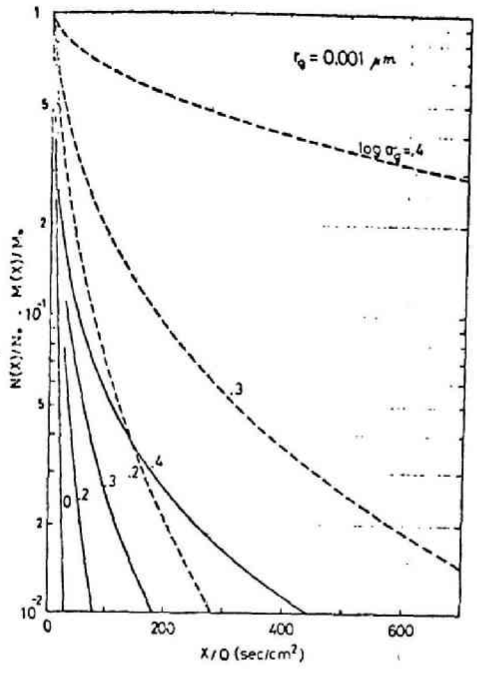

a. Geometric mean radius = 0.001 μm.

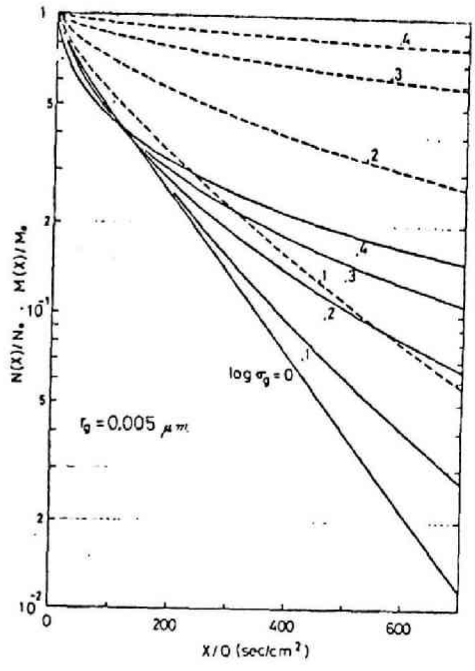

b. Geometric mean radius = 0.005 μm.

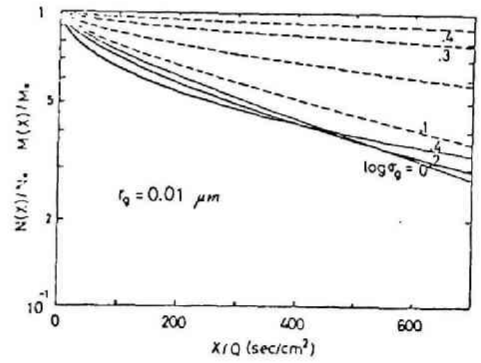

c. Geometric mean radius = 0.01 μm.

Fig. 5-1. N / N_o and M / M_o as a function of X / Q.
(Number and mass fraction of aerosol particles leaving tube to those entering tube)

$(N/N_o, X/Q)$ does not correspond to a unique particle size distribution function. This means that the particle size distribution satisfying a value of $(N/N_o, X/Q)$ can be expressed by a line on the r_g - $\log\sigma_g$ plane. So that, if a group of $(N/N_o, X/Q)_1, \cdots\cdots, (N/N_o, X/Q)_m$ were experimentally obtained, the most probable size distribution can be estimated from a crossing point of those lines corresponding to each value of $(N/N_o, X/Q)_m$. An experimental example of this method is shown in Fig.5-2.

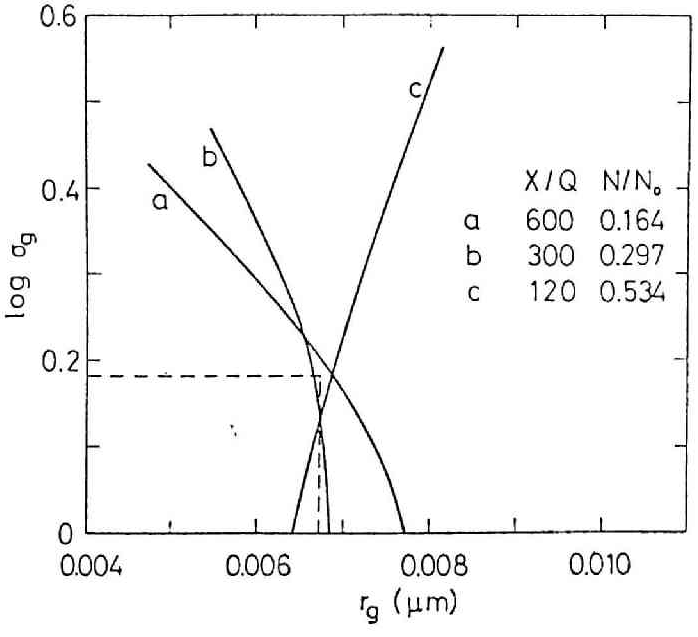

Fig. 5-2. An example of particle size determination.

(sulfuric acid : $r_g = 0.0067$ μm, $\log\sigma_g = 0.18$)

In usual practice, the particle size determination can be made by the number fraction measurement, while mass fraction measurement is applicable when the chemical quantitative analysis or radioactivity measurement is rather convenient.

An alternative method determining the particle size distribution from the measurement of deposited particles can be referred in other papers [20-22].

5.3 Experimental Equipment and Procedure

Particle size distribution of aerosols formed photochemically by ultraviolet (u.v.) irradiation of sulfur dioxide in pure air was determined for various combinations of SO_2 concentration, relative humidity and irradiation time. The experimental determination were made in the following ranges of environmental factors.

Table 5-1. Ranges of environmental factors used in this study

SO_2 concentration (s)	: 0.05 - 10 ppm
relative humidity (h)	: Dry - 80% r.h.
irradiation time (τ)	: 100 - 750 sec

On the other hand, sulfuric acid concentration of particles was determined for the environmental conditions of $s = 1$ ppm, 60% r.h. and $\tau = 500$ sec, and of $s = 10$ ppm, 60% r.h. and $\tau = 300$ sec.

The average u.v. intensity of light source used in those determinations was 0.15 m watt/cm^{2}sterad at the center of the irradiation box, and it is roughly 0.05 hr^{-1} of the specific absorption rate constant by SO_2.

Experimental equipments and procedure to form aerosol particles were the same to those descibed in Chapter 4.

Particle size distribution of aerosol formed by photochemical oxidation of sulfur dioxide was determined by diffusion tube method on the assumption of log-normal distribution. Four kinds of Teflon tube of 2, 5, 10 and 15 m in length and 5 mm in diameter were used as the diffusion tube. The number concentrations of particles both entering and leaving the tube were measured by the CNC for four kinds of Teflon tube, i.e. for four sets of values of X/Q, in each run. One of the original data obtained in the determination of size distribution by diffusion tube method is shown in Appendix 5-2. The geometric mean radius and the geometric standard deviation were determined by comparing (X/Q,

N/N_o) curve obtained experimentally with those obtained theoretically under the assumption of log-normal particle size distribution.

In addition to the experiments of particle size distribution determination by diffusion tube method, determination of sulfuric acid concentration of particles was attempted by measuring pH change of sulfuric acid particles deposited in the diffusion tube. Irradiated sample gas containing aerosol particles was passed through a Teflon diffusion tube of 20 m long for 75 - 270 sec. For reference, non-irradiated blank gas was also drawn from the flow control valve and passed through another diffusion tube under the same condition. And then, each tube was sufficiently washed by sodium borate solution of about pH 7. Sulfuric acid concentration of a particle was determined from the difference of hydrogen ion concentration between Sample and Blank, and from the experimental data of particle number concentration and particle radius.

5.4 Results and Discussion

5.4.1 Physical Properties of Aerosols

(1) Variation of particle size with irradiation time

Particle radii of aerosols produced by u.v. irradiation of 100, 200, 300, 500 and 750 sec were determined for the six combinations of SO_2 concentration and relative humidity. In this section, Run $r_\tau(s,h)$ represents the experimental run of the variation of particle radius r with irradiation time τ under SO_2 concentration of s ppm and relative humidity of h%.

Particle radius and particle number concentration are illustrated in Figs.5-3 and 5-4, respectively, as a function of irradiation time for above six Runs r_τ. In the figures, every point is the average of at least two separate measurements for each run

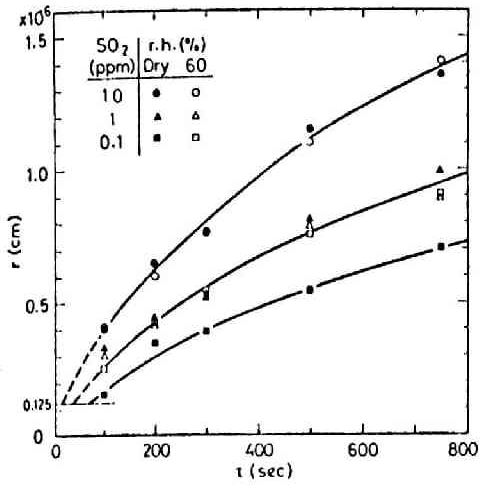

Fig. 5-3. Variation of particle radius of aerosols with irradiation time under various environmental conditions.

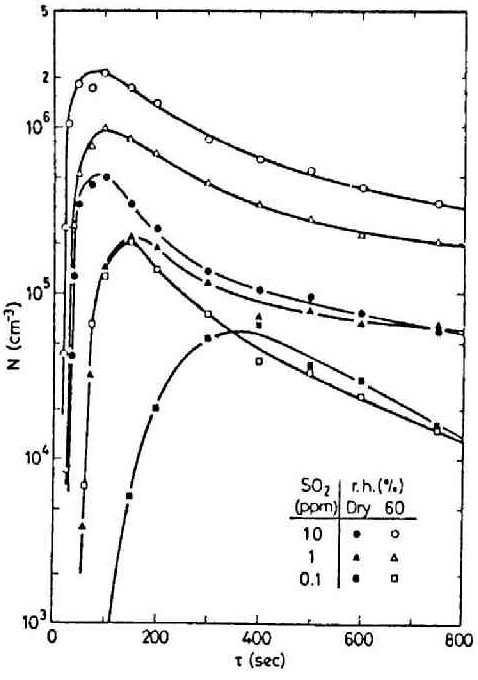

Fig. 5-4. Variation of particle number concentration of aerosols with irradiation time for various environmental conditions.

performed on different day. In this study, particle radius means a geometric mean radius under the assumption of log-normal size distribution. For any environmental condition, particle radius enlarged with irradiation time, particularly more quickly in a shorter region of irradiation time. Particle radius ranged from 0.0015 μm (τ = 100 sec, s = 0.1 ppm, h = Dry) to 0.014 μm (τ = 750 sec, s = 10 ppm, h = 60% r.h.) under the condition of this experiment. For the two higher SO_2 concentration, particle size and its growth rate were independent of relative humidity. But at the low SO_2 concentration (0.1 ppm), they were dependent evidently on relative humidity. The particle radius and its growth rate were also dependent strongly on SO_2 concentration in both cases of Dry and 60% r.h. The effects of SO_2 concentration and relative humidity on particle radius will be discussed in more detail in Figs. 6-8 and 6-9.

From a rough estimation of geometric standard deviation by applying diffusion tube method, it was summarized that the particle size distribution was almost homogeneous ($\log\sigma_g = 0$) at the shorter period of irradiation time than 300 sec and after that it broadened. However, the value of $\log\sigma_g$ is unlike to exceed 0.1 or 0.2 for SO_2 concentrations of 0.1 and 1 ppm or 10 ppm, respectively.

As was discribed in Chapter 4, the variation of particle number concentration of aerosol with irradiation time shows that, after some period (τ_o) from the onset of irradiation, the particle number concentration of aerosol increases rapidly. τ_o was dependent on both SO_2 concentration and relative humidity, and ranged from 15 sec (s = 10 ppm, h = 60% r.h.) to 85 sec (s = 0.1 ppm, h = Dry). On the other hand, the irradiation times (τ_c), when particle radius of 0.00125 μm is observed on the particle growth curve in Fig.5-3, ranged from 15 to 80 sec. From those data of τ_o and τ_c, it is verified that the detectable radius of the CNC is about 0.00125 μm which was given from the manufacturer.

(2) Variation of volume concentration and surface area concentration with irradiation time

The volume concentration (total volume of particles per unit air volume, V) and the surface area concentration (total surface area of particles per unit air volume, S) were calculated on the assumption that the shape of particle is spherical and that the particle size distribution is monodisperse. Figs.5-5 and 5-6 show the variations of V and S with irradiation time for the six different environmental conditions. Also in Fig.5-7, the particle number concentration N, V and S are illustrated on a linear scale as a function of irradiation time for Run rτ(1,60).

The volume concentration increased almost linearly with the increase of τ. The slope of V - τ line, $dV/d\tau$, represents the volume change per unit time and is called the volumetric formation

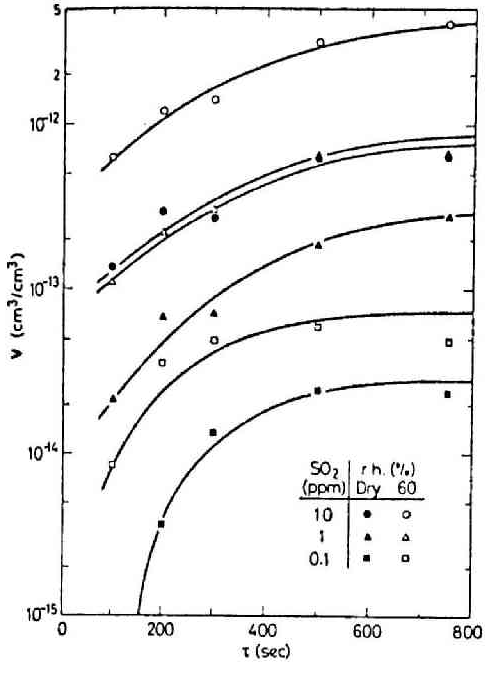

Fig. 5-5. Variation of volume concentration with irradiation time under various environmental conditions.

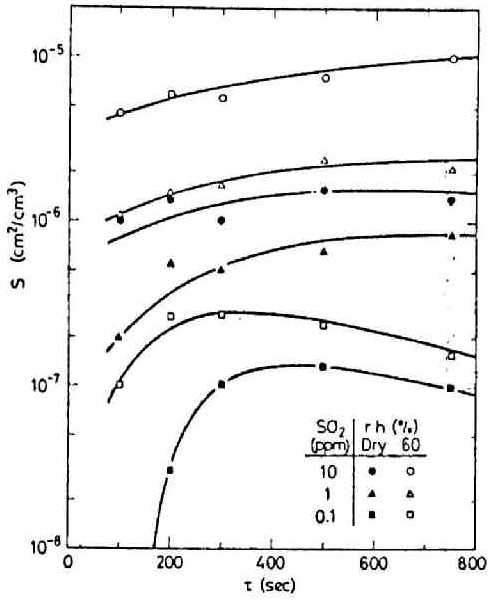

Fig. 5-6. Variation of surface area concentration with irradiation time under various environmental conditions.

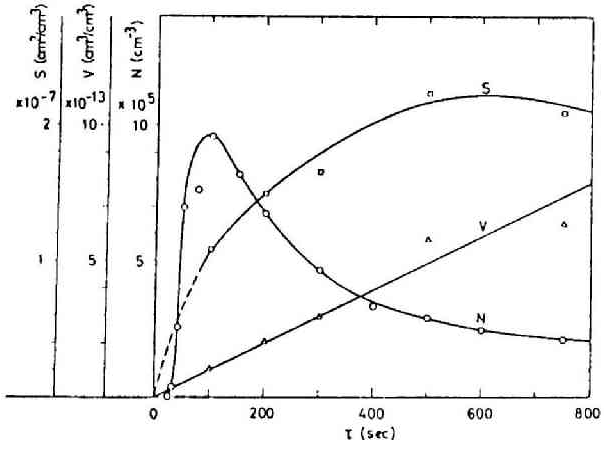

Fig. 5-7. Variation of particle number concentration, volume concentration and surface area concentration with irradiation time for Run rτ(1,60).

rate hereafter. The volumetric formation rate obtained for each Run r_τ ranges from 0.15 to 18.7 $\mu m^3/cm^3hr$ as shown in Table 5-2, and is very close to the data given by Clark [26].

Table 5-2. Volumetric formation rate for Run r_τ, ($\mu m^3/cm^3hr$)

SO_2 / r.h.	10 ppm	1 ppm	0.1 ppm
60 %	18.7	3.7	0.53
Dry	3.9	1.1	0.15

The surface area concentration increased first with irradiation time, and was found to reach an equilibrium value at a higher SO_2 concentration or to decrease gradually after reaching the maximum value at a lower SO_2 concentration.

At long irradiation time, since sulfuric acid gas consumption rate is constant and the volume of newly formed particles is negligibly small comparing with the total volume of already existing particles, the total volume increases linearly with τ as shown in Fig.5-7, i.e. $dV/d\tau$ = constant. According to the diffusional control growth theory, as the particle size is sufficiently smaller than the mean free path of gas molecules, $dV/d\tau$ is proportional to the surface area concentration S. Therefore, S is expected to be constant with respect to τ for long period of irradiation time. In fact, Clark [26] showed that S increases with the increase of τ at first and reaches to an equilibrium value.

At a longer irradiation time, in which the particle size distribution deviated from monodisperse, experimental values of V and S were sometimes lower than the values expected from above consideration. It is considered that the low value is partially due to the assumption of monodisperse particle size distribution. The

values of V and S will be 1.3 and 1.1 times as much for the particles of log-normal distribution with $\log \sigma_g = 0.1$, and 2.6 and 1.5 times as much for $\log \sigma_g = 0.2$.*

At a shorter irradiation time, the experimental values of V and S were also extremely low, especially at low SO_2 concentration and low relative humidity. It is considered to be due to a time lag of aerosol formation from sulfuric acid gas to sulfuric acid particle.

(3) Effects of sulfur dioxide concentration and relative humidity

In order to make detailed investigation of the effect of environmental condition on the particle size, SO_2 concentration and relative humidity were changed from 0.05 to 10 ppm and from Dry to 80% r.h., respectively. Determination of particle radius was performed for the cases of 28 combinations of SO_2 concentration and relative humidity. The experimental run for s ppm SO_2 concentration and h % r.h. is expressed by Run r(s,h). Irradiation time of 300 sec was adopted, because it was enough long to form considerable number of particles even for the case of Run r(0.05,Dry) in which the aerosol formation was the slightest in the range of this study, and because the particle size distribution could be regarded almost homogeneous in every conditions as mentioned above.

The geometric mean radius are illustrated in Figs.5-8 and 5-9 as a function of SO_2 concentration and relative humidity, respectively. From those figures and Fig.5-3, the following deductions are drawn ; Particle radius depends strongly on SO_2 concentration, and it increases with the increase of SO_2 concentration. On the other hand, the effect of relative humidity on particle

---

* $\log r_v = \log r_g + 3.454 \log^2 \sigma_g$; r_v = volume mean radius
$\log r_s = \log r_g + 2.303 \log^2 \sigma_g$; r_s = area mean radius

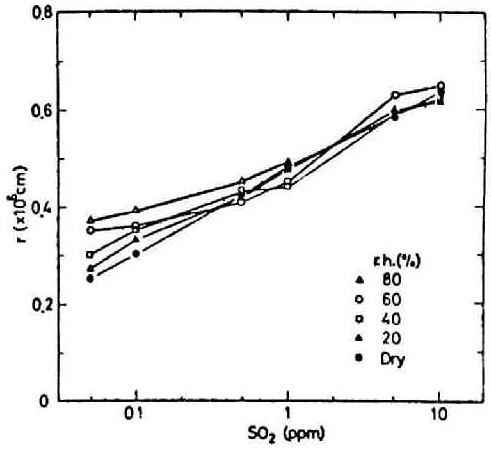

Fig. 5-8. Effects of sulfur dioxide concentration on particle radius at various relative humidities.

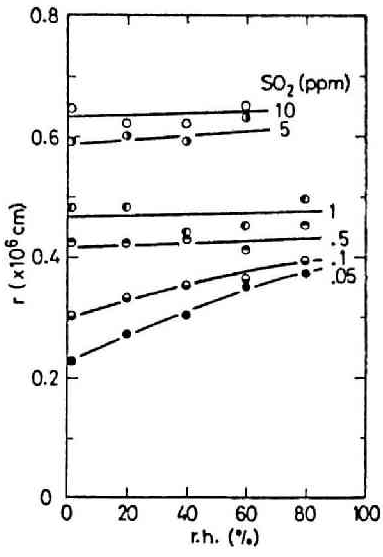

Fig. 5-9. Effects of relative humidity on particle radius at various sulfur dioxide concentrations.

radius is not uniform. At lower two SO_2 concentration (0.05 and 0.1 ppm), it increases evidently with relative humidity. At higher SO_2 concentration, however, there is no notable difference in particle radius with respect to relative humidity. Figs.5-10 and 5-11 show the volume concentration and surface area concentration, respectively, as a function of SO_2 concentration for various relative humidities. The volume concentration and the surface area concentration increase with the increases of SO_2 concentration and/or relative humidity. The rapid increases in lower SO_2 concentration and in lower relative humidity is thought to be due to the fact that the fraction of particulate sulfuric acid is low under those conditions as shown later in theoretical study of Chapter 6.

As a whole, it is considered that SO_2 concentration and relative humidity have effects on the formation and evolution processes of aerosol particles in the following manner ; Within this experimental condition, sufficient number of water molecule exist

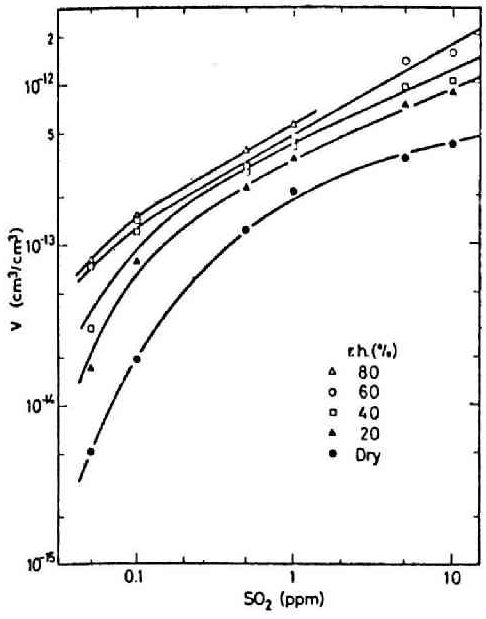

Fig. 5-10. Effect of sulfur dioxide concentration and relative humidity on volume concentration.

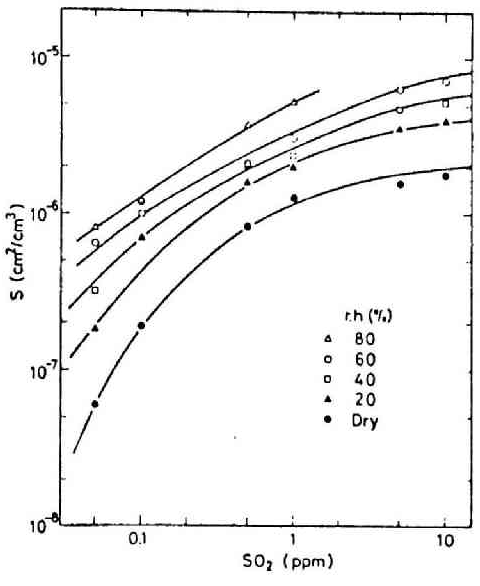

Fig. 5-11. Effect of sulfur dioxide concentration and relative humidity on surface area concentration.

comparing with sulfur dioxide molecule even at relative humidity of Dry, so that SO_2 concentration has almost proportional effect on the photochemical oxidation of sulfur dioxide and the continued hydration to form sulfuric acid gas by Reaction (4.1). The nucleation of sulfuric acid embryo by Reaction (4.2) depends on the amount of both sulfuric acid gas and water vapor molecules. As SO_2 concentration is higher, the nucleation is fast and large. And as relative humidity is higher, the fraction of sulfuric acid in the embryos is small, and the nucleation is also fast and large. Therefore, in the early stage of reaction in which the particle formation dominant rather than the particle growth, the particle formation process by Reaction (4.2) is strongly dependent on sulfuric acid gas concentration, i.e. SO_2 concentration and relative humidity, and the particle formation rate increases with the

increase of SO_2 concentration and relative humidity. With the growth of aerosol particles, Reaction (4.3) becomes dominant rather than Reaction (4.2). And then the most of sulfuric acid gas formed by Reaction (4.1) is consumed by Reaction (4.3). On the other hand, the absorption of water vapor molecules in Reaction (4.3) is restricted by the critical pressure of water vapor in a sulfuric acid particle, and is determined by particle size of aerosol and relative humidity of ambient air. So that, the particle growth by Reaction (4.3) is influenced mainly by number concentration and particle size of already existing aerosol particles, and by sulfuric acid vapor concentration, i.e. SO_2 concentration.

The effect of relative humidity on the particle growth is understood as follows ; Essentially, the increase of relative humidity has an effect of enhancing both nucleation rate and particle growth. The increase of nucleation rate implies rapid formation of smaller particles and reduction of average particle size. Resultantly, average size of all particles will be determined by the combined effect of these mechanisms. The effect of particle growth for already existing aerosol is predominant at a lower SO_2 concentration. However, the contributions of both effects associated with the change of relative humidity are possibly becoming comparable order at a higher SO_2 concentration.

As mentioned above, the effects of SO_2 concentration and relative humidity on the formation and evolution process of aerosol particles are generally much complicated. In this work, it is concluded that SO_2 concentration has an effect not only on the formation of aerosol particles but also on the particle growth, and that relative humidity has mainly effect on the formation of aerosol particles. In another word, the particle number concentration is strongly dependent on both SO_2 concentration and relative humidity, and the average particle size is mainly dependent

on SO_2 concentration.

5.4.2 Chemical Properties of Aerosols

The average sulfuric acid volume concentration of a particle $[H_2SO_4]_e$ was determined by the following equation;

$$[H_2SO_4]_e = \frac{3.0 \times 10^{20}\ v\ (10^{-pH_s} - 10^{-pH_b})}{N_o\ (1 - \frac{N_x}{N_o})\ Q_c\ t_s} \cdot \frac{1}{\frac{4}{3}\pi r^3} \cdot V_m$$

$$= 5.3 \times 10^{-3}\ v\ (10^{-pH_s} - 10^{-pH_b}) / (N_o - N_x)\ Q_c\ t_s\ r^3$$

where v is the volume in cc of standard solution (Borax + Bromothymol Blue), pH_s and pH_b are pH values of Sample and Blank, V_m is 7.44×10^{-23} cc/molecule of the molecular volume of sulfuric acid, N_o and N_x are particle number concentrations of aerosols entering and leaving the diffusion tube in particles/cm^3, Q_c is flow rate in the reaction chamber in cm^3/min, t_s is the sampling time in minute and r is particle radius in cm.

Several runs for determination of sulfuric acid concentration has been performed under the environmental conditions of s = 1 ppm, 60% r.h. and τ = 500 sec, and of s = 10 ppm, 60% r.h. and τ = 300 sec. The detailed data obtained are tabulated in Table 5-3.

The sulfuric acid concentration of particle calculated theoretically as a function of particle size and ambient relative humidity was about 42 and 45 weight per cent for 0.91 μm of particle radius at 60% r.h. and for 0.75 μm of particle radius at 60% r.h., respectively. Therefore, the results obtained experimentally show the values about four times as high as the theoretical. The followings are considered as the cause of error; 1) Use of larger value of v : Since some of standard solution remains in the diffusion tube, the real value of v should be less than the value used

Table 5-3. Sulfuric acid concentration of a particle

	s=1ppm, h=60% τ=500sec			s=10ppm, h=60% τ=300sec	
Q_c (cc/min)	300	300	300	500	500
t_s (min)	270	75	75	200	200
$N_o \times 10^{-5}$ (cm^{-3})	9.8	5.1	4.6	6.4	6.6
$N_x \times 10^{-5}$ (cm^{-3})	3.7	1.9	1.8	2.8	2.6
$\Delta H^+ \times 10^7$ (ion/l)[a]	3.3	1.0	0.43	3.0	2.7
v (ml)	20	25	25	20	20
$r \times 10^6$ (cm)	0.92	0.90	0.91	0.77	0.72
H_2SO_4 volume %	91	252	118	191	189
H_2SO_4 weight %	95				

a : ΔH^+ means the average value of $(10^{-pH_s} - 10^{-pH_b})$ calculated from three readings of pH_s and pH_b.

in estimation of sulfuric acid concentration; 2) Possibility that there is some problems on the accuracy of the CNC : The accuracy of the CNC influenced severely on estimation of the volume of particles deposited on the diffusion tube wall. Problems on the accuracy of the CNC is discribed in Appendix 2; 3) Assumption on the particle size distribution : The particle size distribution of aerosols is assumed to be monodisperse; and 4) Chemical analysis : The change of pH is extremely small and seems to be influenced by carbon dioxide in air. The contribution of each cause is uncertain yet.

Although there are differences between experimental and theoretical values by a factor of four, those data are thought to be meaningful because some errors are inevitable in such a

microanalysis technique which consists of both chemical and physical procedures.

5.4.3 Photochemical Oxidation Rate of Sulfur Dioxide

The photochemical oxidation of sulfur dioxide is generally accepted to be of the first order with respect to SO_2 concentration as proposed by Hall [3] and Gerhard and Johnstone [4]. Although the photochemical oxidation rate means strictly the fraction of sulfur dioxide oxidized per unit time, it can be estimated approximately from aerosol formation measurements as,

$$k = \frac{\text{number of } SO_2 \text{ molecules transfered into particles per unit time}}{\text{initial number of } SO_2 \text{ molecules}} \tag{5.8}$$

and calculated actually by the following equation;

$$k = \frac{10^{-12}\, V(\tau)\, \rho\, [H_2SO_4]_t\, (A/W) \times 3600}{2.46 \times 10^{13} [SO_2]\, \tau}$$

$$= 0.90\, V(\tau)\, \rho\, [H_2SO_4]_t \,/\, [SO_2]\, \tau \tag{5.9}$$

where k is the photochemical oxidation rate in hr^{-1}, $V(\tau)$ is the volume concentration at τ in (μm^3 of particle/cm^3 of air), ρ is the density of sulfuric acid in (gr of particle/cm^3 of particle), $[H_2SO_4]_t$ is the weight fraction of H_2SO_4 in sulfuric acid aerosol calculated theoretically as functions of particle radius and ambient relative humidity, A is the Avogadro number, W is the mole weight of sulfuric acid, 2.46×10^{13} is the number of molecules of 1 ppm gaseous matter per 1 cm^3 of air at 1 atm and 25°C $[SO_2]$ is SO_2 concentration in ppm, and τ is irradiation time in sec. Calculation of k for Run $r\tau(1,60)$ is shown in Table 5-4. The average value of k for the remain of Run $r\tau$ were calculated

Table 5-4. Photochemical oxidation rate for Run rτ(1,60)

	τ (sec)				
	100	200	300	500	750
$r \times 10^3$ (μm)	3.0	4.2	5.3	8.0	8.9
$[H_2SO_4]_t$ (%)	46	44	43	42	41
ρ (gr/cm³)	1.3	1.3	1.3	1.3	1.3
V (μm³/cm³)	0.11	0.21	0.29	0.59	0.62
$k \times 10^4$ (hr^{-1})	5.9	5.4	4.9	5.8	4.0

Average of $k = 5.2 \times 10^{-4}$ hr^{-1}

Table 5-5. Photochemical oxidation rates for Run rτ in % hr^{-1}

	SO_2 (ppm)		
	10	1	0.1
60% r.h.	0.028	0.052	0.061
Dry	0.016	0.039	0.046

Average k for Runs rτ = 0.040% hr^{-1}

in similar way and are shown in Table 5-5. The values of k decreases with the increase of SO_2 concentration, that is, the photochemical oxidation of sulfur dioxide deviates from the first order reaction and is apparently lower degree than the first order with respect to SO_2 concentration. However, the photochemical oxidation of sulfur dioxide is considered to be the first order reaction with respect to SO_2 concentration. Because,

as the particle growth is dominant and the reaction rate of Reaction (4.3) is larger than that of Reaction (4.1) by several order, the transfer of sulfuric acid vapor to particles must be proportional to the amount of sulfuric acid vapor, namely SO_2 concentration. The deviation from the first order reaction is thought to be due to some of the following items ; 1) The assumption of monodisperse size distribution for particles. That is, it leads to underestimating the value of $V(\tau)$ as mentioned before. It was confirmed experimentally that the deviation of particle size distribution was large as SO_2 concentration was higher. Therefore, it is possible that the value of k for the higher SO_2 concentration is underestimated ; 2) The accuracy of the CNC, as will be discussed in Appendix 2, and of sulfur dioxide analyzer ; 3) The possibility of transfer of sulfur dioxide molecule into particle without absorbing radiation energy ; 4) Deposition of particle onto the reaction chamber wall and 5) The accuracy of diffusion tube method.

Even though, the possibility still exists that the photochemical oxidation of sulfur dioxide deviates from the first order with respect to SO_2 concentration. In order to make sure this possibility, further experimental study is required by using more sensitive and reliable method.

The values of k for 60% r.h. were about 1.3 - 1.7 times as large as those for Dry. It has been reported by Shirai et al. [27], Katz and Gale [8], and Wilson and Levy [28] that the photochemical oxidation rate increased with the increase of relative humidity.

On the other hand, it is also thought that the scatter in the values of k tabulated in Table 5-5 is sufficiently small considering the accuracy limits of the particle size determination by diffusion tube method. The average value of k for six Runs $r\tau$

is 0.040% hr^{-1}. The effective u.v. intensity in the reaction chamber used in this study was estimated to be approximately equivalent to about $k_a = 0.05\ hr^{-1}$. Where k_a is the specific absorption rate constant of sulfur dioxide. And so, the over-all quantum yield Φ is estimated to be 8×10^{-3}. The value of k_a for noonday sunlight in summer (in Kyoto, N35°) is about 0.85 hr^{-1} as shown in Section 3.4. Therefore, by using the value of 8×10^{-3} for the quantum yield in the atmosphere, the photochemical oxidation rate of sulfur dioxide for noonday sunlight in summer is estimated to be 0.7% hr^{-1}.

Although a number of estimations of the solar photochemical oxidation rate and quantum yield have been reported, there are an apparent lack of agreement in those estimated values as shown in the review of Allen et al. [9]. Especially, the values of quantum yield scatter in the range over several orders. The solar (noonday in summer) photochemical oxidation rate of 0.7% hr^{-1} is slightly larger comparing with the results obtained by Hall [3], Gerhard and Johnstone [4], and Urone et al. [6] and almost agreement with those by Cox et al. [7], and Katz and Gale [8]. And the over-all quantum yield of 8×10^{-3} is within the region of 10^{-3} - 10^{-2} which was obtained by the most of the investigators [3,4,7,9,29].

List of Symbols in Chapter 5

A : Avogadro number, ($mole^{-1}$)

h : relative humidity (r.h.) in system, (%)

k : photochemical oxidation rate, (sec^{-1} or hr^{-1})

k_a : specific absorption rate constant, (sec^{-1} or hr^{-1})

M : mass of aerosols leaving diffusion tube, (gr/cm^3)

M_o : " " " entering diffusion tube, (gr/cm^3)

N : particle number concentration at irradiation time of τ, (cm^{-3})

N_o, N_o or n_o : particle number concentration of aerosols leaving diffusion tube, (cm^{-3})

N_x, N or n : particle number concentration of aerosols entering diffusion tube, (cm^{-3})

Q : flow rate in diffusion tube, (cm^3/sec or cm^3/min)

Q_c : " " in reaction chamber, (cm^3/sec or cm^3/min)

r : particle radius, (cm)

r_g : geometric mean particle radius, (cm)

S : surface area concentration, (cm^2/cm^3)

s : sulfur dioxide concentration, (ppm)

t_s : sampling time, (sec or min)

V : volume concentration, (cm^3/cm^3)

V_m : molecular volume of sulfuric acid, (cm^3/molecule)

v : volume of standard solution, (cc)

W : molecular weight of sulfuric acid, (gr/mole)

X : length of the diffusion tube, (cm)

ρ : density of sulfuric acid, (gr/cm^3)

σ_g : geometric standard deviation of particle size distribution, (-)

τ : irradiation time, (sec)

τ_o : time when detectable particle are first formed, (sec)

Φ : over-all quantum yield, (-)

References

[1] Endow, N., Doyle, G. J. and Jones, J. L. (1963) : The nature of some model photochemical aerosol, J. Air Poll. Contr. Assoc., Vol.13, pp.141-147.

[2] Altshuller, A. P., Kopczynski, S. L., Lonneman, W. A., Becker, T. L. and Wilson, D. L. (1968) : Photochemical of propylene with nitrogen oxide in presence of sulfur dioxide, Environ. Sci. Tech., Vol.2, pp.696-698.

[3] Hall, T. C. (1953) : Photochemical studies of nitrogen dioxide and sulfur dioxide, Ph.D. Thesis, Univ. of California at Los Angeles.

[4] Gerhard, E. R. and Johnstone, H. F. (1955) : Photochemical oxidation of sulfur dioxide in air, Ind. Eng. Chem., Vol.47, pp.972-976.

[5] Renzetti, N. A. and Doyle, G. J. (1960) : Photochemical aerosol formation in sulfur dioxide - hydrocarbon systems, Int. J. Air Poll., Vol.2, pp.327-345.

[6] Urone, P., Lutsep, H., Noyes, C. M. and Parcher, J. F. (1968) : Static studies of sulfur dioxide reactions in air, Environ. Sci. Tech., Vol.2, pp.611-618.

[7] Cox, R. A. and Penkett, S. A. (1970) : The photo-oxidation of sulfur dioxide in sunlight, Atmos. Environ., Vol.4, pp.425-433.

[8] Katz, M. and Gale, S. B. (1970) : Mechanism of photooxidation of sulfur dioxide in atmosphere, 2nd Int. Clean Air Congress, Washington, D. C., CP1E pp.336-343.

[9] Allen, E. R., McQuigg, R. D. and Cadle, R. D. (1972) : The photooxidation of gaseous sulfur dioxide in air, Chemosphere, Vol.1, pp.25-32.

[11] Pollak, L. W. and Metnieks, A. L. (1957) : On the determination of the diffusion coefficients of heterogeneous aerosols by the dynamic method, Geofisica Pura e Applicata, Vol.37, pp.183-190.

[12] Fucks, N. A., Stechkina, I. B. and Strosselskii, V. I. (1962) : On the determination of particle size distribution in polydisperse aerosols by diffusion method, Brit. J. Appl. Phys., Vol.13, pp.280-281.

[13] Sansone, E. B. and Weyel, D. A. (1971) : A note on the penetration of a circular tube by an aerosol with a log-normal size distribution, J. Aerosol Sci., Vol.2, pp.413-415.

[14] Twomey, S. (1963) : The determination of aerosol size distributions from diffusional decay measurements, J. Franklin Inst., Vol.275, pp.121-138.

[15] Thomas, J. W. (1966) : Distribution of radioactivity on a polydisperse aerosol by the diffusion method, Health Phys., Vol.12, pp.765-768.

[16] Ikebe, Y. (1972) : Determination of the size distribution of polydisperse submicron aerosols by a response matrix method, Pure Appl. Geophys., Vol.98, pp.197-212.

[17] Ikebe, Y. and Hata, S. (1972) : Determination of the size distribution of submicron aerosols by diffusion method (in Japanese), Oyo Butsuri, Vol.41, pp.77-79.

[18] Fuchs, N. A. and Sutugin, A. G. (1963) : Generation and investigation of high-dispersed sodium chloride aerosols, Brit. J. Appl. Phys., Vol.14, pp.39-42.

[19] Meagaw, W. J. (1965) : The absorption of iodine on atmospheric particles, J. Nuclear Energy, Vol.19, pp.585-595.

[20] Browning, Jr. W. E. and Ackley, R. D. (1962) : Characterization of millimicron radioactive aerosols and their removal from gases, TID - 7641, pp.130-147.

[21] Takahashi, K. (1966) : Experiments on adsorption of radioactive iodine vapor on small metallic fume particles, J. Nuclear Sci. Tech., Vol.3, pp.401-403.

[22] Takahashi, K. (1967) : Application of diffusion tube method to characterization of gas-particle mixture (in Japanese), Hoken Butsuri (J. Japan Health Phys. Soc.), Vol.2, pp.115-120.

[23] Berezhnoi, V. M. and Kirichenko, V. V. (1964) : Theory of diffusive deposition of decay products of inert gases in circular and flat channels, Sov. J. Atomic Energy, Vol.17, pp.300-302.

[24] Gormley, P. G. and Kennedy, M. (1949) : Diffusion from a stream flowing through a cylindrical tube, Proc. Roy. Irish Acad., Vol.A-52, pp.163-169.

[25] Millikan, R. A. (1923) : The general law of fall through a gas, Phys. Rev., Vol.22, pp.1-23.

[26] Clark, W. E. (1972) : Measurements of aerosol produced by the photochemical oxidation of SO_2 in air, Ph.D. Thesis, Univ. Minnesota.

[27] Shirai, T., Hamada, S., Takahashi, H., Ozawa, T., Ohmuro, T. and Kawakami, T. (1962) : Photooxidation of sulfur dioxide in air (in Japanese), Kagaku Zashi (J. Chem. Soc. Japan), Vol.65, pp.1906-1911.

[28] Wilson, Jr. W. E. and Levy, A. (1970) : A study of sulfur dioxide in photochemical smog, I. Effect of SO_2 and water vapor concentration in the 1-butene/NO_x/SO_2 system, J. Air Poll. Contr. Assoc., Vol.20, pp.385-390.

[29] Sethi, D. S. (1971) : Photo-oxidation of sulfur dioxide, ibid., Vol.21, pp.418-420.

Chapter 6

6. Kinetic Model of Aerosol Formation from Photochemical Oxidation of Sulfur Dioxide

Theoretical approach is also important and effective way to make clear the mechanism of aerosol formation from photochemical oxidation of sulfur dioxide. In this chapter, the nucleation rate for a system of water and sulfuric acid vapor is calculated according to Reiss's theory, and a kinetic model of the photochemical aerosol formation process from sulfur dioxide in air is proposed and some calculated examples are shown.

6.1 Introduction

Sulfur dioxide in air is oxidized photochemically to form sulfuric acid aerosol particles. The formation process of aerosols consists of three stages, namely photochemical oxidation and hydration, nucleation, and growth, and can be schematized as Reactions (4.1), (4.2) and (4.3).

As was described in detail in Section 2.7, the kinetic model of phase transition in two component, such as sulfuric acid mist from sulfur trioxide and water vapor, has been first presented by Reiss [1]. The quasi - thermodynamic approach to Reiss's theory was tried by Doyle [2]. On the basis of Reiss - Doyle theory, Doyle, Kiang et al. [3,4], and Mirabel and Katz [5] calculated the nucleation rate of embryo from a binary system of sulfuric acid and water vapor.

Walter [6] calculated the changes of concentration and size distribution of condensation aerosols with time when there is a constant rate of production of primary particles of uniform size. Also Stauffer et al. [7] calculated the growth of sulfuric acid droplets originating from the binary homogeneous system of sulfuric acid and water vapor.

6.2 Nucleation of Sulfuric Acid Embryos

According to the theoretical study by Reiss [1], the nucleation rate I from a binary system such as sulfuric acid and water vapor can be expressed as,

$$I = C \exp(-\Delta G / \kappa T) \ , \tag{6.1}$$

where C is a factor containing the probability of capture of molecule of vapor by critical embryo, κ is the Boltzmann constant, T is the absolute temperature, and ΔG is the free energy of formation of embryo consisting of n_1 sulfuric acid and n_2 water molecules and is expressed as,

$$\Delta G = ({}^2\mu_1 - {}^1\mu_1)\, {}^2n_1 + ({}^2\mu_2 - {}^1\mu_2)\, {}^2n_2 + 4\pi r^2 \sigma \ , \tag{6.2}$$

where μ is chemical potential, r is embryo radius and σ is surface tension. The anterior super script denotes the phase, 1 for gas and 2 for liquid (embryo). The posterior subscript denotes the component (here, 1 for sulfuric acid, 2 for water).

Formation of embryo of critical size r_o will take place at the saddle point condition of ΔG in respect to the amount of each component, that is,

$$\left(\frac{\partial\, \Delta G}{\partial\, n_1}\right)_{n_2} = \left(\frac{\partial\, \Delta G}{\partial\, n_2}\right)_{n_1} = 0 \ . \tag{6.3}$$

This leads to the "critical" free energy.

$$\Delta G_o = \frac{4\pi}{3} r_o^{\,2}\, \sigma_o \ . \tag{6.4}$$

The subscript o denotes values at the saddle point. On the other hand, the frequency factor C at the saddle point is given by the following equation [1];

$$C = \frac{\beta_1 \beta_2}{\beta_1 \sin^2\theta + \beta_2 \cos^2\theta} (N_1 + N_2) S_f \left(-\frac{P}{Q}\right)^{1/2} \qquad (6.5)$$

where β_i represents the rate at which molecules of component i strike unit area of embryo surface ($cm^{-2}sec^{-1}$), θ is the angle that the radius vector make with the original axis, and N_i is the molecular concentration of component i (cm^{-3}), S_f is surface area of embryo at saddle point (cm^2) and P and Q are, respectively, second partial derivative of ΔG in direction of steepest descent and of steepest ascent at the saddle point.

The nucleation rate in the sulfuric acid - water system was calculated by substituting Eqs.(6.4) and (6.5) into Eq.(6.1) for the relative humidities of 10, 30, 50, 60, 70 and 90%, and for the temperature of 25°C. In the calculation, the values of surface tension and density of sulfuric acid solution were obtained from the texts of I.C.T. [8] and Perry [9]. Fig.6-1 shows calculated values of I and I / N_g, where N_g is the number concentration of sulfuric acid vapor molecule in air. Eq.(6.1) has been also calculated for a system of water and sulfuric acid system by Doyle [2] at 50% r.h., by Kiang et al.[3,4] and by Mirabel and Katz [5] at various relative humidities. Our results give smaller values than Doyle's, and somewhat larger than

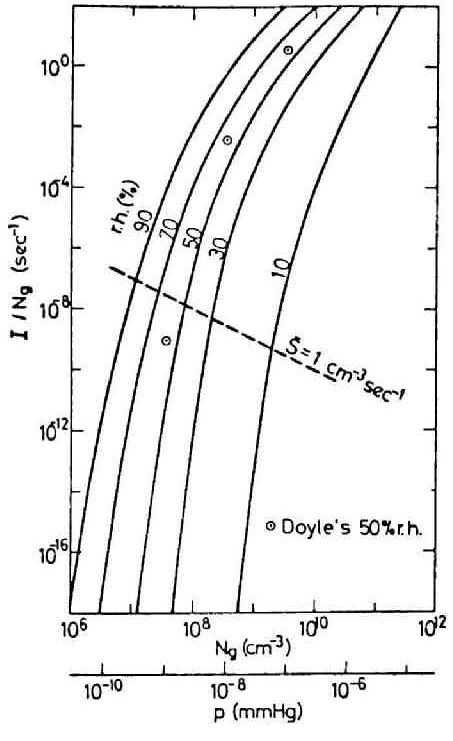

Fig.6-1. Nucleation rate of sulfuric acid embryo at 25°C. p is the sulfuric acid vapor pressure.

those by Kiang et al. The differences in the results, however, small at higher vapor pressure of sulfuric acid and less than three orders of magnitude even at very low vapor pressure. The nucleation rate increases rapidly with the increase of sulfuric acid vapor pressure, and it is strongly dependent on relative humidity. As was noted by Doyle [3] and Kiang et al. [10], the values of nucleation rate especially for low concentration of sulfuric acid vapor may be in error by at least two orders of magnitude, mainly due to the uncertainity of vapor pressure for such a small embryo.

Here, for the convenience of calculation, the values of nucleation rate were approximated by,

$$y = -238.7 + 69.87\,x - 6.90\,x^2 + 0.2333\,x^3 \quad ; \text{for 90\% r.h.} \quad (6.6a)$$

$$y = -489.1 + 147.4\,x - 15.0\,x^2 + 0.5167\,x^3 \quad ; \text{for 60\% r.h.} \quad (6.6b)$$

$$y = -593.4 + 179.4\,x - 18.3\,x^2 + 0.6333\,x^3 \quad ; \text{for 50\% r.h.} \quad (6.6c)$$

$$y = -326.3 + 57.20\,x - 2.50\,x^2 \quad ; \text{for 10\% r.h.} \quad (6.6d)$$

where, $x = \log_{10}(N_g)$, and $y = \log_{10}(I / N_g)$.

Fig.6-2 shows the calculated results for the number of total molecule of water and sulfuric acid per embryo, mole fraction of sulfuric acid, and the radius of critical embryo. From these results, we find that the critical size of embryo is about 10^{-7} cm, and a critical embryo contains 5 to 20 molecules of sulfuric acid.

6.3 Kinetic Model of Aerosol Formation and Growth

As was illustrated before, various gaseous components such as sulfur dioxide, sulfur trioxide, sulfuric acid and water, and various sized aerosol particles exist in the system. Here, taking two components of sulfuric acid vapor and particle into account, the

following equation for the number concentration of each component is formulated.

$$\frac{d N_g}{d \tau} = S - (\alpha + \beta_g + \gamma N_p) N_g \tag{6.7}$$

$$\frac{d N_p}{d \tau} = \frac{\alpha}{i_o} N_g - \beta N_p - K N_p^2 + S_p \tag{6.8}$$

where, N_p is the number concentration (cm^{-3}) of aerosol particles formed including embryos, τ is the time (sec) of aerosol formation and irradiation continues throughout this time, S is the conversion rate ($cm^{-3} sec^{-1}$) of sulfur dioxide to sulfuric acid by photochemical oxidation (named photochemical oxidation rate hereafter) and is given as a function of sulfur dioxide concentration and irradiation light intensity, α is the conversion rate of sulfuric acid vapor to embryo (sec^{-1}) and equated by $I = \alpha N_g / i_o$, β_g and β is, respectively, the deposition rate (sec^{-1}) of sulfuric acid vapor and particle to boundary surfaces, γ is the deposition rate (cm^3/sec) of sulfuric acid vapor to already formed aerosol particles, i_o is the number of sulfuric acid molecules contained in a nucleated

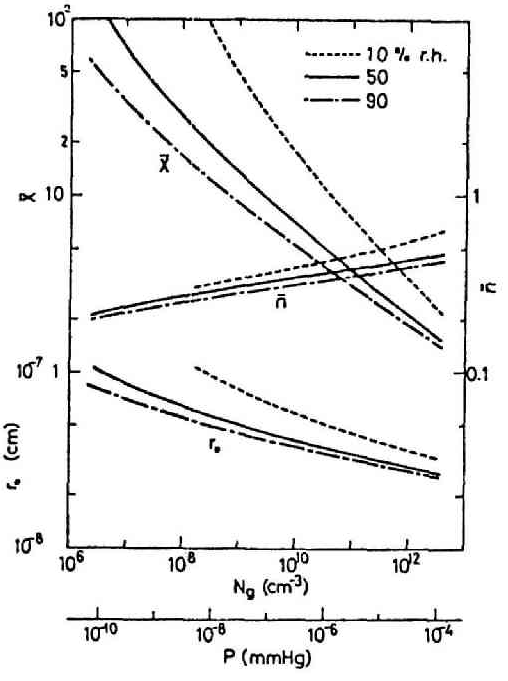

Fig. 6-2. Properties of critical embryo of sulfuric acid. X is total number of molecule, n is mole fraction of sulfuric acid, and r_o is radius of embryo.

embryo, K is the coagulation constant (cm^3/sec), and S_p represents the foreign particle sources other than photochemical reaction. In another word, S_p is the number of sulfuric acid particles added into the system or formed by other mechanism than photochemical reaction in the system, per unit volume per unit time ($cm^{-3}sec^{-1}$).

A newly nucleated embryo consists of certain number of sulfuric acid molecule and also of water molecule. As the time passed, sulfuric acid molecules condense on the particle and, as a result, the concentration of sulfuric acid become higher. Simultaneously, water molecules will also condense on the particle causing it to grow until the water vapor pressure attains equilibrium with the relative humidity of ambient air. This means that the particle size is time dependent, so that γ, β and K are also time dependent.

Neglecting the coagulation effect, the time change of the number of sulfuric acid molecules contained in a particle can be given by,

$$i = i_o + \int_0^\tau \gamma N_g \, d\tau \tag{6.9}$$

and, by ignoring the latent heat of condensation, Fuchs'[11] expression for γ is applicable,

$$\gamma = \frac{\pi v r^2}{\frac{1}{\delta} + \frac{v r^2}{4 (r + l) D_g}} \tag{6.10}$$

where, r is the particle radius (cm), v is the mean thermal velocity of vapor molecule (cm/sec), l is the length nearly equal to the mean free path of the gas molecule ($l \doteqdot 10^{-5}$cm), D_g is the diffusivity of vapor molecules in air, and δ is the condensation probability of the molecule onto a particle and is assumed to be unity in this study.

The equilibrium particle radius can be calculated by a trial

and error method using the next equation in conjunction with Eq. (6.9).

$$\frac{r.h.}{100} = \exp\left(\frac{2\,\sigma\,M}{\rho\,R\,T\,r}\right)\cdot A \qquad (6.11)$$

where, σ and ρ are the surface tension and the density, respectively, of sulfuric acid particles, M is the molecular weight of water, and A is the chemical activity of water in a particle. The physical and chemical properties of sulfuric acid and water vapor are tabulated in Table 6-1.

Table 6-1. Values of physical and chemical properties of H_2SO_4 and H_2O vapor, at 20°C and 1 atm.

	H_2SO_4	H_2O
M : molecular weight (gr/mole)	98	18
V_m : molecular volume (cm^3/molecule)	8.78×10^{-23}	2.99×10^{-23}
v : mean thermal velocity (cm/sec)	2.48×10^4	5.94×10^4
D_g : diffusivity (cm^3/sec in air)	0.0972	0.20
ρ : density (gr/cm^3)	1.854	0.998
σ : surface tension (dyne/cm)	54.6	72

Substituting these values in Eq.(6.10), γ for sulfuric acid and water vapor become as follows;

$$\gamma_{H_2SO_4} = 7.785 \times 10^4 r^2 / [1 + 6.37 \times 10^4 r^2 / (r + 10^{-5})] \qquad (6.12a)$$

$$\gamma_{H_2O} = 1.866 \times 10^5 r^2 / [1 + 7.43 \times 10^4 r^2 / (r + 10^{-5})] \qquad (6.12b)$$

The surface tension and density of sulfuric acid particle depend on the amounts of sulfuric acid and water in particles. On the

basis of the data from Mellor's text [12], they were formulated as a function of the weight fraction of sulfuric acid, w, as,

$$\begin{aligned} \sigma &= 72.0 + 11.0\ w && ;\ \text{for } w \leq 0.4 \\ &= 87.08 - 74.9\ w + 172.5\ w^2 - 130.0\ w^3 && ;\ \text{for } w > 0.4 \end{aligned} \tag{6.13}$$

$$\begin{aligned} \rho &= 0.9999 + 0.6191\ w + 0.398\ w^2 && ;\ \text{for } w \leq 0.85 \\ &= 1.853 + 0.2045\ (1-w) - 3.746\ (1-w)^2 && ;\ \text{for } w > 0.85 \end{aligned} \tag{6.14}$$

On the other hand, chemical activity, A, can be given by Raoult law for a solution of low concentration as expressed by Mason [13]. And a more generalized form for higher concentrations was described by Low [14]. However, as was pointed out by Vohra and Nair [15], the chemical activity for higher concentrations should be determined experimentally. Hence, based on the values in Meller's text [12], the following approximation was applied for the chemical activity of sulfuric acid solution at the temperature of 25°C.

$$A = \exp\left(-1.274\ w + 4.304\ w^2 - 11.47\ w^3\right) \tag{6.15}$$

where, w is the weight fraction of sulfuric acid. Fig.6-3 shows the equilibrium water vapor pressure as a function of particle size

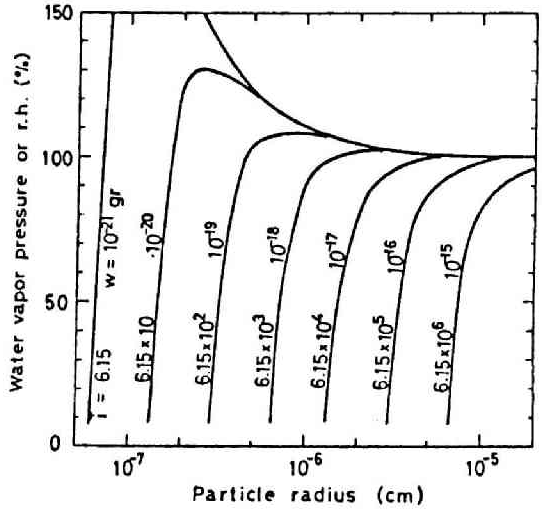

Fig.6-3. Equilibrium water vapor pressure of particle containing sulfuric acid at 25°C. w is sulfuric acid mass per particle, and i is number of sulfuric acid molecule.

and amount of sulfuric acid per particle.

6.4 Computational Method

The numerical computations were performed with digital electronic computer FACOM 230 - 60. An example of flow chart and programme are shown in Fig.6-4 and Appendix 3, respectively.

Eqs.(6.7) through (6.15) were calculated applying the Improved Cauchy - Polygon method with the time interval of 0.3 sec ($=\Delta\tau$). The method is schematized in Fig.6-5, that is,

1) Consider N_{g1} and N_{p1} to be the concentration of sulfuric acid vapor and particles at J $\Delta\tau$ sec.
2) The approximate value of N_g at $(J+1)\Delta\tau$ sec, N_{g2}, can be determined from Eq.(6.7) with N_{g1} and N_{p1} both as the temporary representative values (T.R.V.) and as the initial concentration (I.C.) of N_g and N_p at (J+1)-th step.
3) The approximate value of N_p at $(J+1)\Delta\tau$ sec, N_{p2}, is determined from Eq.(6.8) with N_{g3} and N_{p1} as T.R.V. and with N_{g1} and N_{p1} as I.C., where N_{g3} is the average value of N_{g1} and N_{g2}. And similarily $N_{p3} = (N_{p1} + N_{p2}) / 2$.
4) Since N_{g3} and N_{p3} are considered to be the representative values (R.V.) between $J\Delta\tau$ and $(J+1)\Delta\tau$ sec, the final value of N_g at $(J+1)\Delta\tau$ sec can be calculated from Eq.(6.7) with N_{g3} and N_{p3} as R.V. and with N_{g1} and N_{p1} as I.C.
5) The final value of N_p at $(J+1)\Delta\tau$ sec can be calculated from Eq.(6.8) with N_{g4} and N_{p3} as R.V. and with N_{g1} and N_{p1} as I.C., where N_{g4} is the average of N_{g1} and N_g.

The accuracy of numerical computation can not be determined clearly, but from trial computations by changing the time interval and from the consideration of the magnitude of various factors included in Eqs.(6.7) and (6.8), this time interval was thought to be small enough for the present work.

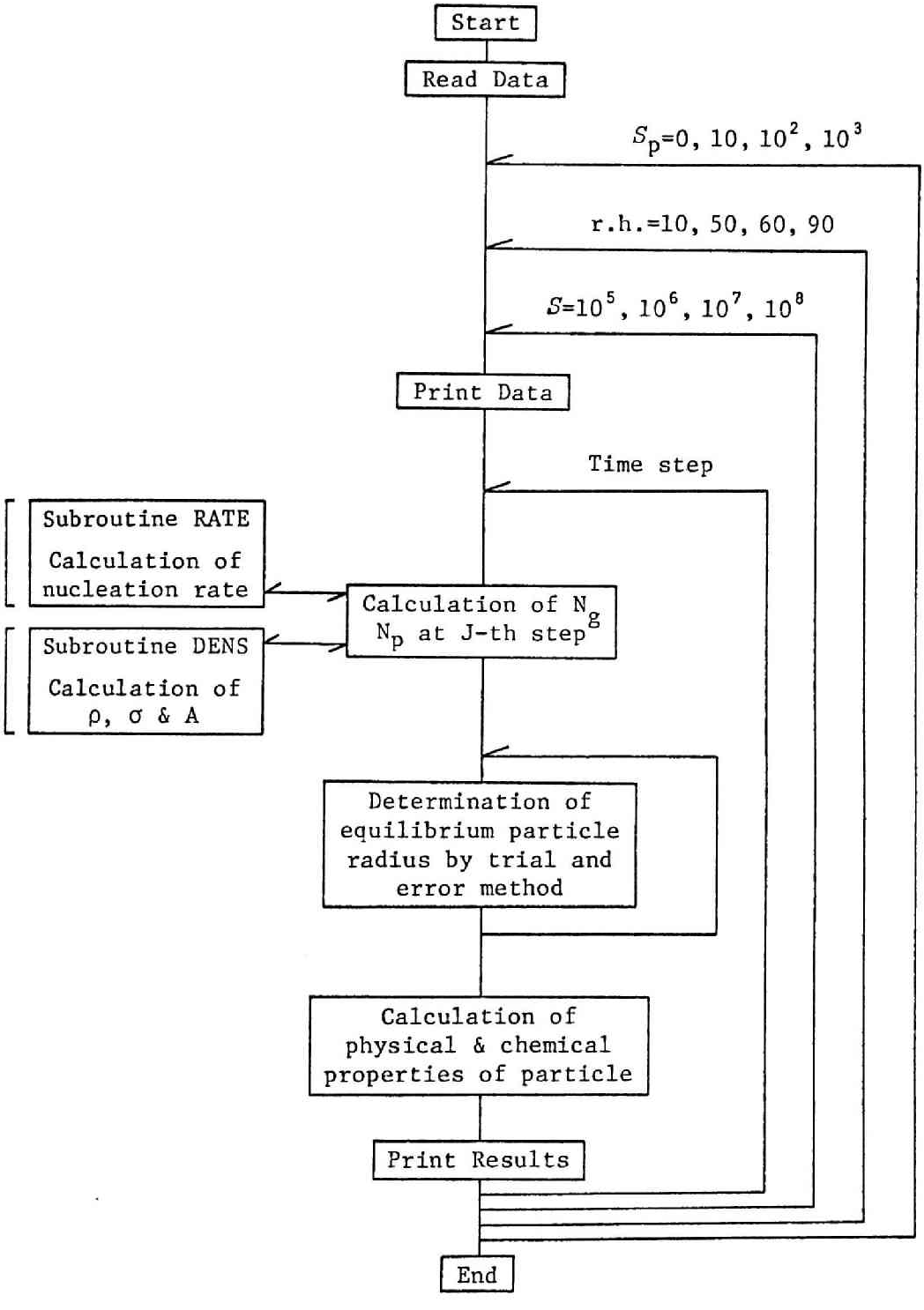

Fig.6-4. Flow chart for numerical computaion of kinetic model

1) Determination of the representative values of N_g and N_p between $J\Delta\tau$ and $(J+1)\Delta\tau$ sec., i.e. at $(J+1)$-th step.

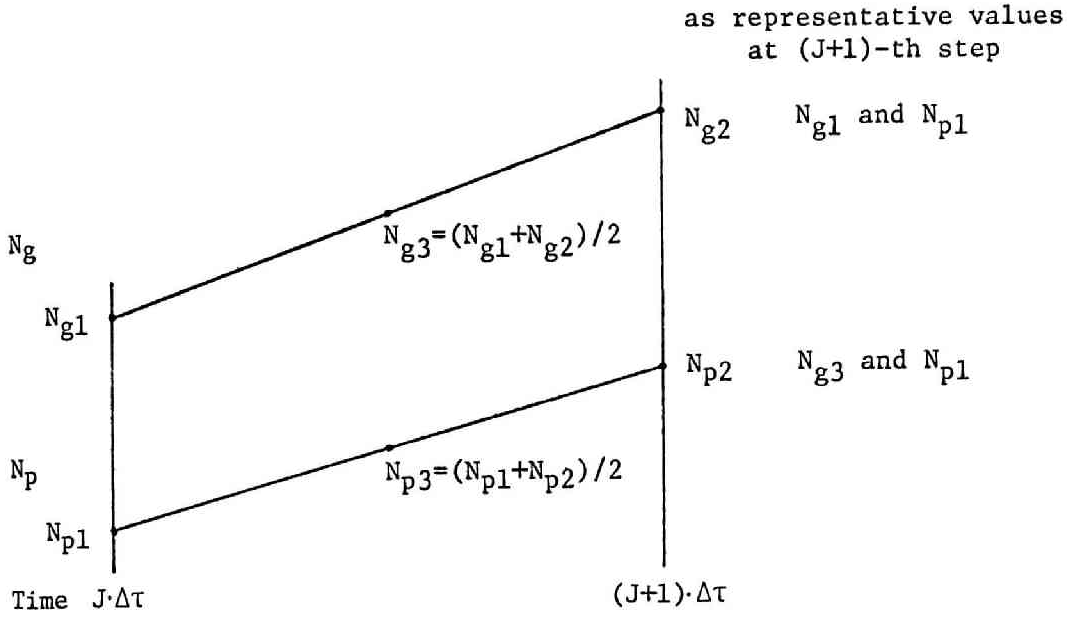

2) Determination of N_g and N_p at $(J+1)\Delta\tau$ sec.

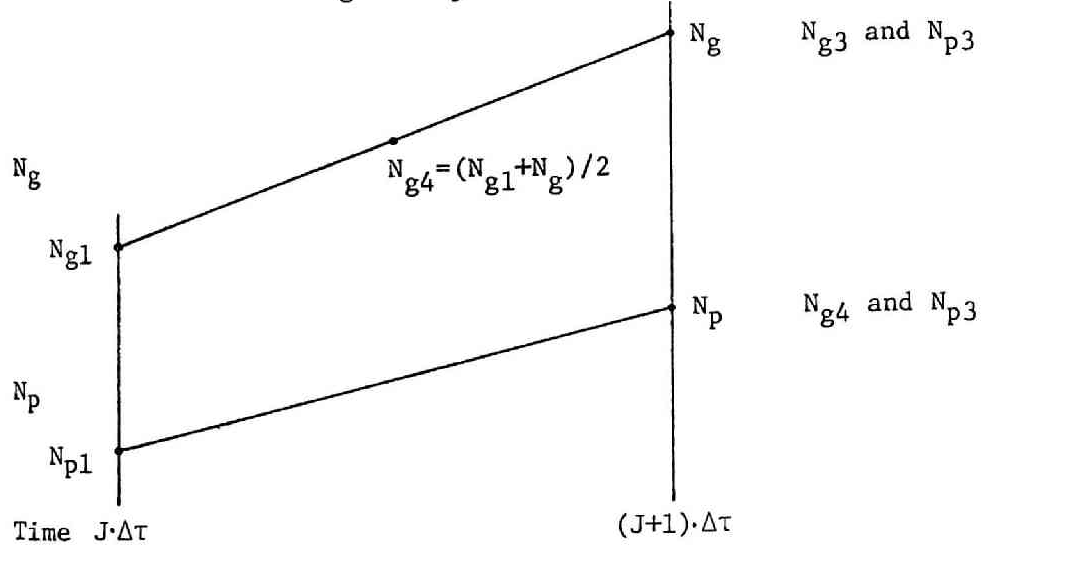

Fig.6-5. Schema of computation by Improved Cauchy - Polygon method

The calculations were carried out assuming a constant photochemical oxidation rate, S, during a run of computation. From the experimental results obtained separately using batch system, it is estimated that the order of diffusional deposition rate of particles onto the boundary surface is $10^{-4}sec^{-1}$. Accordingly, $10^{-4}sec^{-1}$ was applied as the values of β_g and β. For the value of K, taking the polydispersity effect into account and referring the values given by Walter [6], K was selected to be $10^{-8}cm^3/sec$.

As to the initial properties of nucleated particles, when we take the case of $I = 1\ cm^{-3}sec^{-1}$, the values of Table 6-2 are given from Figs.6-1 and 6-2.

Table 6-2. Initial properties of newly formed particles applied in this study.

r.h. (%)	90	60	50	10
N_g (cm^{-3})	10^7	5×10^7	10^8	2×10^9
r_o (cm)	7×10^{-8}	7×10^{-8}	6.5×10^{-8}	7×10^{-8}
i_o	7.5	8	8	13

However, as will be seen later from the calculated results shown in Fig.6-7, the concentration of sulfuric acid vapor which is most likely to occur is somewhat higher for r.h. = 50 and 90% and lower for r.h. = 10% than the values shown above. So that we selected as the initial particle radius to be 6×10^{-8}cm, and as i_o to be 10 in all cases.

Particles consist of newly nucleated embryos and grown particles, so that particle size and sulfuric acid concentration can not be homogeneous. Though, for simplicity, particle size and concentration were assumed to be homogeneous in all cases. This assumption implies that sulfuric acid contained in each particle

is the average amount by particle number at every time step of computation. In the case with foreign source of aerosol particles, the radius and other properties of particles from this source is assumed to be just the same to those of particles formed by photochemical reaction.

6.5 Results and Discussion

The calculations of the kinetic model of sulfuric acid formation are classified into two cases of "without" and "with" foreign source of particles. At first, the peculiarities in the formation and growth process of aerosols in the former case are discussed. And the effects of particles from foreign source on those peculiarities are successively discussed.

6.5.1 Variation of Various Factors with Time

Fig.6-6 shows the typical calculated example of variations of various factors with time for $S = 10^6$ $cm^{-3}sec^{-1}$ at 50% r.h.

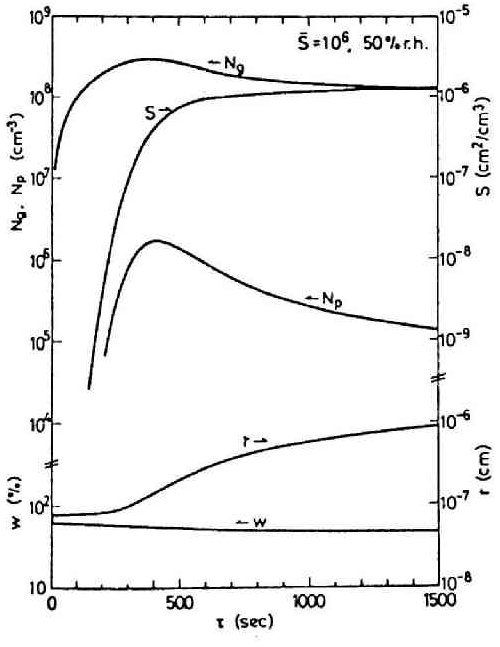

Fig.6-6. Time change of some characteristic values in aerosol formation at 50% r.h. and $S = 10^6$ $cm^{-3}sec^{-1}$. w is weight fraction of sulfuric acid in a particle, and S is particle surface area per unit volume of air.

Generally, vapor molecule concentration increases rapidly at the start of irradiation and decreases slowly after reaching the maximum value. Also, the particle number concentration increases rapidly after some period from the start of irradiation and decreases slowly after reaching the maximum value, in the same manner as shown in the experimental results. The maximum particle number concentration appears a little later than for vapor concentration, but this time lag is not large.

Surface area of particles per unit volume of air approaches an equilibrium value. This implies that at the early stage of the

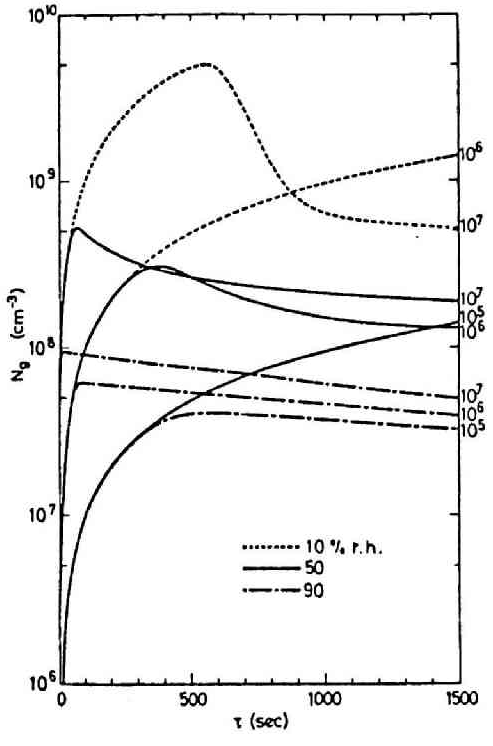

Fig. 6-7. Time change of number concentration of sulfuric acid vapor molecule. $S = 10^5$, 10^6 and 10^7 cm^{-3}sec^{-1} for the case of 10, 50 and 90% r.h.

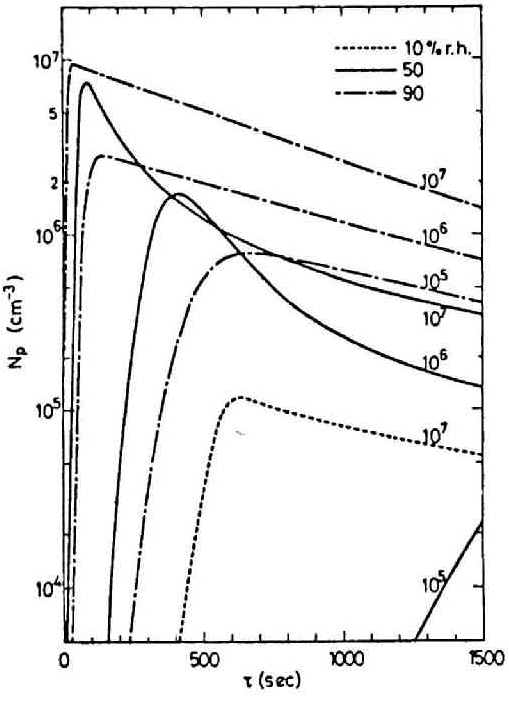

Fig. 6-8. Time change of particle number concentration. $S = 10^5$, 10^6 and 10^7 cm^{-3}sec^{-1} for the case of 10, 50 and 90% r.h.

process nucleation is predominant, however, condensation of vapor becomes significant in the later stage. These mechanisms have been discussed by Husar and Whitby [16] from the view point of self-preserving size spectra.

Figs.6-7 and 6-8 show the changes of sulfuric acid vapor molecule and particle number concentration with time, respectively, for various values of photochemical oxidation rate and relative humidities. As can be predicted from the value of nucleation rate shown in Fig.6-1, particle number concentration is strongly influenced by relative humidity, particularly at a low value of photochemical oxidation rate.

6.5.2 Maximum Number Concentration of Vapor Molecule and Particle

Denote the maximum number concentration of vapor molecule and particle by $N_{g,max}$ and $N_{p,max}$, respectively, and also the time needed to reach $N_{g,max}$ and $N_{p,max}$ by $\tau_{g,max}$ and $\tau_{p,max}$, respectively, hereafter. For various relative humidities, $N_{g,max}$ and $\tau_{g,max}$, and

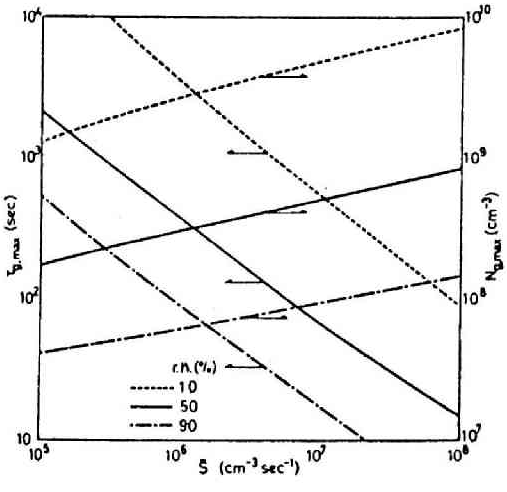

Fig.6-9. Maximum number concentration of vapor molecule and time to reach the maximum concentration.

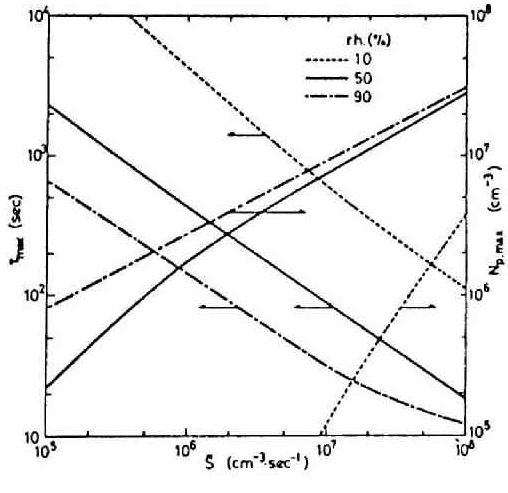

Fig.6-10. Maximum particle number concentration and time to reach the maximum concentration.

$N_{p,max}$ and $\tau_{p,max}$ are shown, respectively, in Figs.6-9 and 6-10 as a function of photochemical oxidation rate S. And also, $N_{g,max}$, $N_{p,max}$, $\tau_{g,max}$ and $\tau_{p,max}$ are illustrated similarly in Figs.6-11a, 6-11b and 6-11c at 10, 50 and 90% r.h., respectively.

The relations between $\tau_{g,max}$ or $\tau_{p,max}$ and S are given approximately by $\tau_{g,max}$ (or $\tau_{p,max}$) $\propto S^{-m}$ where m is a constant such that m increases with the decrease of relative humidity and ranges from 0.5 to 0.8.

The dependence of maximum particle number concentration on photochemical oxidation rate is thought to arise as follows; If the maximum concentrations for both vapor molecule and particle are attained coincidently, $d N_g / d\tau = d N_p / d\tau = 0$. And at the maximum number concentration of vapor molecule and particle, β_g and β of 10^{-4} sec^{-1} are estimated to be negligibly small comparing with the term of $(\alpha + N_p)$ by Fig.6-7 and comparing with the term of $K N_p^2$ by Fig.6-8 in the most cases, respectively. Therefore, the following equations are obtained;

$$N_g = \frac{S}{\alpha + \gamma N_p} \tag{6-16}$$

$$N_p = \left(\frac{\alpha}{i_o K} \cdot \frac{S}{\alpha + \gamma N_p} \right)^{1/2} \tag{6-17}$$

In which, α is also dependent on S indirectly, however, if $\alpha \gg \gamma N_p$ holds, Eq.(6-17) reduces to

$$N_p = \left(\frac{S}{i_o \cdot K} \right)^{1/2} \tag{6-18}$$

And it is found that $N_{p,max}$ and the slope of the line indicated in Fig.6-11 is very close to this relation.

The dependence of particle number concentration on photochemical

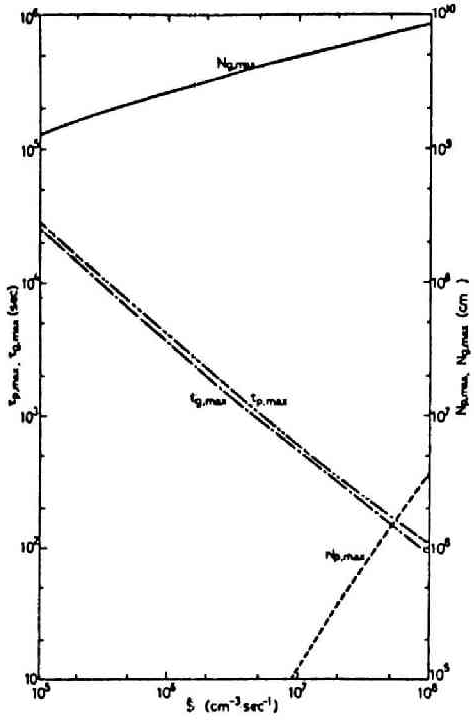

a. 10% r.h.

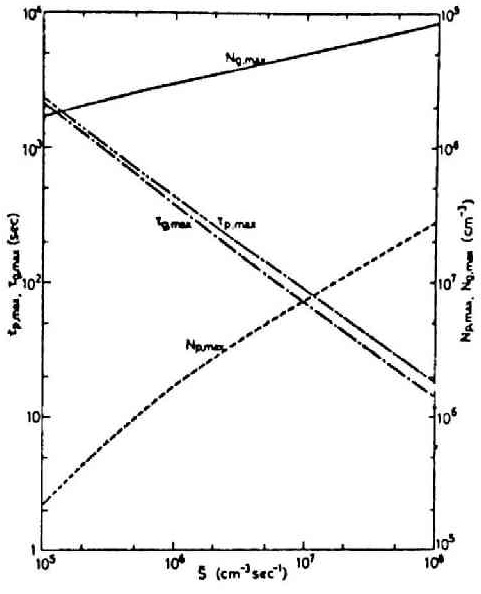

b. 50% r.h.

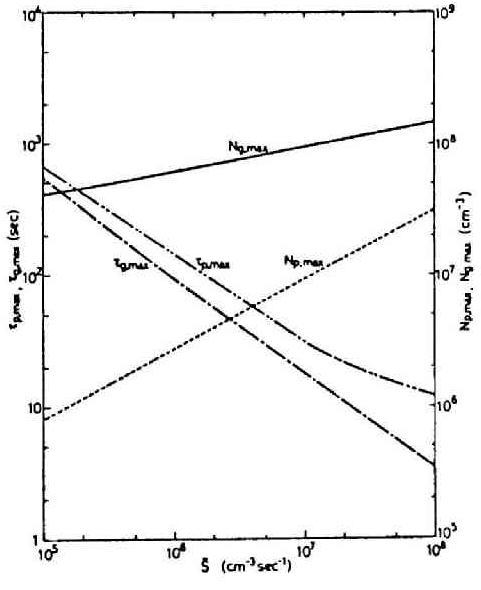

c. 90% r.h.

Fig.6-11. Maximum number concentration of vapor molecule and particle, and time to reach the maximum concentration.

oxidation rate after longer time periods can be understood in similar way. Namely, if equilibrium concentrations for both sulfuric acid vapor, N_g^*, and particle, N_p^*, can be assumed, the relations of Eqs.(6.17) and (6.18) will be also attained in most cases. Hence, in the case shown in Fig.6-6, the order of magnitude of α and γN_p^* are 2×10^{-6} sec^{-1} and 10^{-2} sec^{-1}, respectively. This leads to N_g^* is about 2×10^5 cm^{-3}. The fact that the actual value of N_g^* is about 10^5 cm^{-3} is caused by neglecting the term of βN_p. However, at high relative humidity, the order of magnitude of α becomes significant comparing with γN_p^*.

6.5.3 Maximum Number Formation Rate

The maximum number formation rate of particle, F, which was defined as $(d N_p/d \tau)_{max}$ in Section 4.3, was calculated. The values of F for various relative humidities are shown in Fig.6-12 as a function of photochemical oxidation rate, S. Since the maximum number formation rate appears at the very early stage of reaction in which particle formation is considered to be dominant rather than growth, it should be theoretically equal to the value of nucleation rate. In fact, the values of F are in approximate agreement with the values of nucleation rate estimated in Fig.6-1.

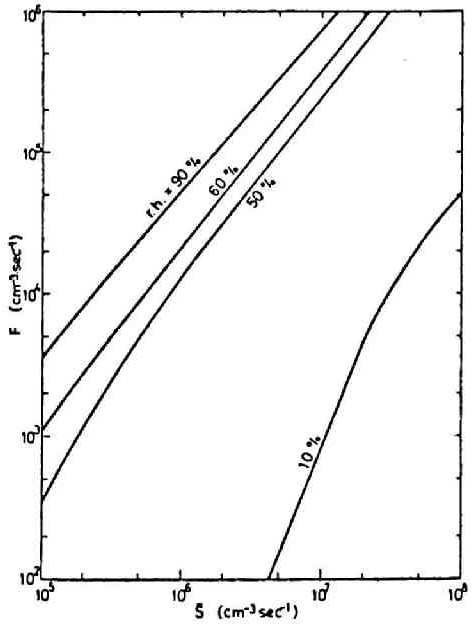

Fig.6-12. Maximum number formation rate for various relative humidities.

The value of F increases with the increase of relative

humidity, particularly at lower relative humidity. It is in slightly higher degree than the first order with respect to S in lower values of F, and the relation between F and S approaches to the first order as F increases.

6.5.4 Particle Radius and Volumetric Formation Rate

Average particle radius increases with time due to condensation and coagulation. However, in the early stages of particle formation in which nucleation is predominant, the vapor concentration is not always high enough for effective condensation to occur leading to grow in particle size. On the other hand, in some cases of low relative humidity, the nucleation rate is very small so that most of the sulfuric acid vapor condenses to make the particles grow larger. Consequently, as shown in Fig.6-13, the growth rate is characterized by relative humidity and photochemical oxidation rate.

The volume concentration of particles was calculated on the assumption that the shape of particle is spherical. Fig.6-14

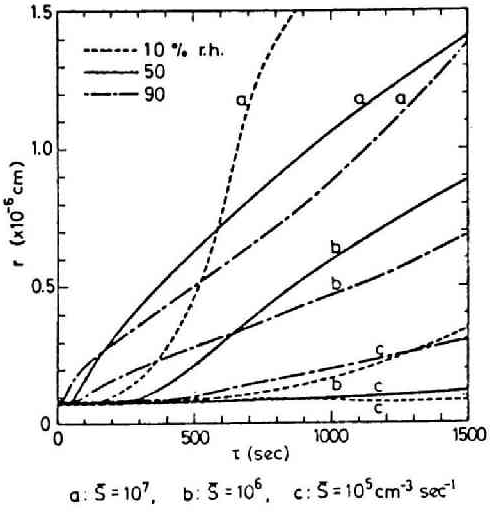

Fig.6-13. Growth of averaged particle size.

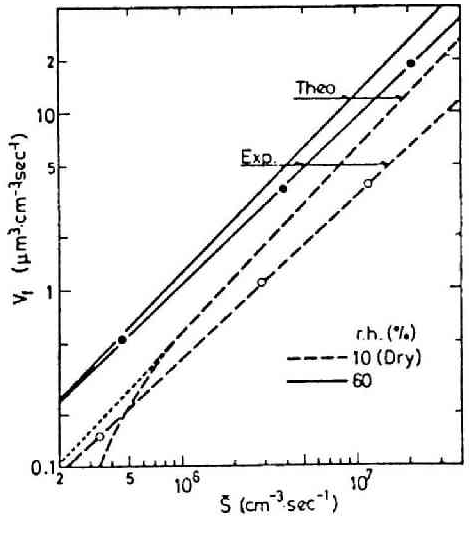

Fig.6-14. Volumetric formation rate of particle.

shows the volumetric formation rate, V_f, which was defined in Section 5.2, as a function of photochemical oxidation rate. At that, V_f is the averaged value for the time long enough to attain a steady particle formation. It is noted that theoretical values of V_f are close to the experimental in every cases.

6.5.5 Particulate Fraction of Sulfuric Acid

As the condensation of vapor becomes effective sulfuric acid concentration in particles increases, however, its time change is very slow as shown in Fig.6-6. And the lower the relative humidity, the higher is the sulfuric acid concentration. As the aerosol formation proceeds, most of the sulfuric acid produced becomes incorporated in the particles as shown in Fig.6-15.

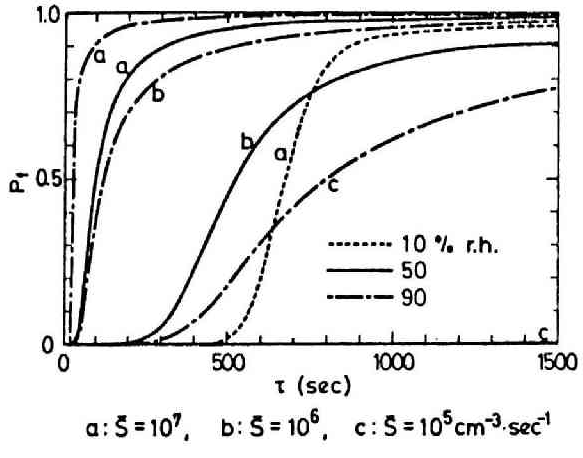

a: $\bar{S}=10^7$, b: $\bar{S}=10^6$, c: $\bar{S}=10^5 cm^{-3}\cdot sec^{-1}$

Fig.6-15. Particulate fraction of sulfuric acid.

6.5.6 Effect of Particles from Foreign Source

The additional rate, S_p, of particles from foreign source was varried between 10 and 10^3 $cm^{-3}sec^{-1}$, and the effects of foreign particles on the peculiarities in the formation and growth process of sulfuric acid aerosols were examined.

Fig.6-16 shows the effects of foreign particles on time change of various factors, such as concentrations of vapor molecule and particles, surface area concentration, particle radius and weight fraction of sulfuric acid. Figs.6-17a to 6-17d also

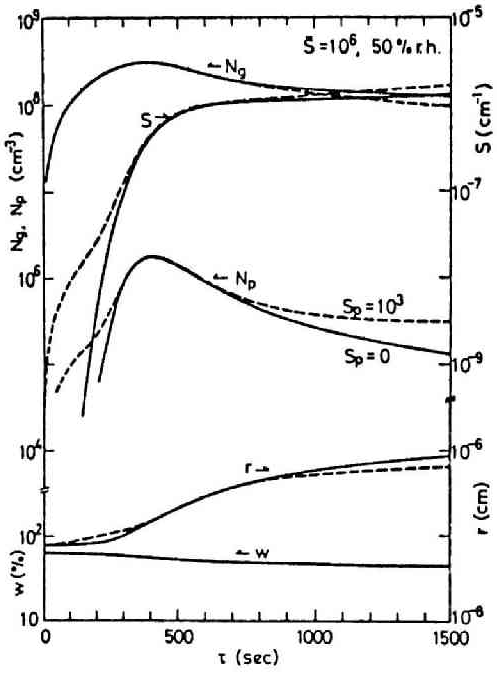

Fig.6-16. Effect of foreign particles on change of various factors with time.

shows the effect of foreign particles on the variation of particle number concentration with time for various maximum number formation rates, F.

The effects of foreign particle are summarized as follows;

1) The effect of foreign particle on particle number concentration is very complicated and depends strongly upon the maximum number formation rate as shown in Figs.6-17a to 6-17d. It is generally found that the addition of foreign particle increases particle number concentration just after the start of irradiation and at longer irradiation time. It is also found as shown in Figs.6-17a and 6-17b that when the additional rate of foreign particles is larger than the maximum number formation rate, the variation of particle number concentration with time is dominated only by the foreign particle.

2) The effect of foreign particle, of which particle radius is assumed to be critical size (6×10^{-8} cm), on the particle size is as follows; At the early stage of aerosol formation (around 200 sec in Fig.6-16), in which particle formation is dominant, the average particle radius is enlarged by addition of foreign particle, because foreign particle added before has grown larger already. At longer period of irradiation time,

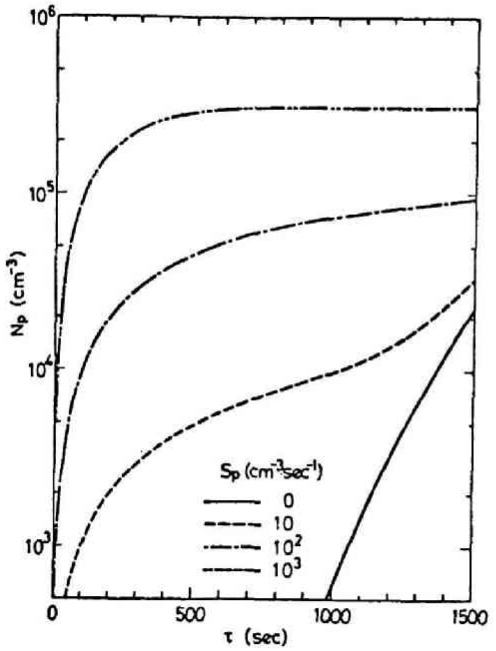

a. $F = 3.5 \times 10^2\ cm^{-3}sec^{-1}$. *(*$S = 10^5\ cm^{-3}sec^{-1}$, *50% r.h.)*

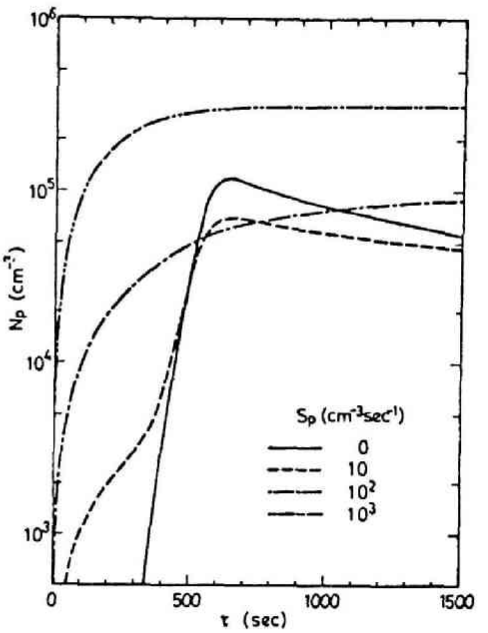

b. $F = 8.5 \times 10^2\ cm^{-3}sec^{-1}$. *(*$S = 10^7\ cm^{-3}sec^{-1}$, *10% r.h.)*

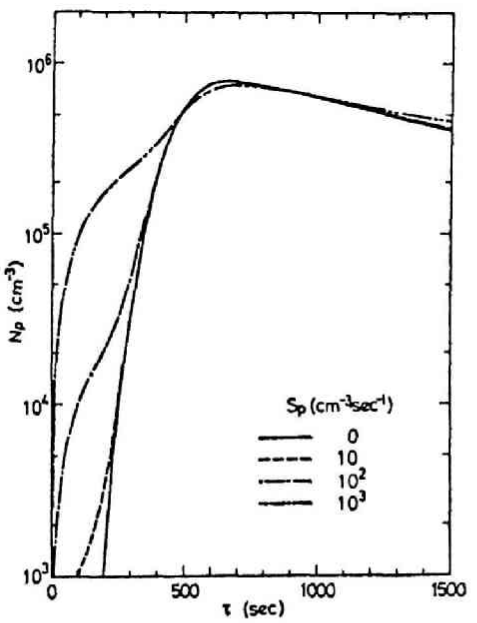

c. $F = 3.6 \times 10^3\ cm^{-3}sec^{-1}$. *(*$S = 10^5\ cm^{-3}sec^{-1}$, *90% r.h.)*

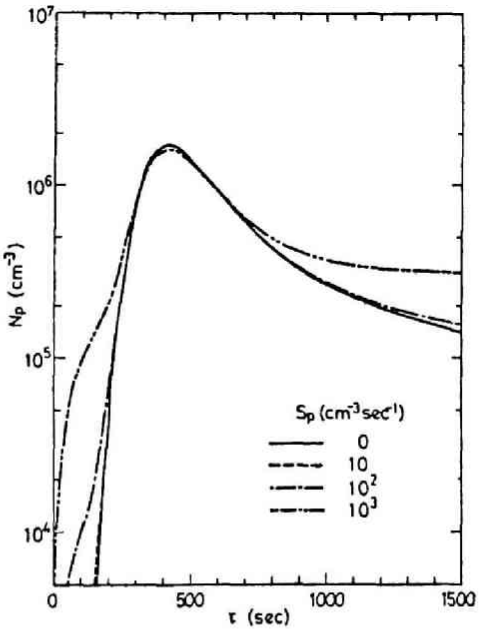

d. $F = 1.3 \times 10^4\ cm^{-3}sec^{-1}$. *(*$S = 10^6\ cm^{-3}sec^{-1}$, *50% r.h.)*

Fig.6-17. Effects of foreign particles on particle number concentration change with time.

the average particle radius is diminished by addition of foreign particle, because size of foreign particle is much smaller than that of growing particle.

3) As shown in Table 6-3, when the additional rate of foreign particle is less than the maximum number formation rate or is in comparable order of this, the surface area concentration and volume concentration of particles are unaffected by addition of foreign particle. However, when the additional rate is considerably larger than the maximum number formation rate, these concentrations increase apparently with the increase of additional rate of foreign particle. Consequently, the amount of sulfuric acid vapor absorbed by particles increases too, and the concentration of sulfuric acid vapor decreases as shown in Fig.6-16.

6.5.7 Comparison of Theoretical Calculation with Experimental Results

The photochemical oxidation rate, k, obtained experimentally, and both theoretical values calculated by the kinetic model and experimental values of the maximum particle number concentration, N_{max}, the irradiation time to reach the maximum particle number concentration, τ_{max}, the average particle radius, r, and the volumetric formation rate are summarized in Table 6-4.

Comparing with the experimental results, it is found that, in the case of moderate degree of relative humidity, the kinetic model gives larger values for N_{max}, comparable order of magnitudes for τ_{max}, and smaller for r. While, in the case of Dry condition, it gives smaller values for N_{max} and extremly larger values for τ_{max}. The volumetric formation rate shown in the table is the averaged value for the irradiation time enough long to attain a steady particle formation. And it is noted that theoretical values are close to the experimental in every cases as shown in Fig.6-14.

Table 6-3. Effect of foreign particle on volume concentration and surface area concentration

	F[a] (cm^{-3} sec^{-1})	V (cm^3/cm^3)				S (cm^2/cm^3)			
		S_p ($cm^{-3}sec^{-1}$) =				S_p ($cm^{-3}sec^{-1}$) =			
		0	10	10^2	10^3	0	10	10^2	10^3
10% r.h.									
$S = 10^5$ $cm^{-3}sec^{-1}$		1.4-37[b]	1.9-16	1.6-15	8.4-15	5.3-30	3.8- 9	2.9- 8	1.4- 7
10^6	1.8	1.4-20	4.5-14	1.6-13	2.2-13	1.2-13	1.5- 7	6.4- 7	1.2- 6
10^7	8.6+2	2.4-12	2.4-12	2.4-12	2.5-12	3.3- 6	3.2- 6	3.9- 6	6.0- 6
10^8	5.2+4	2.5-11	2.5-11	2.5-11	2.5-11	1.7- 5	1.7- 5	2.0- 5	2.8- 5
50% r.h.									
$S = 10^5$ $cm^{-3}sec^{-1}$	3.5+2	1.3-16	5.9-16	3.7-15	1.6-14	3.6- 9	1.1- 8	5.3- 8	2.1- 7
10^6	1.4+4	3.9-13	3.7-13	3.7-13	3.7-13	1.3- 6	1.3- 6	1.3- 6	1.7- 6
10^7	1.8+5	4.1-12	4.2-12	4.2-12	4.3-12	8.8- 5	8.9- 6	9.0- 6	9.7- 6
10^8	4.0+6	4.2-11	4.3-11	4.3-11	4.4-11	6.1- 5	6.2- 5	6.2- 5	6.3- 5
90% r.h.									
$S = 10^5$ $cm^{-3}sec^{-1}$	3.6+3	4.7-14	4.6-14	4.7-14	4.8-14	4.7- 7	4.6- 7	4.8- 7	4.9- 7
10^6	5.4+4	9.4-13	9.5-13	9.4-13	9.1-13	4.1- 6	4.2- 6	4.2- 6	4.2- 6
10^7	7.5+5	1.5-11	1.5-11	1.5-11	1.5-11	3.4- 5	3.4- 5	3.4- 5	3.4- 5
10^8	4.7+6	2.2-10	2.3-10	2.3-10	2.3-10	2.6- 4	2.6- 4	2.6- 4	2.6- 4

(at $\tau = 1500$ sec)

a) : F is the maximum number formation rate at $S_p = 0$.

b) : The value of 1.4-37, for example, means 1.4×10^{-37}.

Table 6-4. Experimental results of photochemical oxidation rate and some other factors, and comparison with theoretical values.

SO_2 (ppm)	r.h.[1] (%)	k (% hr^{-1})	$S \times 10^{-6}$ ($cm^{-3} sec^{-1}$)	N_{max} (cm^{-3})		τ_{max} (sec)		r ($\times 10^{-6}$ cm)[2]		dV/dτ ($\mu m^3 cm^{-3} sec^{-1}$)	
				Exp.	Theor.	Exp.	Theor.	Exp.	Theor.	Exp.	Theor.[3]
10	60	0.028	21	2.3×10^6	1.2×10^7	60	30	1.42	0.84	18.7	26.1
	Dry	0.016	12	5.0×10^5	1.6×10^5	90	540	1.35	1.37	3.9	7.3
1	60	0.052	3.9	9.5×10^5	5.1×10^6	110	120	0.90	0.60	3.7	4.9
	Dry	0.039	2.9	2.2×10^5	1.3×10^4	160	1800	1.00	0.27	1.1	1.7
0.1	60	0.061	0.46	2.1×10^5	1.3×10^6	150	510	0.90	0.25	0.53	0.55
	Dry	0.046	0.34	8.0×10^4	9.1×10	235	10800	0.70	0.081	0.15	0.10

1) Theoretical values for Dry condition are calculated at r.h.=10 %.
2) Average radius at τ = 750 sec.
3) average values for τ = 0 - 15,000 sec.

The discrepancies between the theoretical and the experimental are thought to be due to the facts that : 1) the CNC used in the experiment is unable to count very small particles such as just nucleated embryos, 2) there is considerable wall deposition of gaseous matter and small particles, and 3) there may be some error in the calculated values of nucleation rate, particularly at very low relative humidity.

The greater discrepancy in the case of very low relative humidity at a lower SO_2 concentration is not clearly understood yet, however, it is possibly due to some effective nucleation mechanisms as shown in consideration of particles from foreign source, for example, nucleation by natural ionizing radiation, nucleation from some trace level impurities contained in sample gas as was shown by Vohra et al. [17] and Bricard et al. [18].

In the atmosphere, the concentration of sulfur dioxide is in the order of 0.01 - 0.1 ppm, namely, $2.7 \times 10^{11} - 2.7 \times 10^{12}$ molecules/cm^3 at S.T.P. The photochemical conversion rate of sulfur dioxide to sulfuric acid in noonday sunlight in summer has been derived to be 0.7% hr^{-1} (2×10^{-6} sec^{-1}) experimentally. Consequently, the value of S ranges $5 \times 10^5 - 5 \times 10^6$ $cm^{-3}sec^{-1}$, therefore the case shown in Fig.6-6 is probably realistic.

The kinetic model and the calculated results given in this chapter are thought to be useful for understanding the photochemical aerosol formation process in the real atmosphere. However, there remains the problem of the assumption for the particle size distribution change with time. Furthermore, when this kinetic model is applied to experimental result obtained in a smog chamber, the flow pattern of the air should be taken into consideration.

List of Symbols in Chapter 6

A : chemical activity of water, (-)

C : factor containing the probability of capture of molecule, (cm^{-3} sec^{-1})

D_g : diffusivity of gas molecule, (cm^2/sec)

ΔG : free energy, (erg/molecule)

I : nucleation rate, ($cm^{-3}sec^{-1}$)

i : number of sulfuric acid molecule in a particle, (-)

K : coagulation constant, (cm^3/sec)

l : length nearly equal to mean free path, (cm)

M : molecular weight of water, (gr/mole)

N_p : number concentration of particle, (cm^{-3})

N_g : number concentration of gas molecule, (cm^{-3})

n : number of molecule in embryo, (cm^{-3})

n : mole fraction of sulfuric acid, (-)

P_f : particulate fraction, (-)

p : Planck's constant, (erg sec)

R : gas constant, (erg/deg molecule)

r : particle radius, (cm)

r_o : radius of critical embryo, (cm)

S ($\bar{S}$ in figures) : conversion rate of sulfur dioxide to sulfuric acid, ($cm^{-3}sec^{-1}$)

S_p : additional rate of foreign particle from source other than photochemical reaction, ($cm^{-3}sec^{-1}$)

T : absolute temperature, (°K)

V_f : volume formation rate of particle, ($\mu m^3/cm^3$ sec)

v : mean thermal velocity of gas molecule, (cm/sec)

w : weight fraction of sulfuric acid, (-)

X : number of total molecule of sulfuric acid and water per embryo, (cm^{-3})

α : conversion rate of vapor to embryo, (sec^{-1})

β : diffusion deposition rate of particle, (sec^{-1})

β_g : " " " of vapor molecule, (sec^{-1})

γ : deposition rate of sulfuric acid vapor to particle, (cm^3/sec)

δ : condensation probability of vapor molecule, (-)

κ : Boltzmann's constant, (erg/deg)

ν : frequency of light, (sec^{-1})

ρ : density of solution of sulfuric acid particles, (gr/cm^3)

σ : surface tension of sulfuric acid particles, (dyne/cm)

τ : irradiation time, (sec)

subscript g : vapor

subscript p : particle

subscript o : critical state at the saddle point of ΔG

References

[1] Reiss, H. (1950) : The kinetics of phase transitions in binary system, J. Chem. Phys., Vol.18, pp.840-848.

[2] Doyle, G. J. (1961) : Self-nucleation in the sulfuric acid-water system, J. Chem. Phys., Vol.35, pp.795-799.

[3] Kiang, C. S., Stauffer, D., Mohnen, V. A., Bricard, J. and Vigla, D. (1973) : Heteromolecular nucleation theory applied to gas-to-particle conversion, Atmos. Environ., Vol.7, pp. 1279-1283

[4] Kiang, C. S. and Stauffer, D. (1973) : Chemical nucleation theory for various humidities and pollutants, Preprint for the Faraday Symposium of the Chemical Society.

[5] Mirabel, P. and Katz, J. L. (1974) : Binary homogeneous nucleation as a mechanism for the formation of aerosols, J. Chem. Phys., Vol.60, pp.1138-1144.

[6] Walter, H. (1973) : Coagulation and size distribution of condensation aerosols, Aerosol Sci., Vol.4, pp.1-15.

[7] Stauffer, D., Mohnen, V. A. and Kiang, C. S. (1973) : Heteromolecular condensation theory applied to particle growth, Aerosol Sci., Vol.4, pp.461-471.

[8] International Critical Table (1928), Vol.4, McGraw-Hill.

[9] Perry, J. H. (Editor) (1950) : Chemical engineer's handbook, McGraw-Hill.

[10] Kiang, C. S., Stauffer, D., Walker, G. H., Puri, O. P., Wise, Jr. J. D. and Patterson, E. M. (1971) : A reexamination of homogeneous nucleation theory, J. Atmos. Sci., Vol.28, pp. 1222-1232.

[11] Fuchs, N. A. (1959) : Evaporation and droplet growth in gaseous media, Pergamon Press.

[12] Mellor, J. W. (1931) : A comprehensive treatise on inorganic and theoretical chemistry, Vol.X, Chapter LVII, Longman Green.

[13] Mason, B. J. (1960) : Nucleation of water aerosols, Disc. Faraday Soc., No.30, pp.20-38.

[14] Low, R. D. H. (1969) : A generalized equation for the solution effect in droplet growth, J. Atmos. Sci., Vol.26, pp. 608-611.

[15] Vohra, K. G. and Nair, P. V. N. (1971) : Stability of submicron aqueous solution droplets in the atmosphere, J. Atmos. Sci., Vol.28, pp.280-285.

[16] Husar, R. B. and Whitby, K. T. (1973) : Growth mechanisms and size spectra of photochemical aerosol, Environ. Sci. Tech., Vol.7, pp.241-247.

[17] Vohra, K. G., Nair, P. V. N. and Muraleedharan, T. S. (1972) : Possible role of singlet oxygen in an ion-induced reaction mechanism of nucleus formation by sulfur dioxide, Aerosol Sci., Vol.3, pp.225-236.

[18] Bricard, J., Cabane, M., Madelaine, G. and Vigla, D. (1972) : Formation and properties of neutral ultrafine particles and small ions conditioned by gaseous impurities of the air, J. Colloid Interface Sci., Vol.39, pp.42-58.

Chapter 7

7. Conclusions and Recommendations

The results obtained in this study must lead to better understanding of formation and evolution mechanism of aerosol particles from photochemical oxidation of sulfur dioxide. The principal conclusions in this study are summarized as follows;

1) Under any environmental conditions, particle number concentration of sulfur dioxide increases rapidly after some period from the start of irradiation, and decreases gradually after reaching the maximum concentration. And then every environmental factor of SO_2 concentration, relative humidity and ultraviolet light intensity applied in this study influences strongly on the formation and evolution processes of aerosol particle.

2) The maximum number formation rate of particles is very important factor on the aerosol formation process, and the various characters in the time variation of particle number concentration are expressed as a function of only the maximum number formation rate. In the case of lower number formation rate, it is proportional to the amount of the product of SO_2 concentration and irradiation intensity.

3) In the early stage of reaction, particle formation is dominant rather than particle growth, and so the most sulfuric acid vapor react to form new particles by Reaction (4.2). Reaction (4.2) is remarkably dependent on both SO_2 concentration and relative humidity, and the number formation rate of aerosol particle increases with the increase of SO_2 concentration and/or relative humidity

4) With the growth of aerosol particles, Reaction (4.3) becomes dominant rather than Reaction (4.2). The particle growth by Reaction (4.3) is influenced mainly by number concentration and

size of the already existing aerosol particles and by sulfuric acid vapor concentration. As a whole, particle number concentration is strongly dependent on both SO_2 concentration and relative humidity, and the particle size is mainly dependent on SO_2 concentration.

5) Particle size just after formed is estimated to be smaller than 0.0025 μm, and grows up with time. Volumetric formation rate of particles is also dependent on both SO_2 concentration and relative humidity. The value ranges from 0.15 to 18.7 $\mu m^3/cm^3 hr$ within this experimental condition, and is close to that obtained theoretically in every cases.

6) The photochemical oxidation rate of sulfur dioxide, k, and the over-all quantum yield are 0.04% hr^{-1} and 8×10^{-3}, respectively, in the experimental study. The value of k, 0.04% hr^{-1}, is equivalent to be 0.7% hr^{-1} for noonday sunlight in summer in Kyoto area.

7) Although there are some qualitative differences between the experimental and the theoretical studies, the variation of particle number concentration with time and the properties of particles obtained in the experimental have similar tendencies to those of theoretical study. The kinetic model and the calculated results are thought to be useful for understanding the photochemical aerosol formation process.

8) The effect of foreign particles on the formation and evolution process of photochemical aerosol formation is very complicated and depends markedly upon the maximum number formation rate of particles.

Further investigations are still required on such problems of, a) clarification of the effect of flow condition in the reaction chamber and selection of the most suitable type of reaction chamber, b) determination of chemical properties by more sensitive

and reliable technique, c) determination of the detailed particle size distribution using a measurement instrument for submicron particles such as electrostatic particle sizer, and d) absolute calibration of the CNC.

On the other hand, the study about the role of ultraviolet irradiation on photochemical reaction show that : The information of spectral intensity within the absorption band of substance in question is the most important for the problem of photochemical reaction. The light intensity, particularly at shorter wavelength in the lower atmosphere, is influenced significantly by various environmental factors. Consequently, measurements of ultraviolet light intensity at the earth's surface under various environmental conditions in systematic way is strongly desired.

Atmospheric aerosol particles consist of both primary emitted particles and secondary particles which are converted in the atmospheric air from gaseous substances. Sulfuric acid mist and sulfate particles are the typical example of those secondary produced aerosol particles. Therefore, aerosol formation from photochemical reaction of sulfur dioxide vapor plays very important role in air pollution.

These experimental and theoretical studies are conducted in the most simple system of sulfur dioxide in pure air and considered to be useful as the first step to make clear the formation and growth mechanism of sulfuric acid aerosol in the atmosphere. And so, further investigations are strongly required theoretically and experimentally to clarify the aerosol formation mechanism in the real atmosphere, or in complex systems of SO_2, NO_x and hydrocarbons which are generally recognized to be important reactants for photochemical reaction in the atmosphere.

ACKNOWLEDGMENTS

I would particularly like to express my thanks to Professor Kanji Takahashi for his constant guidance and encouragement during the course of this study. Thanks are also due to the members of the Takahashi's Laboratory of the Institute of Atomic Energy, Kyoto University for generous assistance in carrying out the experiments.

APPENDICES

Appendix 1

Effect of Impurities in Sample Gas on Experimental Studies

Some trace level impurities contained in sample gas contribute to aerosol formation by photochemical reaction and by natural ionizing radiation as was suggested by Bricard et al.* and Vohra et al.**

It was confirmed as shown in Section 4.2, that the effects of gaseous impurities such as sulfur dioxide and nitrogen oxides, and of background particulate matters in pure air can be neglected. Further, the gas chromatographical examination showed that the fraction of gaseous impurities such as aldehydes and ketons is less than 0.5% of SO_2 gas in SO_2 - pure air mixture. Those carbonyl compounds absorb radiation energy to form peroxy radicals with high quantum yield. Peroxy radicals may sometimes play a significant role on the oxidation of SO_2 to SO_3 in the following reactions as has been discussed by Payne et al.***

$$\text{carbonyl compounds} \longrightarrow HO_2 \qquad \text{(A1)}$$

$$HO_2 + SO_2 \longrightarrow HO + SO_3 \qquad \text{(A2)}$$

---

* Bricard, J., Cabane, M., Madelaine, G. and Vigla, D. (1972) : Formation and properties of neutral ultrafine particles and small ions conditioned by gaseous impurities of the air, J. Colloid Interface Sci., Vol.39, pp.42-58.

** Vohra, K. G., Nair, P. V. N. and Muraleedharan, T. S. (1972) : Possible role of singlet oxygen in an ion-induced reaction mechanism of nucleus formation by sulfur dioxide, Aerosol Sci., Vol.3, pp.225-236.

*** Payne, W. A., Stief, L. J. and Davis, D. D. (1973) : A kinetics study of the reaction of HO_2 with SO_2 and NO, J. Am. Chem. Soc., Vol.95, pp.7614-7619.

The formation rate of SO_3 from carbonyl compounds can be evaluated by the following equations ;

$$\frac{d\,(HO_2)}{d\,t} = k_1 \cdot (SO_2)\,x - k_2\,(HO_2)\,(SO_2) \tag{A3}$$

$$\frac{d\,(SO_3)}{d\,t} = k_2\,(HO_2)\,(SO_2) \tag{A4}$$

where k_1 and k_2 are the reaction rates of Reactions (A1) and (A2), respectively, and k_1 is calculated to be 10^{-2} hr^{-1} in this experimental system from Leighton's text. And x is the fraction of carbonyl impurities to SO_2 gas, and so $(SO_2)\,x$ means concentration of carbonyl compounds. From Eqs.(A3) and (A4), concentration of SO_3 attributed to carbonyl compounds, $(SO_3)_c$, is given by,

$$(SO_3)_c = k_1\,x\,(SO_2)\left[t - \frac{1 - \exp\{-k_2(SO_2)\,t\}}{k_2\,(SO_2)}\right]$$

$$< k_1\,x\,(SO_2)\,t \tag{A5}$$

On the other hand, concentration of SO_3 from photochemical oxidation of SO_2, $(SO_3)_s$, is given by

$$(SO_3)_s = k\,(SO_2)\,t \tag{A6}$$

where k is the photochemical reaction rate of SO_2 to SO_3, and is obtained to be 4×10^{-4} hr^{-1} in this work. Therefore, the uttermost contribution, c, of the carbonyl compounds in oxidation of SO_2 can be evaluated by

$$c = \frac{(SO_3)_c}{(SO_3)_s} < \frac{k_1\,x}{k} \tag{A7}$$

Since the fraction of impurities was less than 0.5% of SO_2 gas, the value of c is less than 0.125.

Appendix 2

On the Accuracy of the CNC

There are some problems on the accuracy of this type of the CNC. Liu and Pui* made calibration work of the Environment/One CNC using the Whitby Aerosol Analyzer (WAA), and reported that the CNC has a linear response at concentration levels up to 130,000 particles/cm^3 (indicated concentration by the CNC = 52,500 particles / cm^3), but the indicated concentration is lower than the true concentration by a factor of 2.5. Above 130,000 particles/cm^3 the CNC's response becomes non-linear, and the indicated concentration is lower than true concentration by a factor ranging from 2.5 in the lower linear range to 5.3 at the upper concentration limit of 600,000 particles/cm^3 used in the test.

In our laboratory, although the experimental examination of absolute calibration of the CNC has not performed yet, the linearity of the CNC was tested by a dilution method which had been applied as a basic technique in calibration of Nolan-Pollak counter. And it was confirmed that the CNC used in this study at least responds linearly in the range from 41,000 to 580,000 particles/cm^3. Beside, most of the particle number concentration was measured in the lower range than 300,000 particles/cm^3 in this study. Therefore, if the indicated value of the CNC is different from the true value by a factor f, the results obtained here will be influenced only in the following manner ; (1) The true

---

* Liu, B. Y. H. and Pui, D. Y. H. (1974) : A submicron aerosol standard and the primary, absolute calibration of the condensation nuclei counter, J. Colloid Interface Sci., Vol.47, pp.155-171.

particle number concentrations and the formation rates become f times as much as the values obtained, accordingly the coefficients of Eqs.(4.7), (4.8) and (4.9) vary, (2) Particle size determined by the diffusion tube method is not affected, because the diffusion tube method is based on the measurement of relative particle number concentration, (3) The volume concentration and the surface area concentration become f times as much as the values obtained. Accordingly, the photochemical oxidation rate which is proportional to the volume concentration also becomes f times as much, (4) Since the sulfuric acid concentration of particle is inverse proportion to volume of deposited particles in the wall surface of diffusion tube, it becomes $(1/f)$ times as much as the values obtained, and (5) Other qualitative tendencies, however, are not influenced as far as the CNC responds linearly.

On the other hand, if the CNC responds as was reported by Liu and Pui, the results obtained in this study are affected in the following manner ; (1) The indicated relative number concentration of particles through the diffusion tube will be higher than the true value, and this means that the true particle size will be smaller than the determined size, (2) The influence of the accuracy of the CNC on the values of particle number concentration, volume concentration and sulfuric acid concentration of particle is much complicated, and dependent on the range used to measure the particle number concentration. Accordingly, the photochemical oxidation rate is influenced in complicated way.

Appendix 3. Programme of Kinetic Model of Sulfuric Acid Aerosol Formation from Photochemical Oxidation of Sulfur Dioxide

```
C     SO2 GAS TO SULFURIC ACID MIST
C     PARTICLE GROWTH IN HUMID AIR
C     CASE 1 AND 2
C     CASE 1 : NO FOREIN PARTICLE (SPA IS 0)
C     CASE 2 : FOREIN PARTICLES ARE ADDED CONTINUOUSLY (SPA IS NOT 0)
      REAL NG1,NG2,NG,NP1,NP2,NP,K
      DIMENSION S(5),RH(5),SPA(5)
      COMMON NG1,ALFP,ALFG,AI,X,R1,SD,ST,ZA,ZR,ZC,ZD,R2,RC,RHX
C
      READ(5,450) NC
      READ(5,500) DT
      READ(5,600) K,BETAG,BETAP,RC,AI
      DO 20 I=1,NC
   20 READ(5,700) SPA(I),RH(I),S(I)
      WRITE(6,400) DT,K,BETAG,BETAP,RC,AI
  400 FORMAT(1H1,//////////20X,12HCASE 1 AND 2///
     X            20X,4HDT = F4.1//
     X            20X,3HK = E9.2//
     X            20X,7HBETAG = E9.2/
     X            20X,7HBETAP = E9.2//
     X            20X,4HRC = E9.2//
     X            20X,4HAI = F5.1)
  450 FORMAT(I2)
  500 FORMAT(8F10.0)
  600 FORMAT(8E10.2)
  700 FORMAT(2F10.0,6E10.2)
C
      DO 10 I=1,NC
      SP=SPA(I)
      RHX=RH(I)
      SL=S(I)
      WRITE(6,100) RC,SL,RHX,SP
      WRITE (6,200)
  100 FORMAT(1H1,5H  RC=E11.3,4H  S=E11.3,5H  RH=F5.2,5H  SP=F6.1)
  200 FORMAT(1H0,9H    TIME ,12H       R      ,12H     SURF     ,12H      VOL
     X    ,12H     ALFG     ,12H      NG      ,12H      NP      ,12H      PC
     X  ,12H   SA CONC  ,12H      SPC     ,7H       Y/)
      J=1
      NG2=SL*DT
      NG1=NG2*0.5
      CALL RATE
      NP1=ALFP*NG1*DT*SP*DT
      NG1=NG2
      R1=RC
      R2=RC
      X=1.0/(0.46059+2.5745E22*RC**3/AI)
      SVOL=8.90E-23*AI*NP1
      VOL=4.189*RC**3*NP1
C
    2 J=J+1
      IF(J.GT.5000) GO TO 10
      NG1=NG1
      NP1=NP1
      CALL RATE
      RAMD=ALFG+BETAG
      GAMA=7.785E04*R1**2/(1.0+6.37E04*R1**2/(R1+1.0E-05))
      NG2=NG1-NG1*(RAMD+GAMA*NP1)*DT+SL*DT-SP*AI*DT
      NG1=(NG1+NG2)*0.5
      CALL RATE
      Y=ALFP*NG1*DT+SP*DT
      NP2=NP1+Y-NP1*DT*(NP1*K+BETAP)
      NP1=(NP1+NP2)*0.5
      CALL RATE
      RAMD=ALFG+BETAG
      GAMA=7.785E04*R1**2/(1.0+6.37E04*R1**2/(R1+1.0E-05))
      NG2=NG1-NG1*(RAMD+GAMA*NP1)*DT+SL*DT-SP*AI*DT
      ANG=(NG1+NG2)*0.5
      NG1=ANG
      CALL RATE
      Y=ALFP*ANG*DT+SP*DT
      NP2=NP1+Y-NP1*DT*(NP1*K+BETAP)
      AC=1.0
      ZF=1.0/AC+6.37E04*R1**2/(R1+1.0E-05)
      SVOL=SVOL+8.776E-23*AI*Y+6.832E-18*R1**2*NG1*NP1*DT/ZF
      SMASS=SVOL*1.853
```

Calculation of N_g N_p at J-th step

Appendix 3 (continued)

```
      R2=R2*1.1
   94 YY=(4.189*R2**3*NP2-SVOL)/SMASS
      IF(YY.LT.0.0) GO TO 96
      X=1.0/(1.0+YY)
      CALL DENS
      PC=EXP(ZA-ZD)
      DPC=RHX-PC
      ADPC=ABS(DPC)
      DDPC=RHX*0.05
      IF(ADPC.LT.DDPC) GO TO 90
      IF(DPC.LT.0.0) GO TO 92
   96 R2=R2*1.05
      GO TO 94
   92 R2=R2*0.98
      IF(R2.LT.RC) GO TO 98
      GO TO 94
   98 R2=RC
C
      YY=(4.189*R2**3*NP2-SVOL)/SMASS
      X=1.0/(1.0+YY)
   90 VOL=4.189*R2**3*NP2
      SUF=12.57*R2**2*NP2
      WS=SMASS/(SMASS+1.627E-22*NG2)
C
      IF(J.GT.100) GO TO 80
      IF(MOD(J,10).NE.0) GO TO 1
      GO TO 82
   80 IF(MOD(J,100).NE.0) GO TO 1
   82 T=DT*FLOAT(J)
      IT=IFIX(T+0.1)
      WRITE(6,300)IT,R2,SUF,VOL,ALFG,NG2,NP2,PC,X,SVOL,WS
  300 FORMAT(I9,10E12.4)
    1 NG1=NG2
      NP1=NP2
      R1=R2
      GO TO 2
   10 CONTINUE
      STOP
      END

      SUBROUTINE RATE
      REAL NG1,NG2,NGI,NP1,NP2,NPI,K
      COMMON NG1,ALFP,ALFG,AI,X,R1,SD,ST,ZA,ZB,ZC,ZD,R2,RC,RHX
      AX=ALOG10(NG1)
      IF(RHX.NE.0.5) GO TO 74
      AXX=(-593.4+179.4*AX-18.33*AX**2+0.63333*AX**3)*2.30259
      GO TO 77
   74 IF(RHX.NE.0.9) GO TO 75
      AXX=(-238.7+69.87*AX-6.9*AX**2+0.2333*AX**3)*2.30259
      GO TO 77
   75 IF(RHX.NE.0.1) GO TO 76
      AXX=(-326.3+57.2*AX-2.5*AX**2)*2.30259
      GO TO 77
   76 AXX=(-489.1+147.4*AX-15.0*AX**2+0.5167*AX**3)*2.30259
   77 IF(AXX.LT.-70.0) GO TO 72
      GO TO 73
   72 AXX=-70.0
   73 ALFP=EXP(AXX)
      ALFG=ALFP*AI
      RETURN
      END

      SUBROUTINE DENS
      REAL NG1,NG2,NGI,NP1,NP2,NPI,K
      COMMON NG1,ALFP,ALFG,AI,X,R1,SD,ST,ZA,ZB,ZC,ZD,R2,RC,RHX
      IF(X.GT.0.85) GO TO 5
      SD=0.99987+0.61908*X+0.398*X**2
      GO TO 6
    5 SD=1.8528+0.2045*(1.0-X)-3.746*(1.0-X)**2
    6 IF(X.GT.0.4) GO TO 7
      ST=72.0+11.0*X
      GO TO 8
    7 ST=87.08-74.9*X+172.5*X**2-130.0*X**3
    8 ZA=1.4778E-09*ST/SD/R2
      ZD=1.2738*X-4.304*X**2+11.465*X**3
      RETURN
      END
```

Determination of equilibrium particle radius by trial and error method

Calculation of physical & chemical properties of particle

Subroutine RATE
Calculation of nucleation rate

Subroutine DENS
Calculation of ρ, σ & A

Appendix 4. Aerosol Particle Concentration Passing Through Diffusion Tube

NUMBER FRACTION OF PASSED AEROSOL PARTICLES THROUGH DIFFUSION TUBE
GEOMETRIC MEAN RADIUS=0.0010 MIC.

	N(X)/N(0)									
X/0	LS= 0.000	LS= 0.050	LS= 0.075	LS= 0.100	LS= 0.125	LS= 0.150	LS= 0.200	LS= 0.250	LS= 0.300	LS= 0.400
5	0.390E+00	0.389E+00	0.388E+00	0.386E+00	0.385E+00	0.384E+00	0.384E+00	0.386E+00	0.390E+00	0.398E+00
10	0.185E+00	0.189E+00	0.193E+00	0.198E+00	0.205E+00	0.212E+00	0.228E+00	0.245E+00	0.260E+00	0.288E+00
20	0.418E-01	0.480E-01	0.551E-01	0.640E-01	0.742E-01	0.852E-01	0.108E+00	0.131E+00	0.154E+00	0.193E+00
40	0.213E-02	0.394E-02	0.651E-02	0.104E-01	0.158E-01	0.225E-01	0.389E-01	0.581E-01	0.785E-01	0.119E+00
60	0.109E-03	0.413E-03	0.106E-02	0.241E-02	0.472E-02	0.816E-02	0.185E-01	0.326E-01	0.493E-01	0.856E-01
80	0.556E-05	0.519E-04	0.215E-03	0.688E-03	0.172E-02	0.355E-02	0.101E-01	0.206E-01	0.342E-01	0.665E-01
100	0.284E-06	0.758E-05	0.513E-04	0.228E-03	0.715E-03	0.173E-02	0.610E-02	0.140E-01	0.253E-01	0.540E-01
150	0.167E-09	0.103E-06	0.233E-05	0.223E-04	0.116E-03	0.401E-03	0.219E-02	0.654E-02	0.139E-01	0.359E-01
200	0.985E-13	0.234E-08	0.171E-06	0.329E-05	0.267E-04	0.124E-03	0.979E-03	0.361E-02	0.874E-02	0.263E-01
250	0.580E-16	0.788E-10	0.175E-07	0.635E-06	0.763E-05	0.460E-04	0.500E-03	0.220E-02	0.597E-02	0.204E-01
300	0.342E-19	0.363E-11	0.229E-08	0.149E-06	0.255E-05	0.194E-04	0.279E-03	0.144E-02	0.431E-02	0.164E-01
400	0.118E-25	0.146E-13	0.661E-10	0.122E-07	0.394E-06	0.451E-05	0.105E-03	0.710E-03	0.250E-02	0.115E-01
500	0.411E-32	0.118E-15	0.316E-11	0.148E-08	0.820E-07	0.133E-05	0.469E-04	0.396E-03	0.160E-02	0.854E-02
600	0.142E-38	0.160E-17	0.217E-12	0.234E-09	0.210E-07	0.465E-06	0.234E-04	0.241E-03	0.110E-02	0.665E-02
700	0.000E+00	0.304E-19	0.195E-13	0.451E-10	0.628E-08	0.183E-06	0.127E-04	0.155E-03	0.787E-03	0.534E-02
800	0.000E+00	0.800E-21	0.218E-14	0.102E-10	0.211E-08	0.794E-07	0.736E-05	0.105E-03	0.586E-03	0.439E-02
900	0.000E+00	0.288E-22	0.290E-15	0.260E-11	0.783E-09	0.370E-07	0.448E-05	0.738E-04	0.448E-03	0.368E-02
1000	0.000E+00	0.128E-23	0.446E-16	0.737E-12	0.313E-09	0.184E-07	0.284E-05	0.534E-04	0.351E-03	0.312E-02

MASS FRACTION OF PASSED AEROSOL PARTICLES THROUGH DIFFUSION TUBE
GEOMETRIC MEAN RADIUS=0.0010 MIC.

	M(X)/M(0)									
X/0	LS= 0.000	LS= 0.050	LS= 0.075	LS= 0.100	LS= 0.125	LS= 0.150	LS= 0.200	LS= 0.250	LS= 0.300	LS= 0.400
5	0.390E+00	0.412E+00	0.438E+00	0.472E+00	0.513E+00	0.559E+00	0.659E+00	0.755E+00	0.838E+00	0.931E+00
10	0.185E+00	0.210E+00	0.241E+00	0.282E+00	0.332E+00	0.389E+00	0.517E+00	0.647E+00	0.761E+00	0.895E+00
20	0.418E-01	0.588E-01	0.816E-01	0.115E+00	0.161E+00	0.217E+00	0.356E+00	0.513E+00	0.660E+00	0.845E+00
40	0.213E-02	0.567E-02	0.125E-01	0.264E-01	0.507E-01	0.879E-01	0.204E+00	0.365E+00	0.537E+00	0.775E+00
60	0.109E-03	0.679E-03	0.250E-02	0.780E-02	0.200E-01	0.430E-01	0.133E+00	0.281E+00	0.458E+00	0.724E+00
80	0.556E-05	0.959E-04	0.598E-03	0.271E-02	0.902E-02	0.234E-01	0.925E-01	0.225E+00	0.401E+00	0.683E+00
100	0.284E-06	0.155E-04	0.164E-03	0.106E-02	0.448E-02	0.138E-01	0.676E-01	0.186E+00	0.357E+00	0.649E+00
150	0.167E-09	0.261E-06	0.983E-05	0.142E-03	0.102E-02	0.456E-02	0.352E-01	0.126E+00	0.281E+00	0.581E+00
200	0.985E-13	0.705E-08	0.899E-06	0.267E-04	0.304E-03	0.184E-02	0.207E-01	0.913E-01	0.231E+00	0.530E+00
250	0.580E-16	0.277E-09	0.110E-06	0.627E-05	0.107E-03	0.847E-03	0.132E-01	0.694E-01	0.195E+00	0.488E+00
300	0.342E-19	0.144E-10	0.167E-07	0.173E-05	0.426E-04	0.428E-03	0.886E-02	0.546E-01	0.168E+00	0.453E+00
400	0.118E-25	0.716E-13	0.622E-09	0.187E-06	0.873E-05	0.133E-03	0.449E-02	0.362E-01	0.130E+00	0.398E+00
500	0.411E-32	0.700E-15	0.364E-10	0.281E-07	0.228E-05	0.495E-04	0.254E-02	0.255E-01	0.104E+00	0.354E+00
600	0.142E-38	0.108E-16	0.296E-11	0.533E-08	0.706E-06	0.210E-04	0.154E-02	0.189E-01	0.859E-01	0.319E+00
700	0.000E+00	0.234E-18	0.310E-12	0.120E-08	0.248E-06	0.974E-05	0.991E-03	0.144E-01	0.722E-01	0.290E+00
800	0.000E+00	0.709E-20	0.394E-13	0.311E-09	0.963E-07	0.488E-05	0.664E-03	0.113E-01	0.617E-01	0.265E+00
900	0.000E+00	0.284E-21	0.589E-14	0.900E-10	0.404E-07	0.259E-05	0.461E-03	0.903E-02	0.534E-01	0.244E+00
1000	0.000E+00	0.136E-22	0.101E-14	0.285E-10	0.181E-07	0.144E-05	0.329E-03	0.735E-02	0.467E-01	0.225E+00

Appendix 5. Examples of Original Data in the Experimental Studies

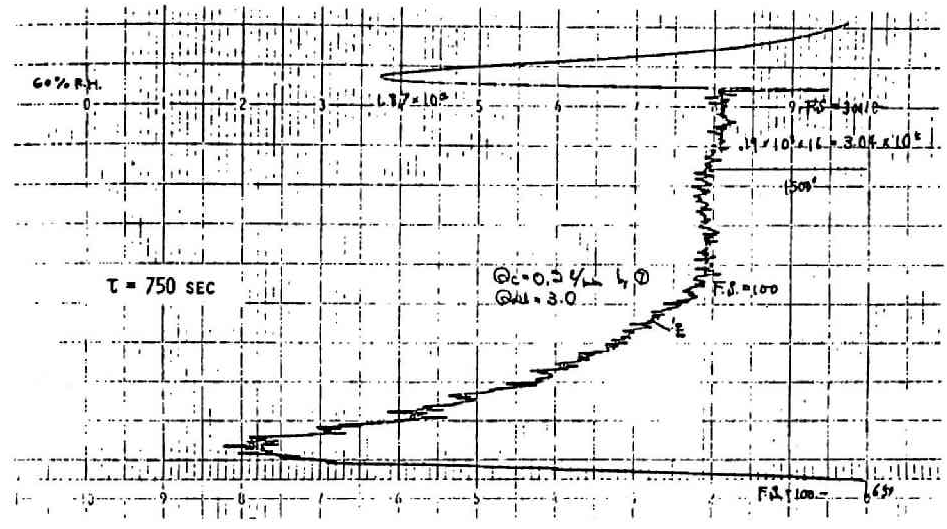

c. τ = 750 sec

b. τ = 200 sec

a. τ = 50 sec

Appendix 5-1. Original experimental data of n - t curves for Run NT(1,60,1)

Appendix 5 (continued)

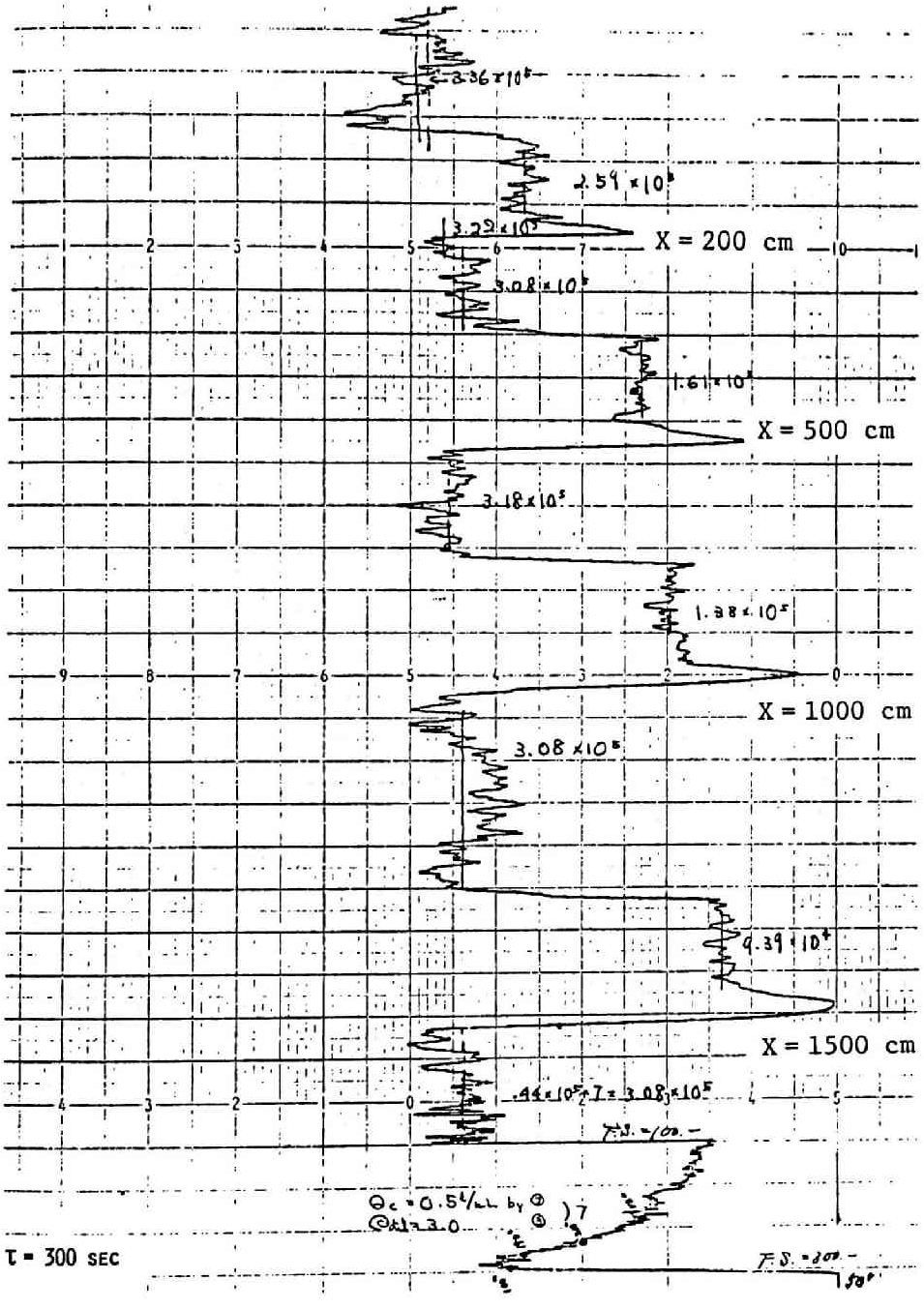

Appendix 5-2. Original data in the determination of size distribution by diffusion tube method for Run rt(1,60)